Analysis Methods of Nonlinear Circuits

and

Stability under Large-Signal Conditions

G.Leuzzi

Dept. Electrical and Information Engineering - Univ. L'Aquila - Italy

Motivation:

Stabilisation of nonlinear circuits under large-signal conditions

* Nonlinear circuits under large-signal drive are subject to unwanted signals at spurious frequencies

* These spurious signals are not detected by standard linear techniques

* A stabilisation approach is highly desirable

Example:

(increasing input power)

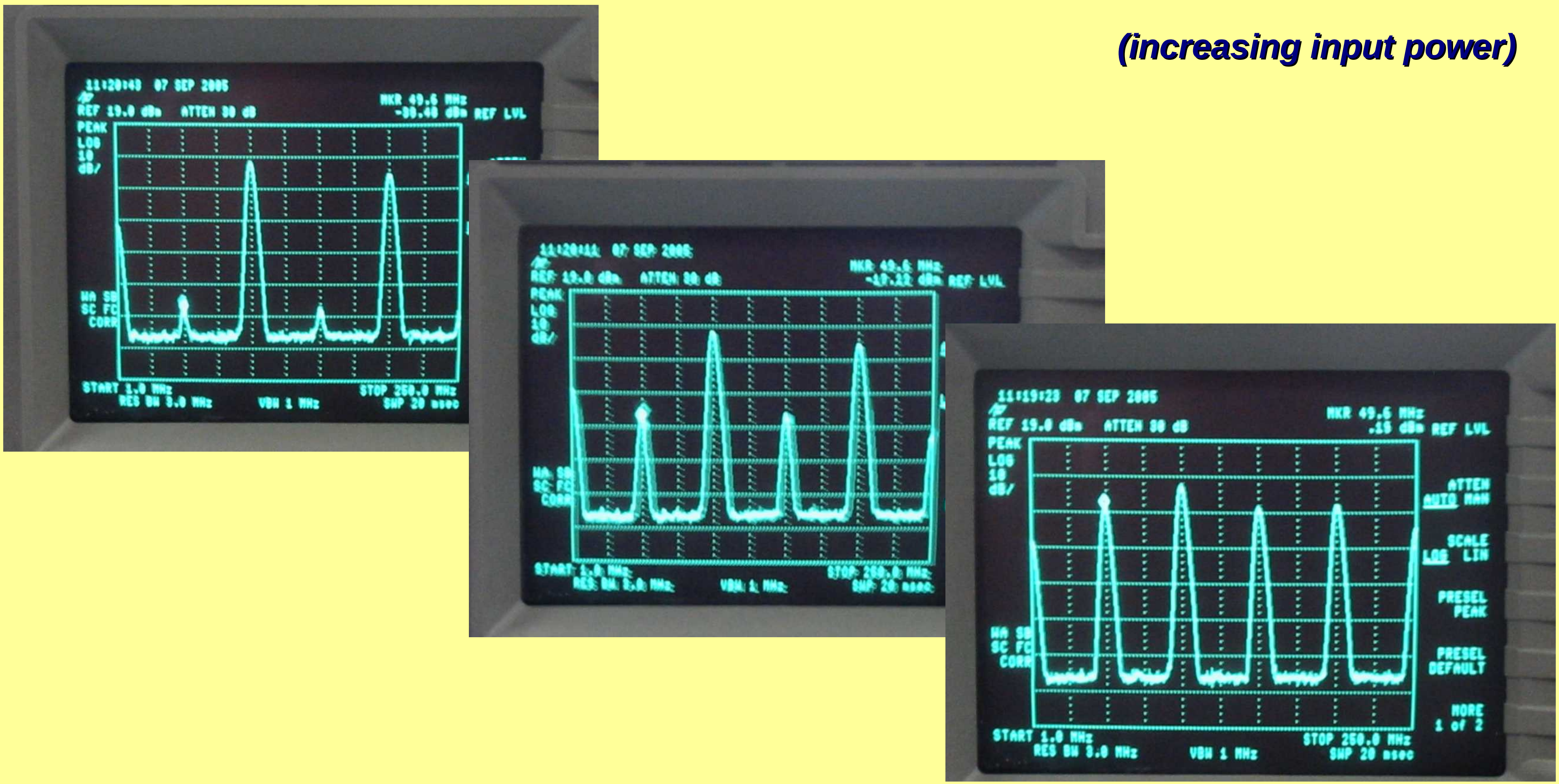

Increasing input power

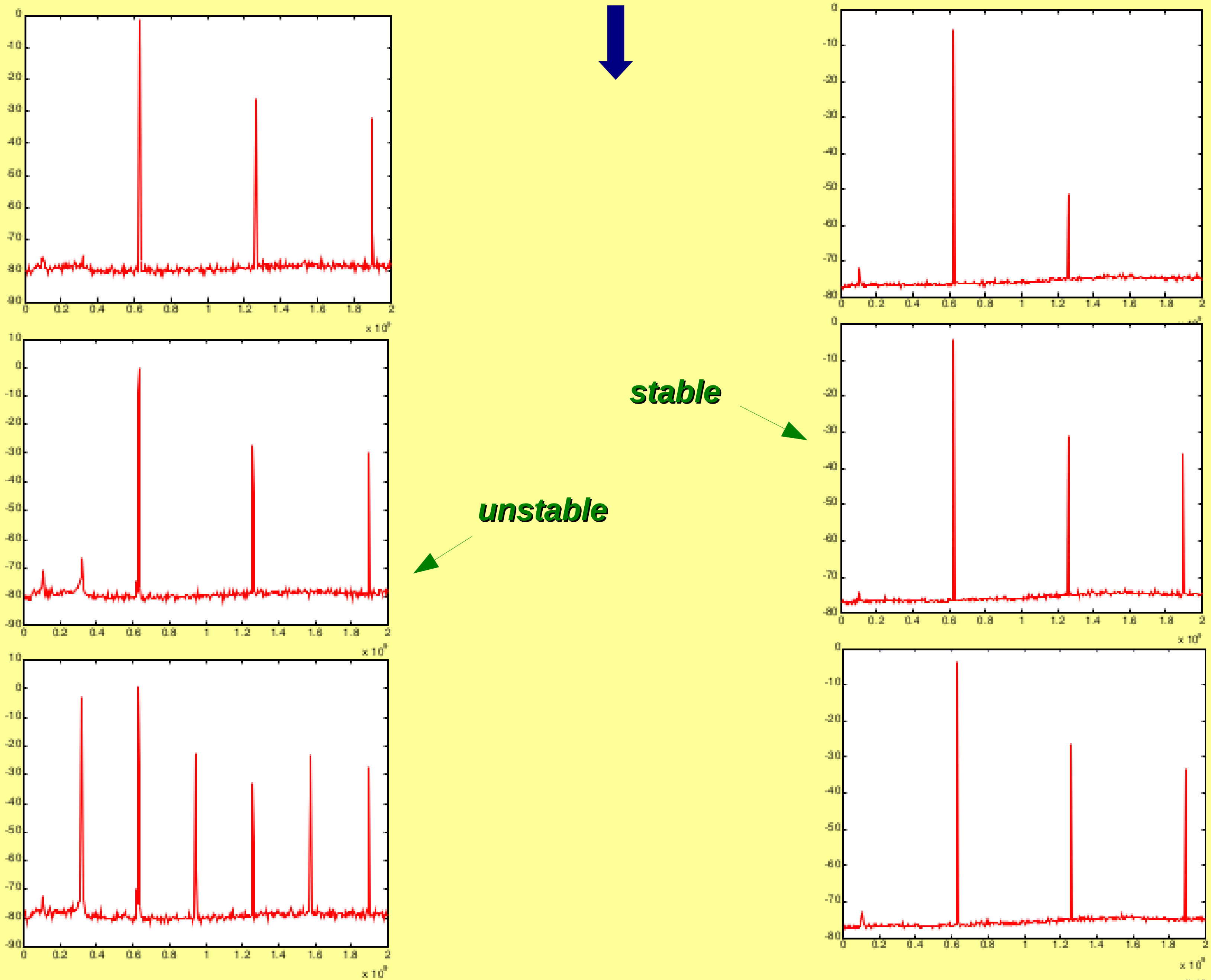

Example: power amplifier

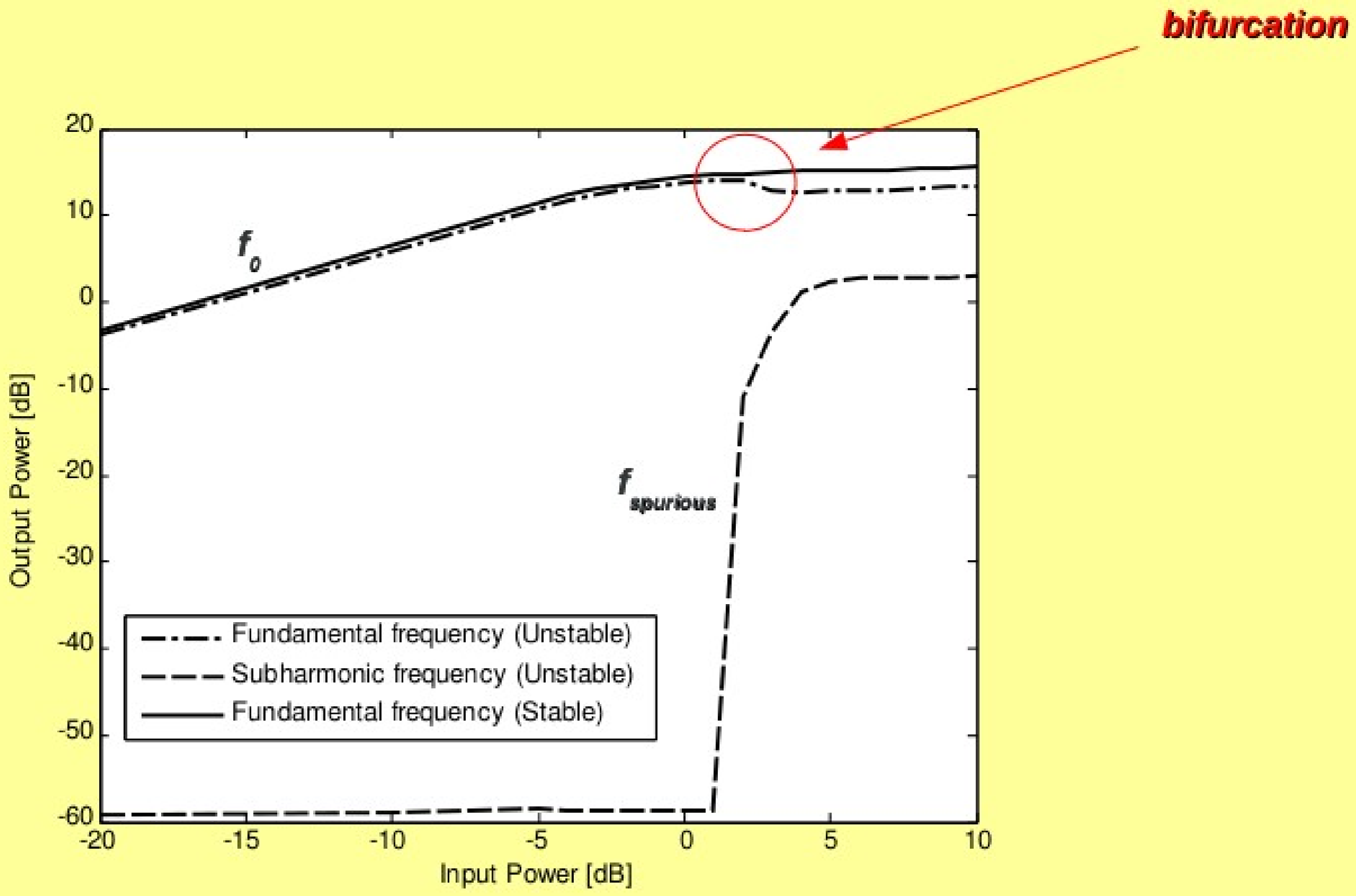

Outline:

* Introduction
* Detection of instabilities via nonlinear CAD simulation
* The conversion matrix: toward a design approach
* Applications: frequency divider, medium-power amplifier
* Conclusions

Stability in small-signal / large-signal conditions:

Small-signal amplifier

(Oscillator)

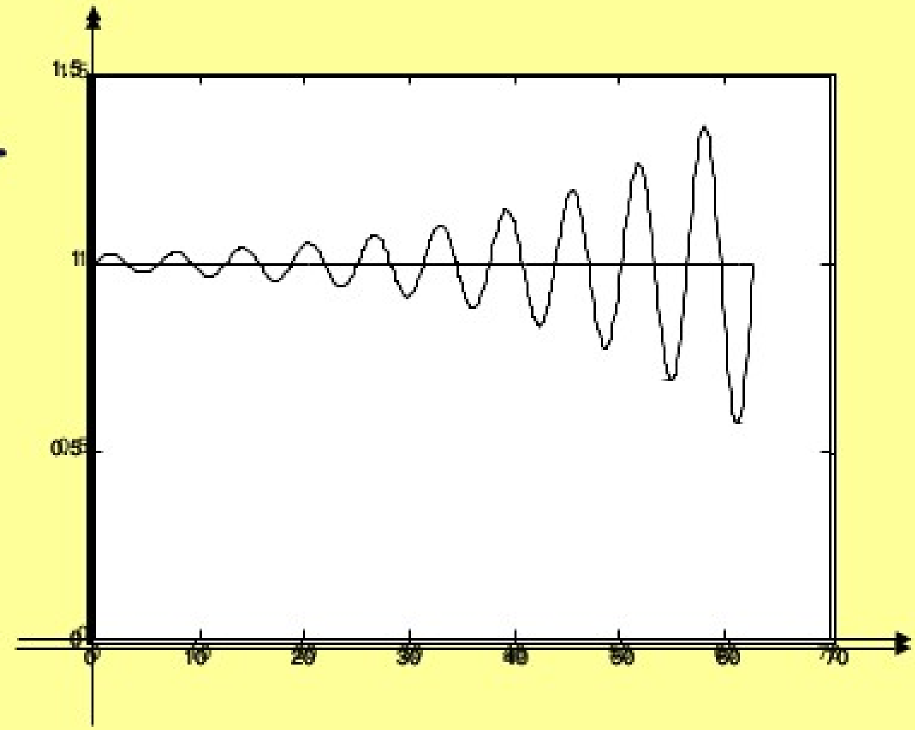

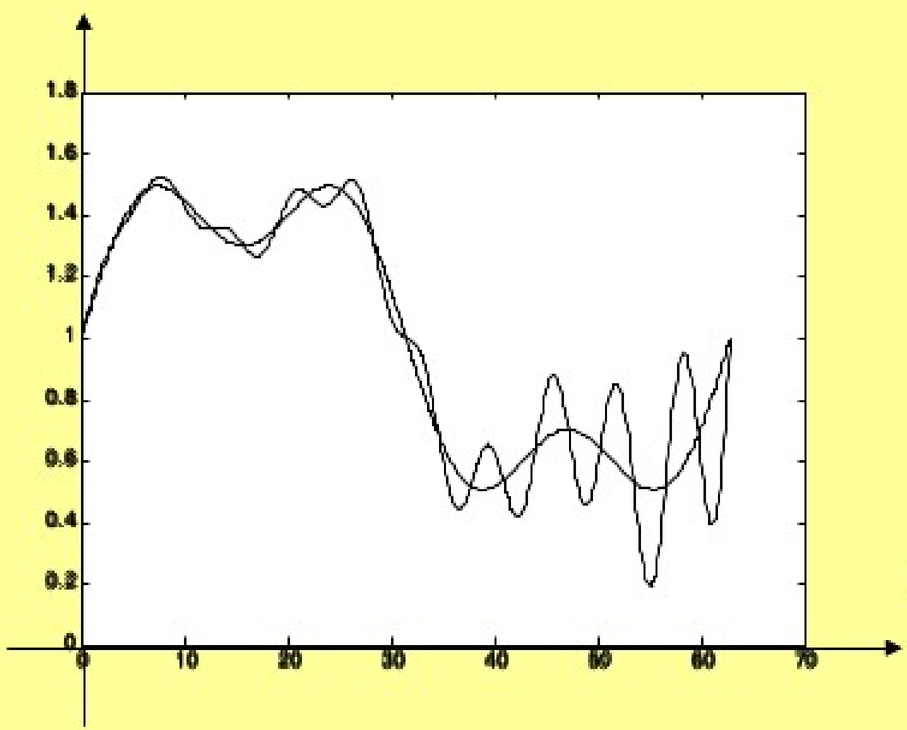

Mixer / Power amplifier

(Frequency divider)

A large signal (DC) and a small signal in a linear amplifier:

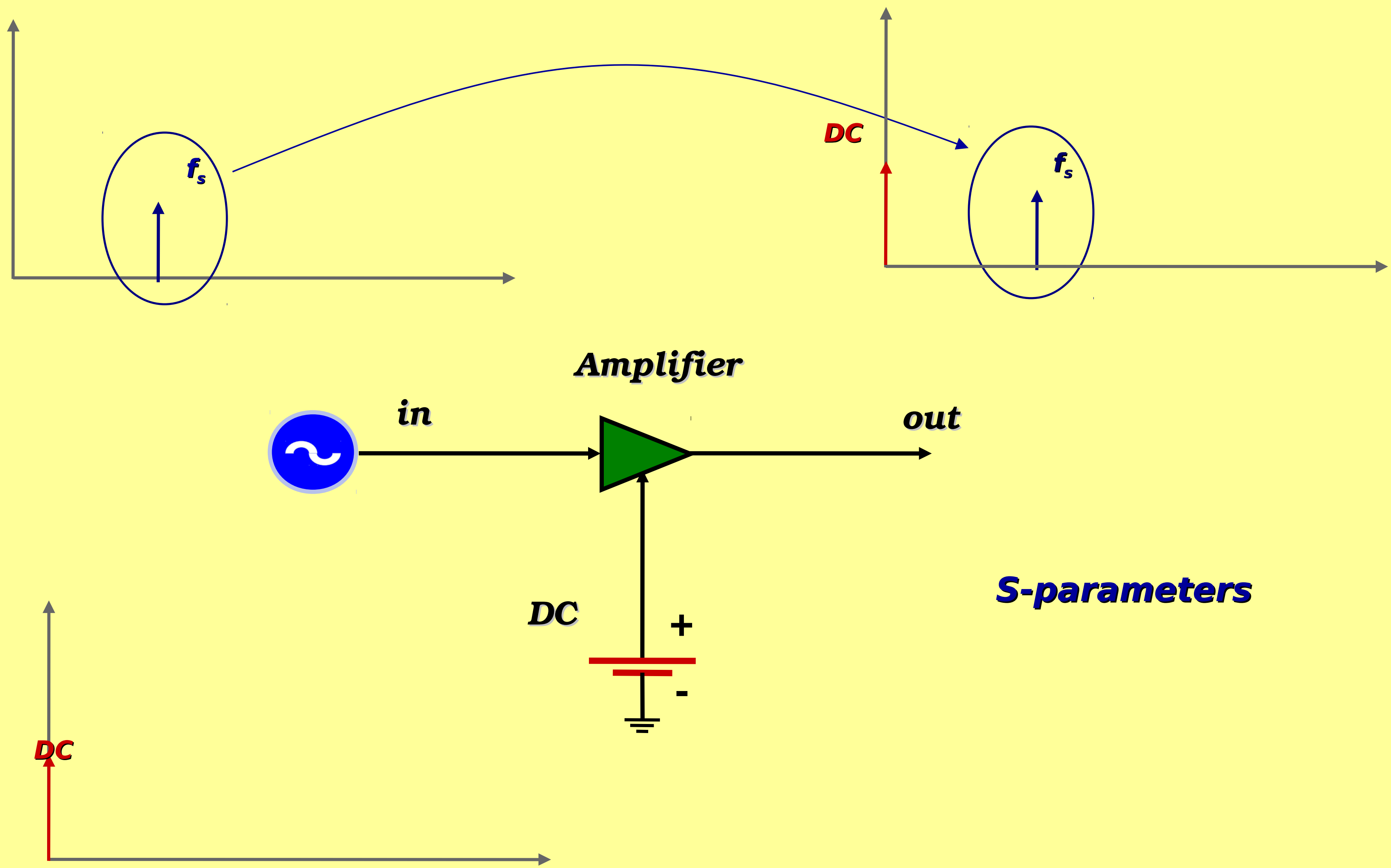

S-parameters

A large signal (RF LO) and a small signal in a mixer:

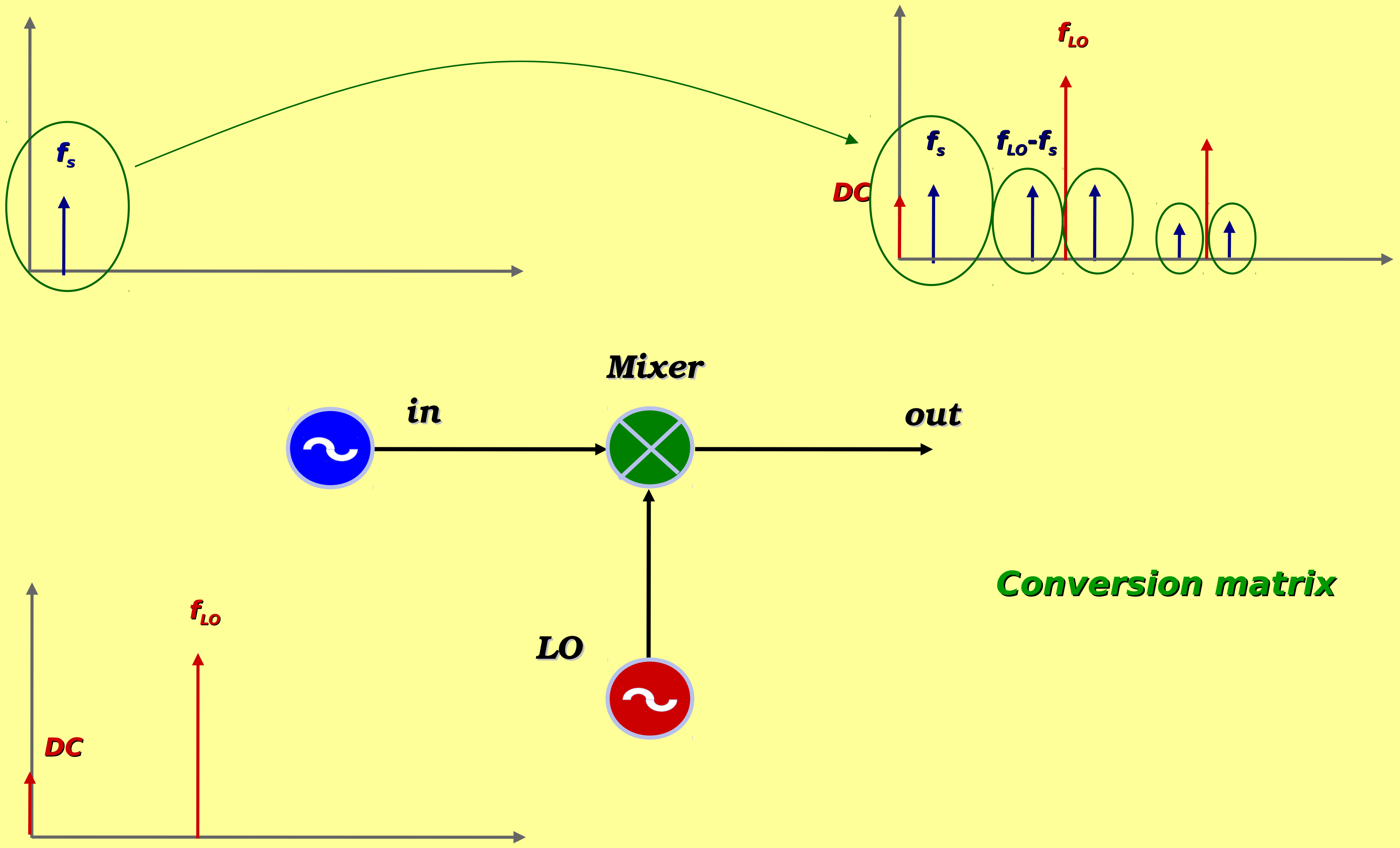

Conversion matrix

A large signal (RF IN) and a small spurious signal in a power amplifier:

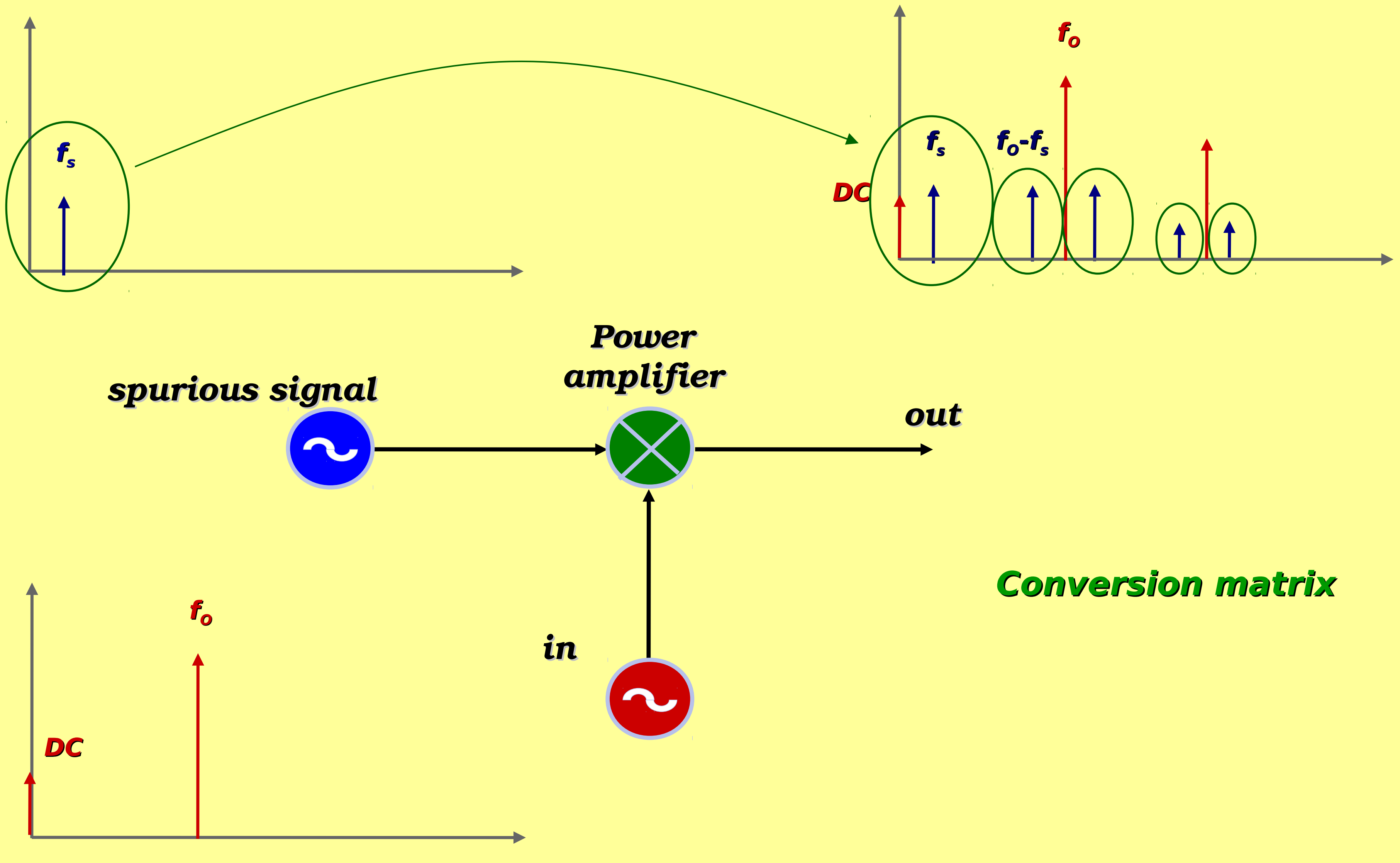

Conversion matrix

Nonlinear computer-aided analysis methods:

Direct time-domain integration:	SPICE Shooting methods Convolution approach
Series expansion:	Fourier series (Harmonic balance) Volterra series
Mixed time-domain / Fourier series:	Transient envelope

Direct time-domain integration:

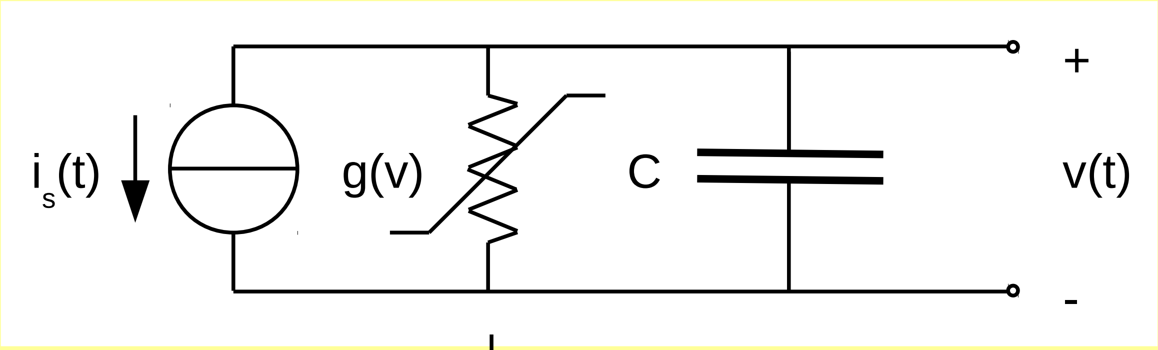

$$i_g = i_{max} \cdot \tanh\left(\frac{g \cdot v}{i_{max}}\right)$$

KCL:

$$i_s(t) + i_{max} \cdot \tanh\left(\frac{g \cdot v(t)}{i_{max}}\right) + C \cdot \left(\frac{dv(t)}{dt}\right) = 0$$

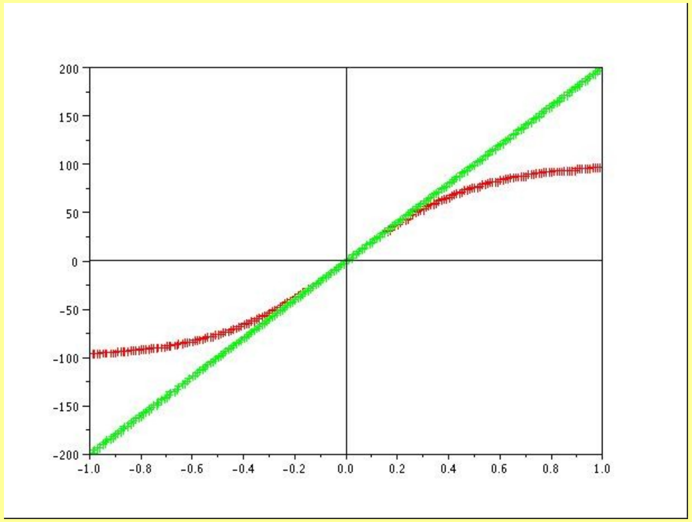

No analytical solution for the unknown function v(t)

Direct time-domain integration:

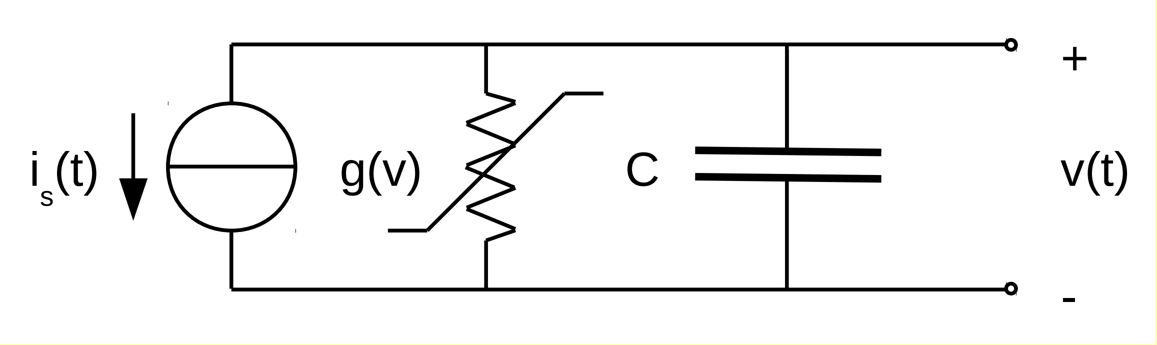

$$i_s(t)+i_{max}\cdot\tanh\left(\frac{g\cdot v(t)}{i_{max}}\right)+C\cdot\left(\frac{dv(t)}{dt}\right)=0$$

$$i_{s,k}(t)+i_{max}\cdot\tanh\left(\frac{g\cdot v_k}{i_{max}}\right)+C\cdot\left(\frac{v_k-v_{k-1}}{t_k-t_{k-1}}\right)=0$$

$$t\Rightarrow t_k$$

$$v(t)\Rightarrow v_k \qquad k=0,1,2\ldots$$

$$v(t_0)\Rightarrow v_0$$

Instead of an unknown function v(t) we look for discrete values v_k

Numerical solution of the nonlinear equation in v_k at each time step t_k starting from $v_0 = v(t_0)$

Direct time-domain integration:

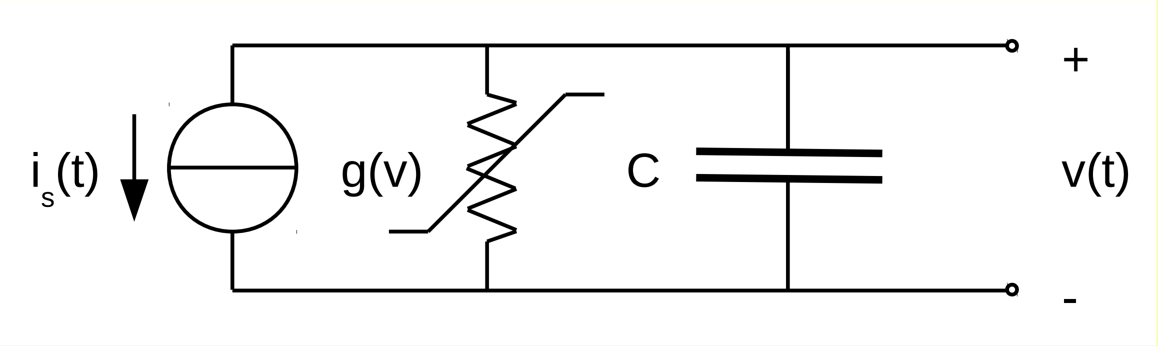

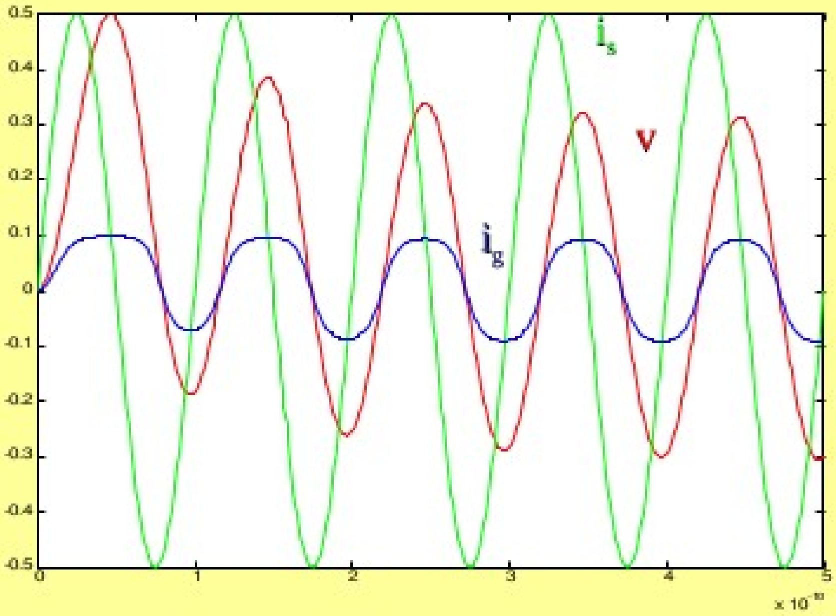

Response to a sine wave (with transient)

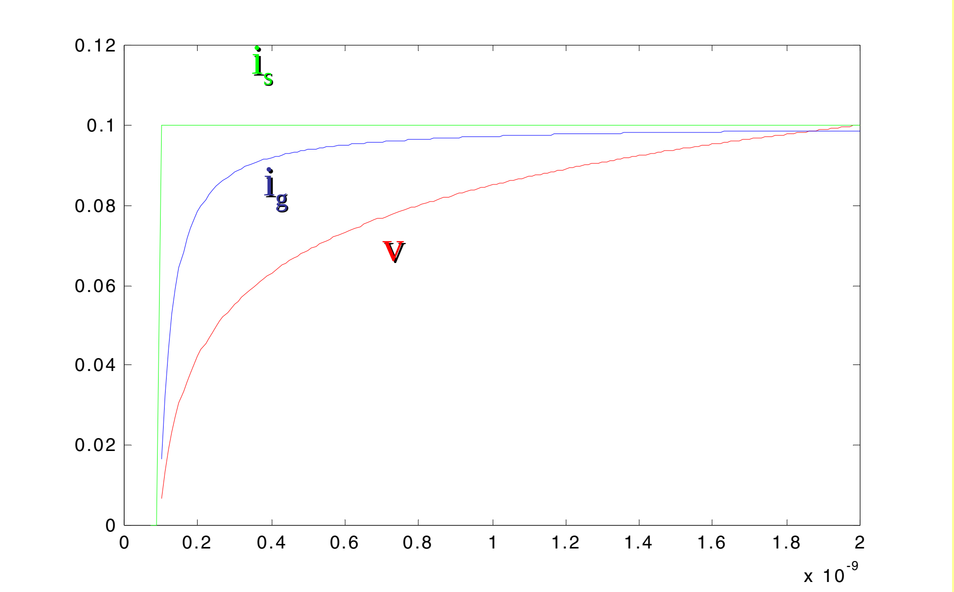

Response to a step

Direct time-domain integration:

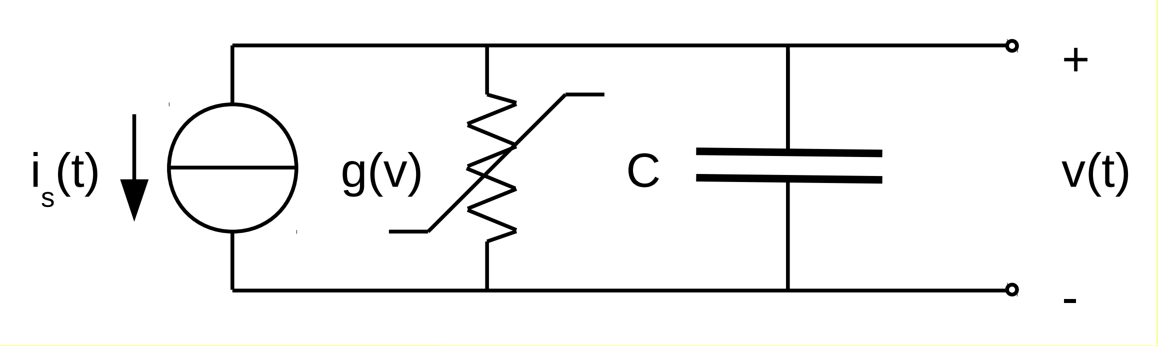

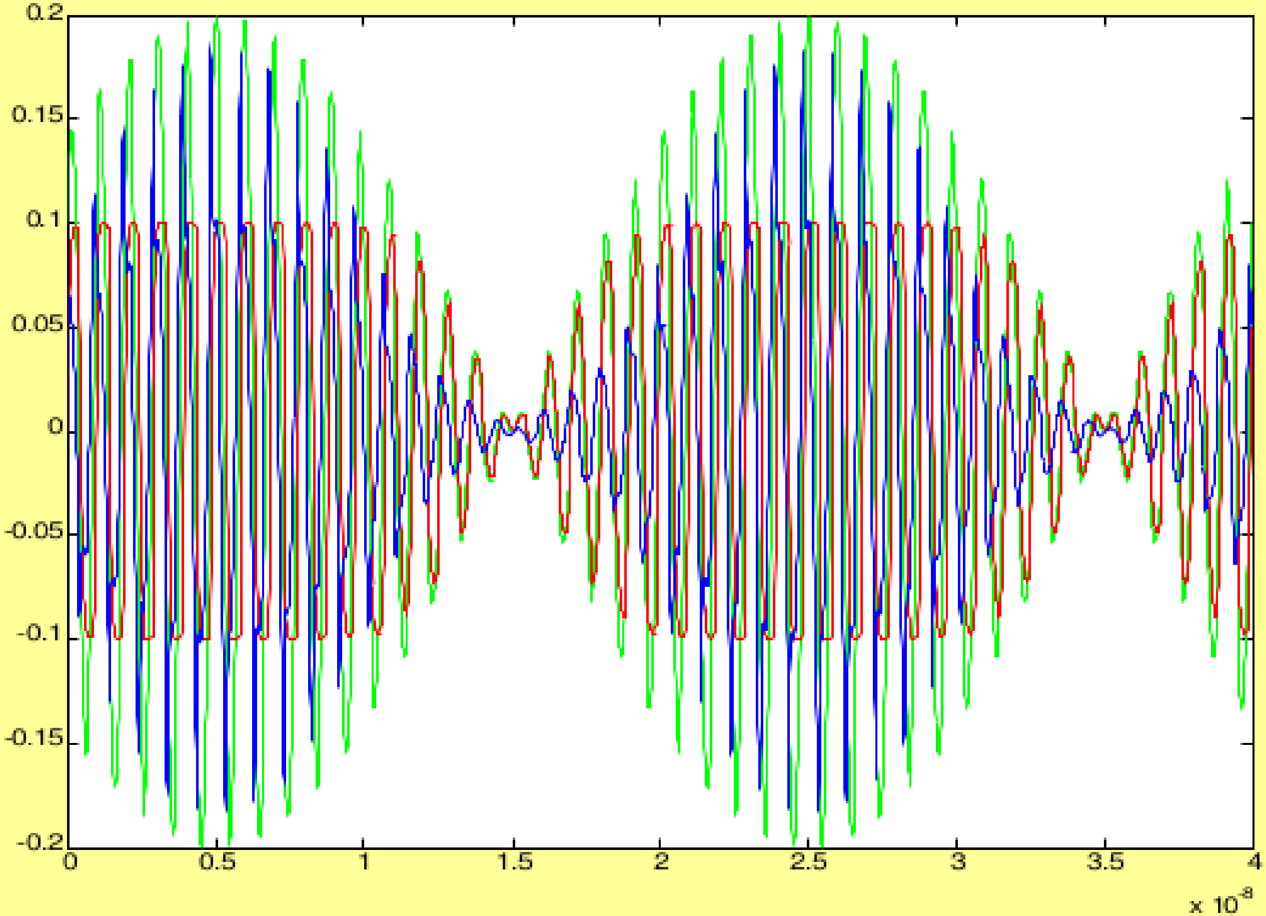

Response to a two-tone quasi-sinusoidal signal

Time-domain solution:

General nonlinearities, even very strong

General solution

Non efficient for steady state

Lumped elements only

Shooting methods

Convolution method

Time-domain solution:

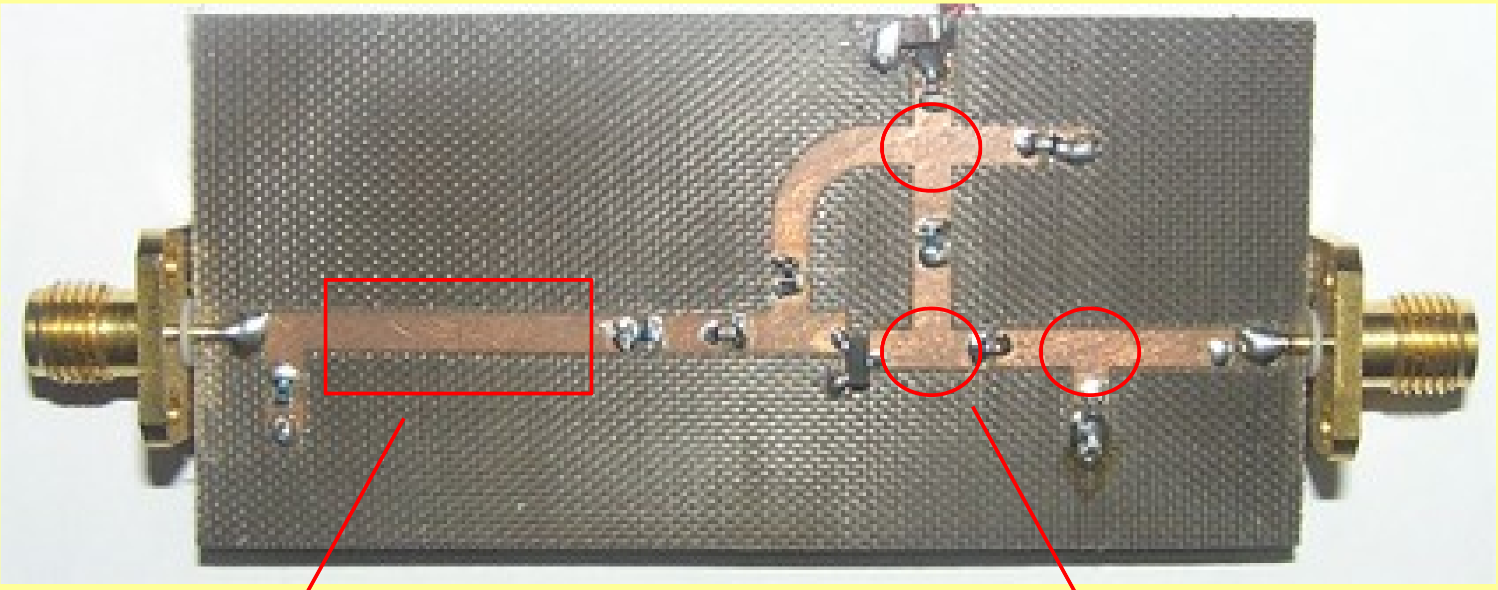

Transmission lines

Discontinuities

$$i(t) = f\,?[v(t)]$$

Convolution method:

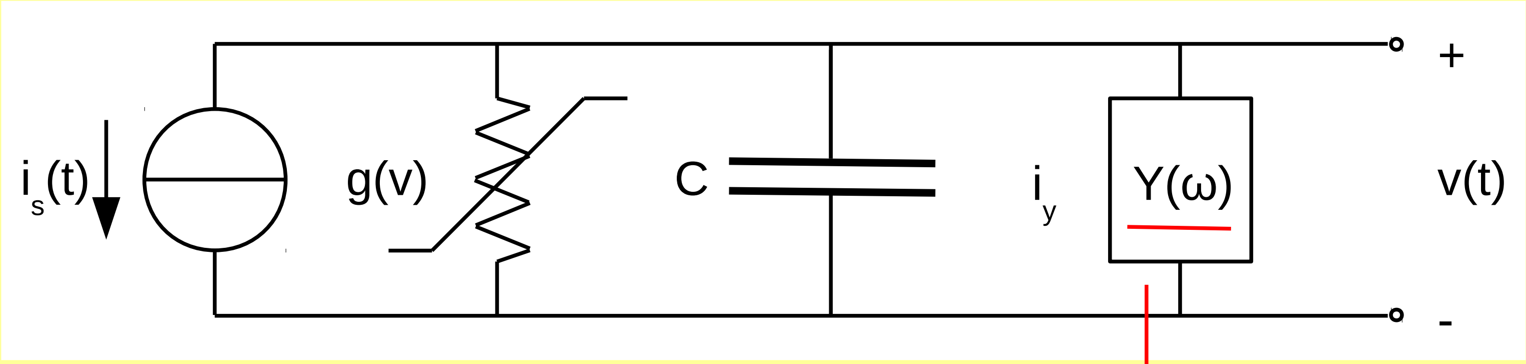

$$i_s(t)+i_{max}\cdot\tanh\left(\frac{g\cdot v(t)}{i_{max}}\right)+C\cdot\left(\frac{dv(t)}{dt}\right)+i_y(t)=0$$

$$I_y(\omega)=Y(\omega)\cdot V(\omega)$$

$$y(t)=\frac{1}{\sqrt{2\pi}}\cdot\int Y(\omega)\cdot e^{j\omega t}\cdot d\omega$$

$$i_y(t)=i_y(t_0)+\int y(t-\tau)\cdot v(\tau)\cdot d\tau$$

$$i_y(t_k)=\sum_{m=0}^{M} y_m\cdot v_{k-m}$$

$$i_{s,k}(t)+i_{max}\cdot\tanh\left(\frac{g\cdot v_k}{i_{max}}\right)+C\cdot\left(\frac{v_k-v_{k-1}}{t_k-t_{k-1}}\right)+\sum_{m=0}^{M} y_m\cdot v_{k-m}=0$$

Unfortunately does not work very well in practice!

Solution by series expansion:

The unknown function is expanded in a suitable series of orthogonal functions $v_n(t)$:

$$v(t) = \sum_{n=-\infty}^{\infty} k_n \cdot v_n(t)$$

- The series is replaced into the 'difficult' equation
- The 'difficult' equation is splitted into infinite 'simpler' equations (using orthogonality)
- Only the first terms of the series (and thence the first equations) are retained
- The unknowns are the coefficients k_n of the series expansion

Fourier series expansion (Harmonic balance):

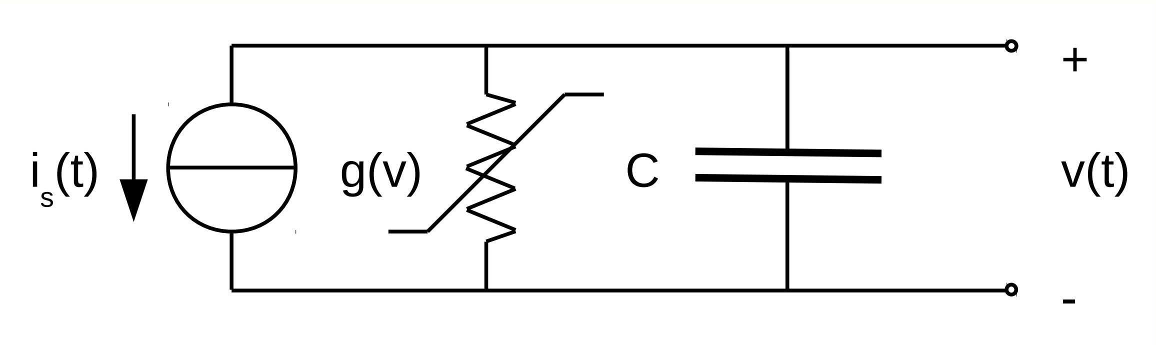

$$v(t)=\sum_{n=-\infty}^{\infty} V_n \cdot e^{jn\omega \cdot t}$$

$$\frac{dv(t)}{dt}=\sum_{n=-\infty}^{\infty} jn\omega C \cdot V_n \cdot e^{jn\omega \cdot t}$$

$$i_s(t)=\sum_{n=-\infty}^{\infty} I_{s,n} \cdot e^{jn\omega \cdot t}$$

$$i_s(t)+i_{max}\cdot \tanh\left(\frac{g\cdot v(t)}{i_{max}}\right)+C\cdot\left(\frac{dv(t)}{dt}\right)=0$$

$$\sum_{n=-\infty}^{\infty} I_{s,n}\cdot e^{jn\omega\cdot t}+i_{max}\cdot\tanh\left(\frac{g\cdot\sum_{n=-\infty}^{\infty} V_n\cdot e^{jn\omega\cdot t}}{i_{max}}\right)+\sum_{n=-\infty}^{\infty} jn\omega C\cdot V_n\cdot e^{jn\omega\cdot t}=0$$

The explicit expression of the Fourier series of the nonlinear current is not available

Fourier series expansion (Harmonic balance):

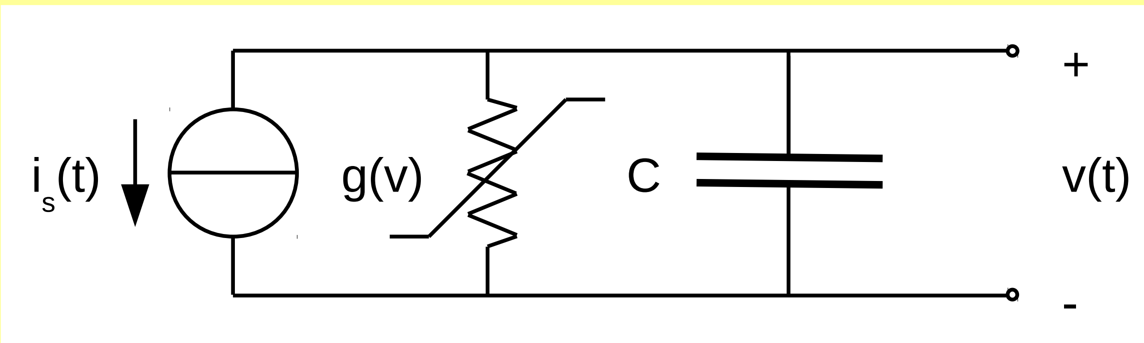

$$i_{max} \cdot \tanh\left(\frac{g \cdot \sum_{n=-\infty}^{\infty} V_n \cdot e^{jn\omega \cdot t}}{i_{max}}\right)$$

$$\Downarrow$$

$$Discrete\ Fourier\ Transform\ (DFT)$$

$$\Downarrow$$

$$\sum_{n=-\infty}^{\infty} I_{g,n} \cdot e^{jn\omega \cdot t}$$

$$\sum_{n=-\infty}^{\infty} I_{s,n} \cdot e^{jn\omega \cdot t} + i_{max} \cdot \tanh\left(\frac{g \cdot \sum_{n=-\infty}^{\infty} V_n \cdot e^{jn\omega \cdot t}}{i_{max}}\right) + \sum_{n=-\infty}^{\infty} jn\omega C \cdot V_n \cdot e^{jn\omega \cdot t} = 0$$

$$\sum_{n=-\infty}^{\infty} I_{s,n} \cdot e^{jn\omega \cdot t} + \sum_{n=-\infty}^{\infty} I_{g,n} \cdot e^{jn\omega \cdot t} + \sum_{n=-\infty}^{\infty} jn\omega C \cdot V_n \cdot e^{jn\omega \cdot t} = 0$$

System of orthogonal nonlinear equations in the unknowns V_n

$$I_{s,n} + I_{g,n}(\vec{V}) + jn\omega C \cdot V_n = 0$$

$$n = -N \div N$$

Harmonic balance:

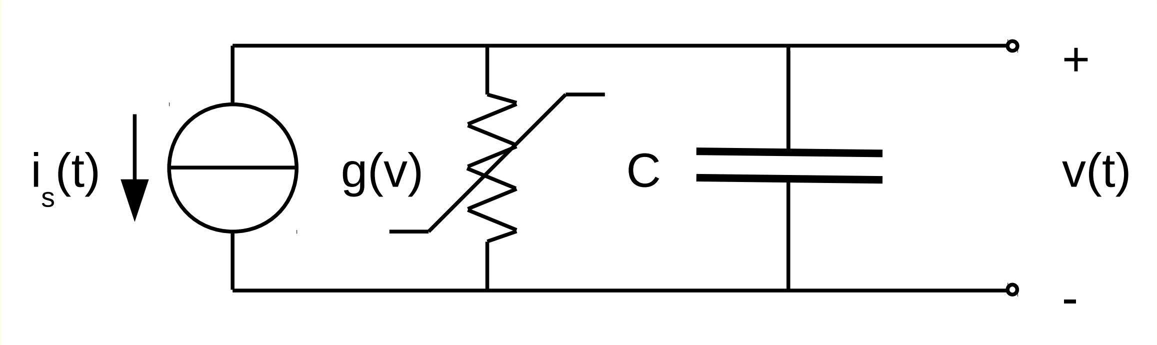

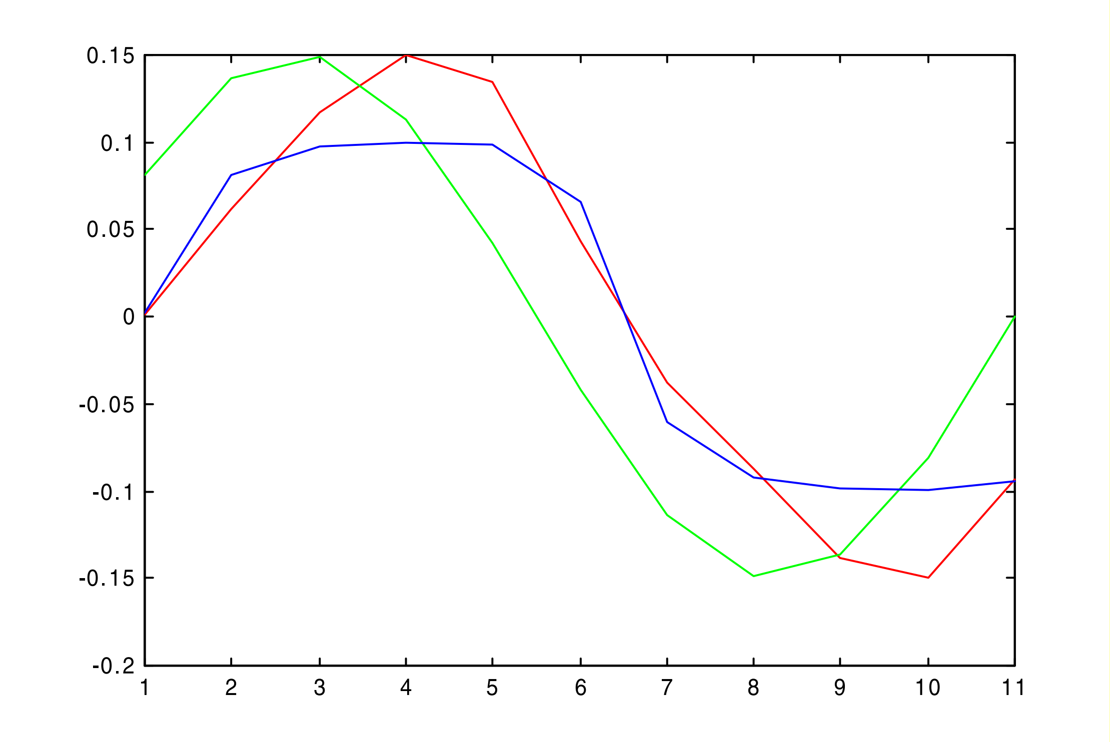

Harmonic balance:

General nonlinearities, weak to moderately strong

Frequency domain linear subcircuits

Steady state only

Not efficient for multi-tone or complex modulation schemes

Envelope transient

Multi-dimensional Fourier transform

Transient envelope:

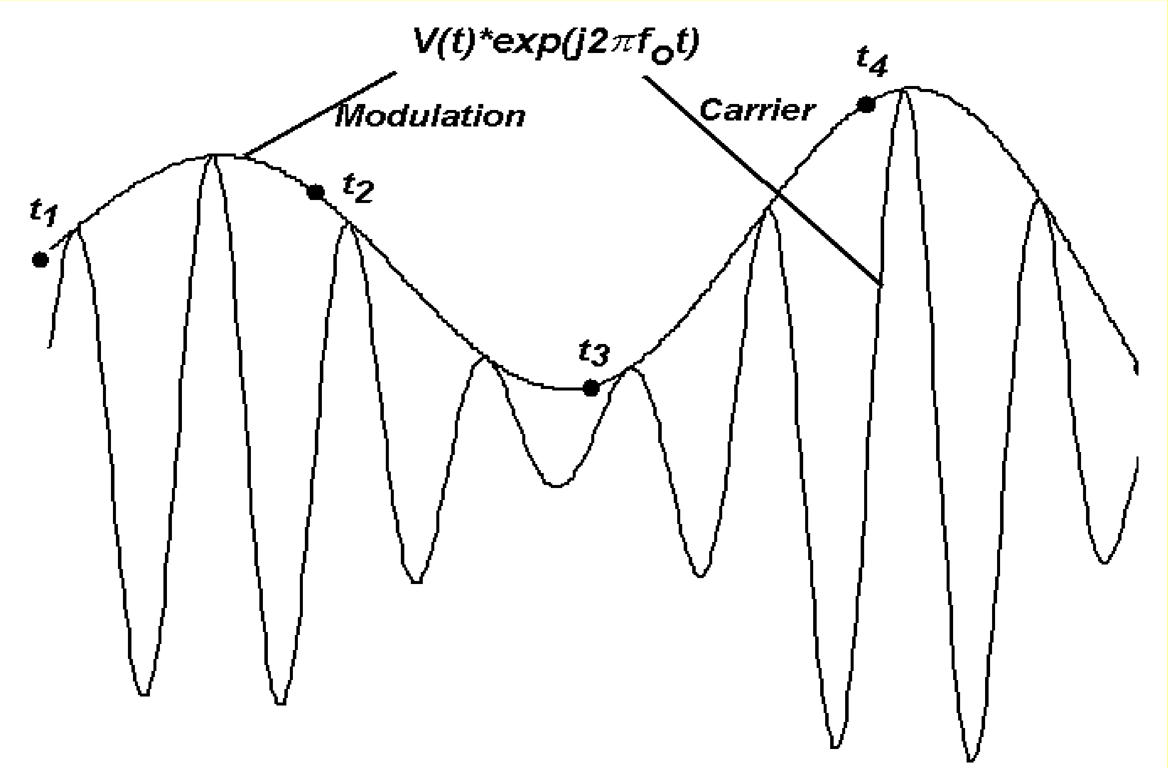

$$v(t)=\sum_{n=-\infty}^{\infty} \underline{V_n(t)}\cdot e^{jn\omega\cdot t}$$

Slowly varying phasors

(narrowband modulation, start-up of oscillation, etc.)

$$\sum_{n=-\infty}^{\infty} I_{s,n}(t)\cdot e^{jn\omega\cdot t}+i_{max}\cdot\tanh\left(\frac{g\cdot\sum_{n=-\infty}^{\infty} V_n(t)\cdot e^{jn\omega\cdot t}}{i_{max}}\right)+C\frac{d\left(\sum_{n=-\infty}^{\infty} V_n(t)\cdot e^{jn\omega\cdot t}\right)}{dt}=0$$

Time-domain discretisation of the values of the slowly varying phasors

CAD detection of instabilities:

Time-domain analysis detects spurious frequencies (instabilities)

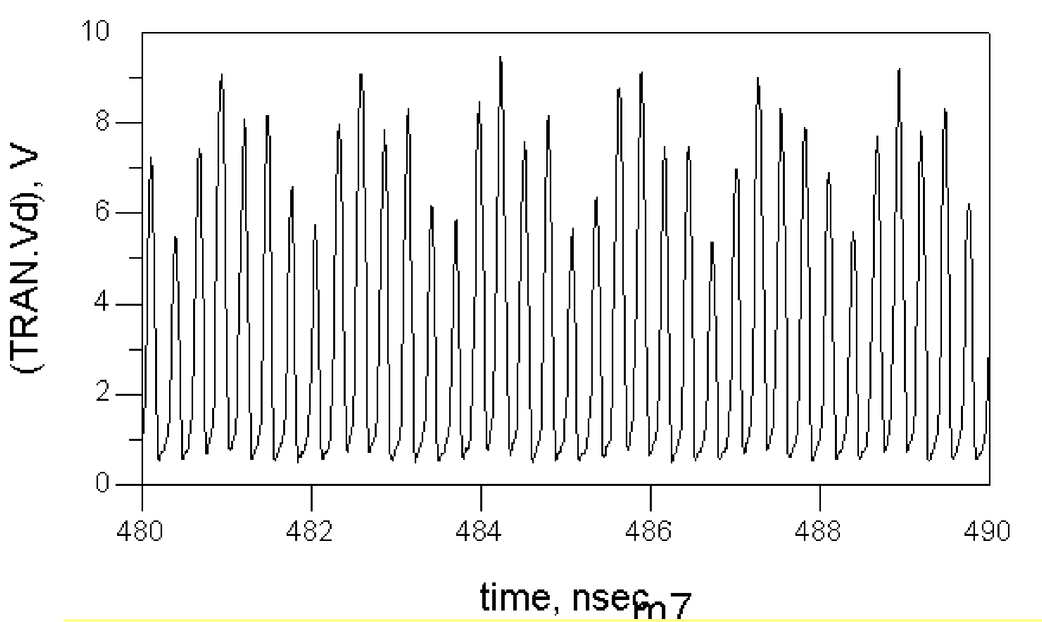

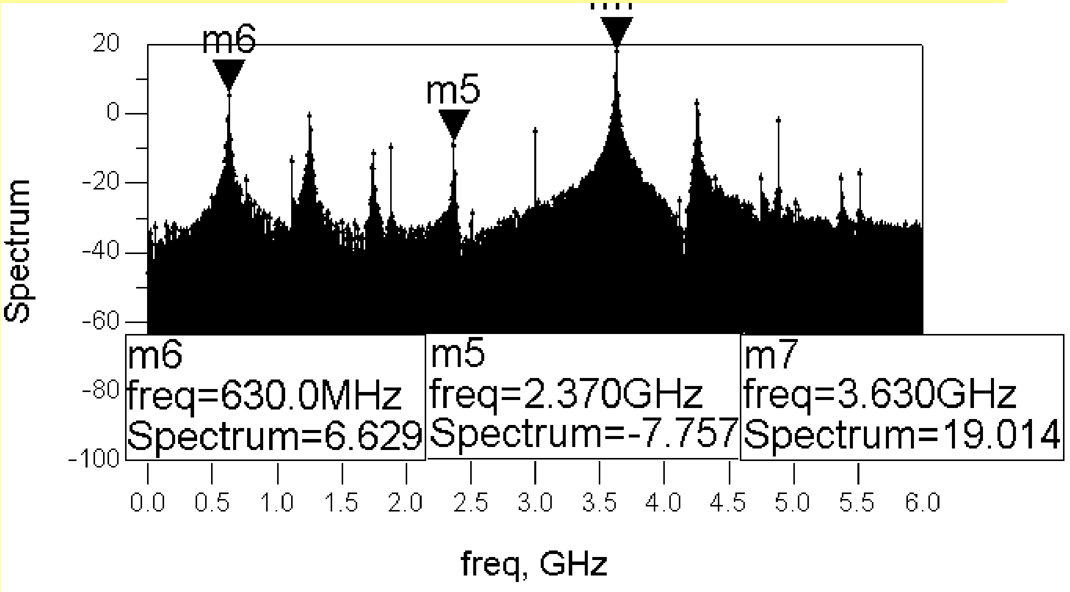

CAD detection of instabilities:

Harmonic balance analysis does not detect spurious frequencies:

$$v(t) = \sum_{n=-\infty}^{\infty} V_n \cdot e^{jn\omega \cdot t}$$

unless included in the frequency list,

or detected by means of an auxiliary generator.

Harmonic balance detection of instabilities: the auxiliary generator

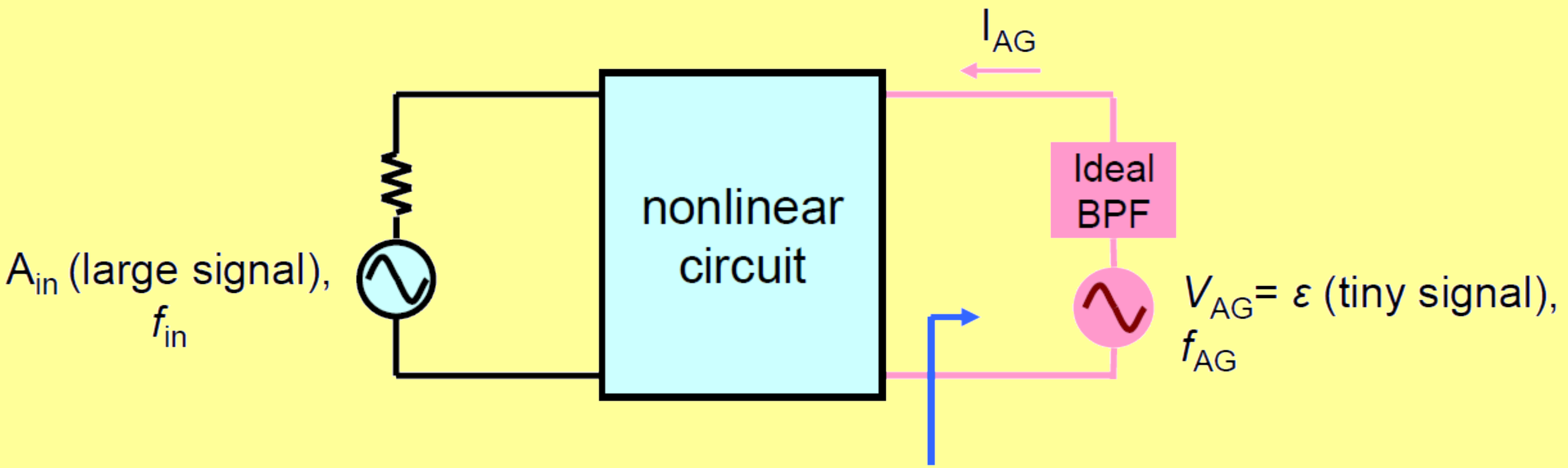

$$Y_{AG} = \frac{I_{AG}}{V_{AG}} = 0 \quad \text{(Non-perturbation condition)}$$

A probing voltage is applied at the spurious frequency, and an oscillation condition is looked for:

Frequency, phase and amplitude of the probing voltage are swept until the non-perturbation condition is found.

The conversion matrix:

Linearisation around a static bias point

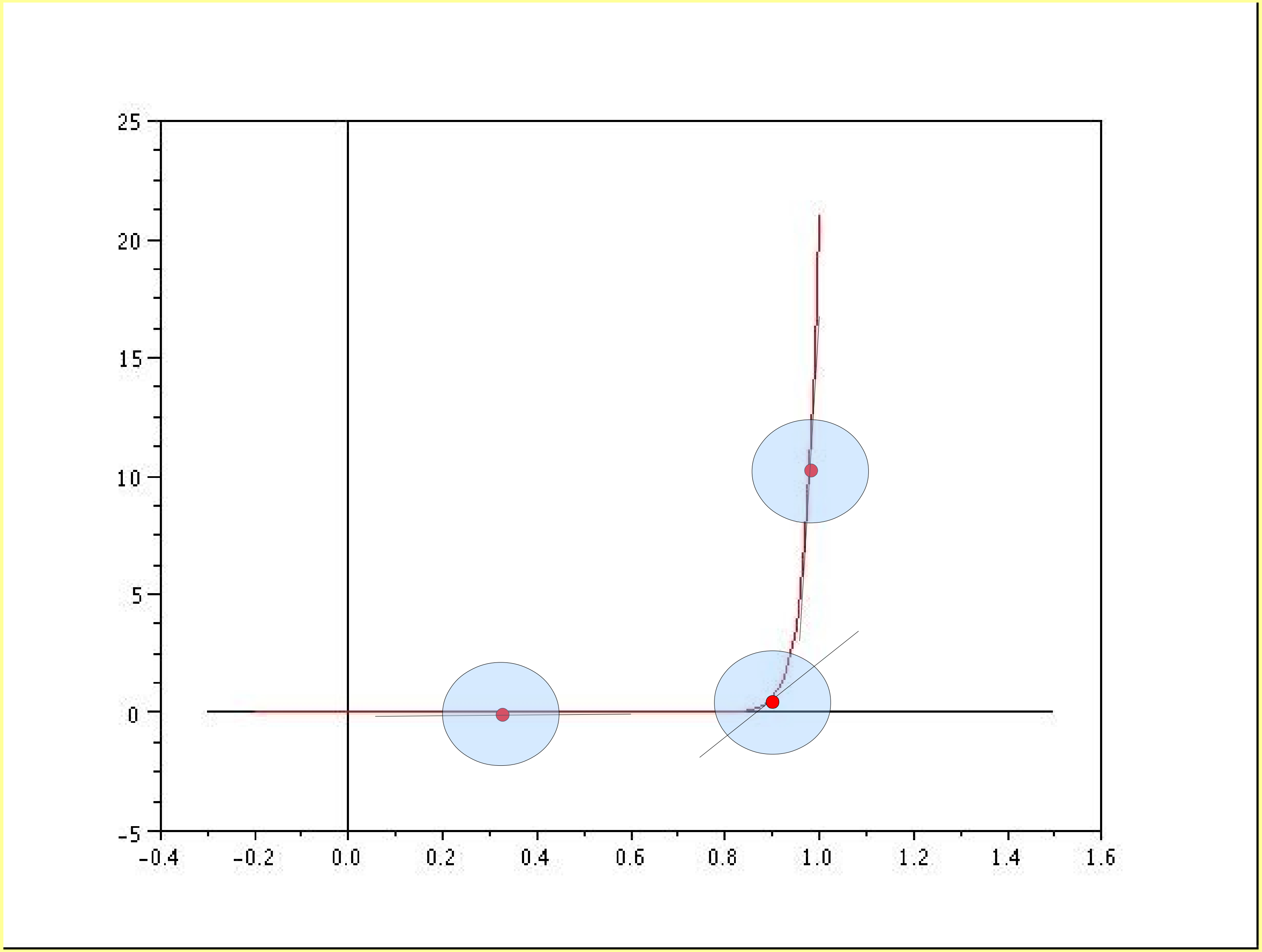

Linearisation around a dynamic bias point

The conversion matrix:

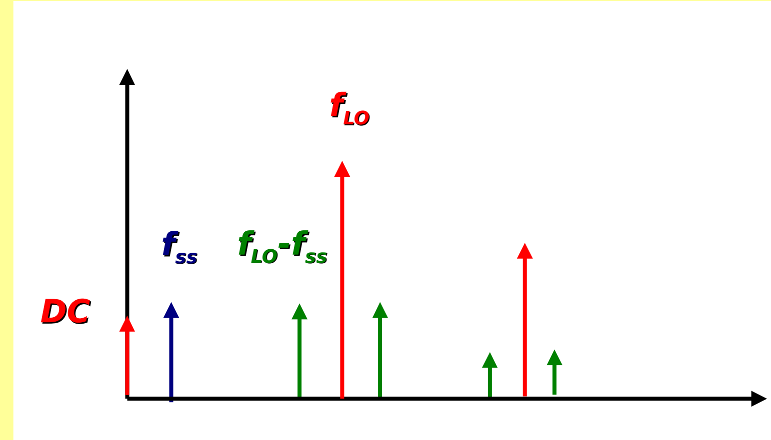

Periodic switching: frequency conversion

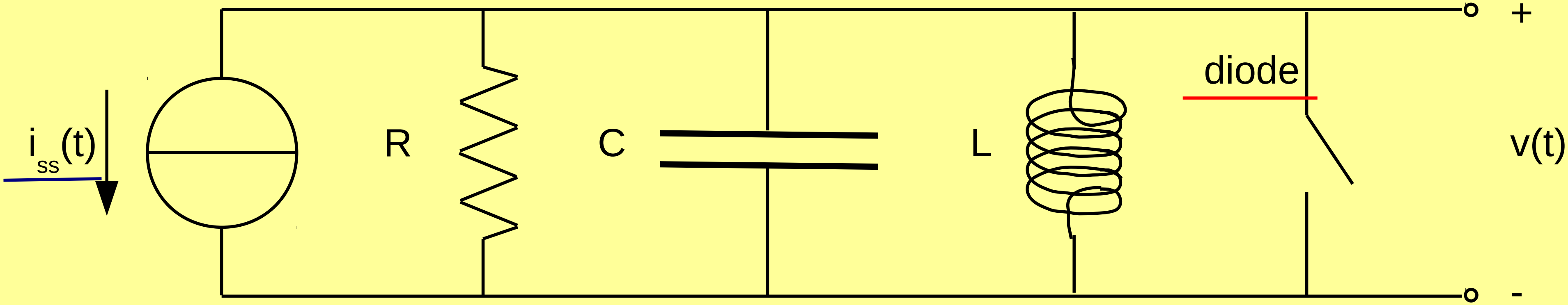

$$v(t)=I_{ss}\sin(\omega_{ss}t)\cdot\sum_{n=-\infty}^{\infty}G_n\cdot e^{-jn\omega_{LO}\cdot t}=\sum_{n=-\infty}^{\infty}[I_{ss}G_n\cdot e^{-jn(\omega_{LO}-\omega_{ss})\cdot t}+I_{ss}G_n\cdot e^{-jn(\omega_{LO}+\omega_{ss})\cdot t}]$$

in — diode — LSB — USB

The conversion matrix:

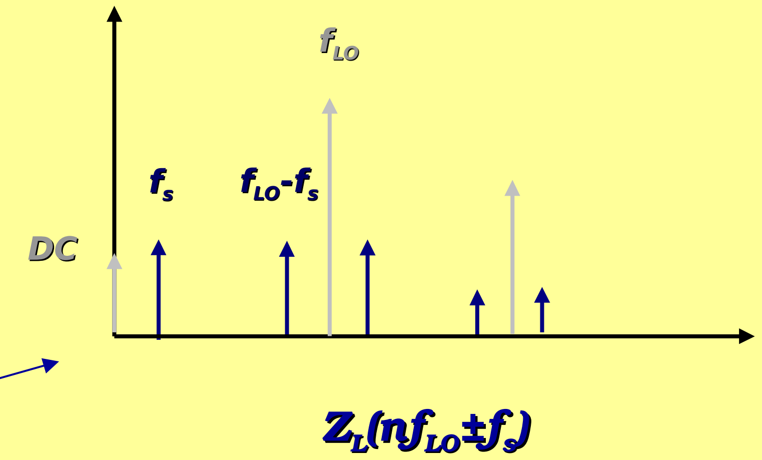

Small-signal (in) behaviour: converted frequencies

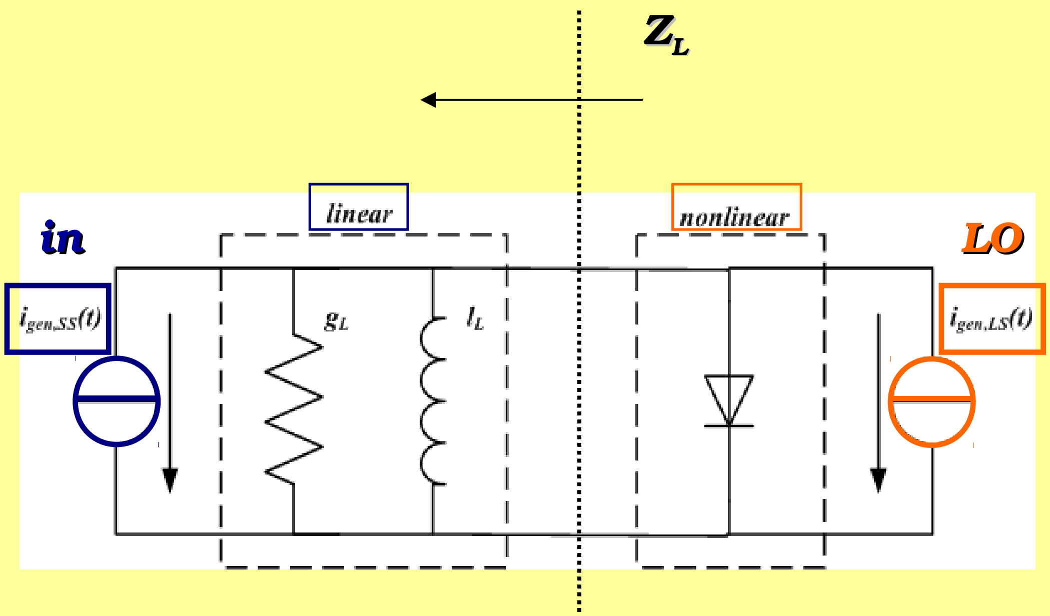

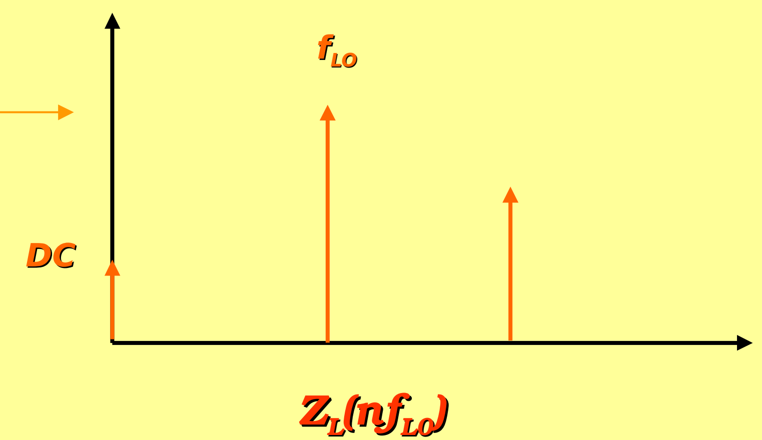

Large-signal (LO) behaviour: fundamental frequency (and harmonics) loads

The conversion matrix:

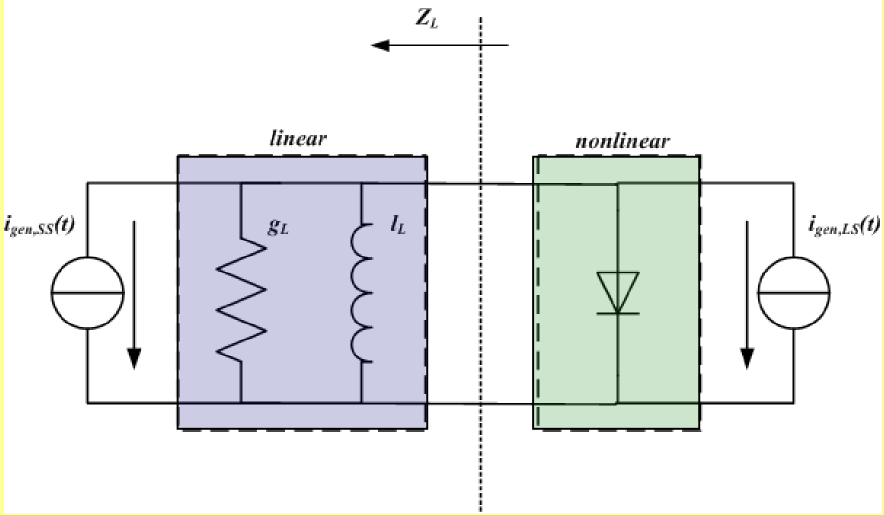

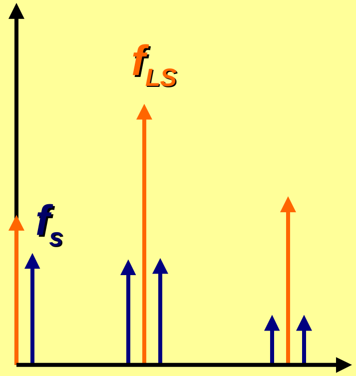

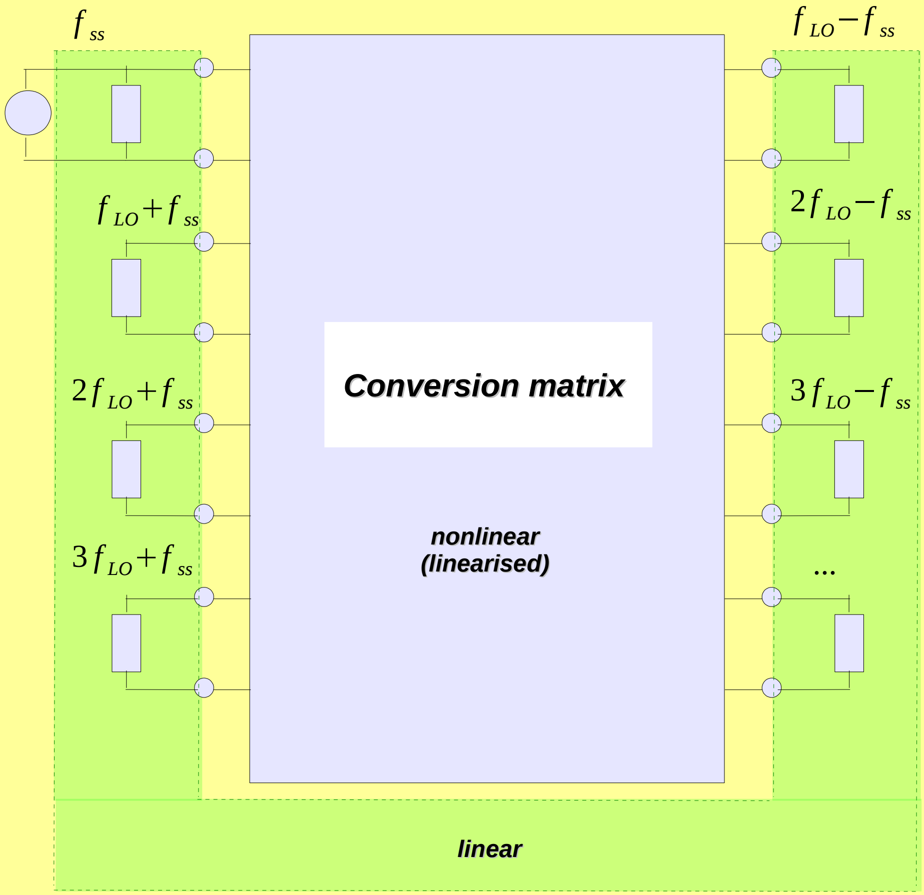

Small-signal operations:

frequency-converting linear network

The conversion matrix:

Active device (+ bias networks) linearised by means of the conversion matrix

Passive matching networks provide the external loads at converted frequencies

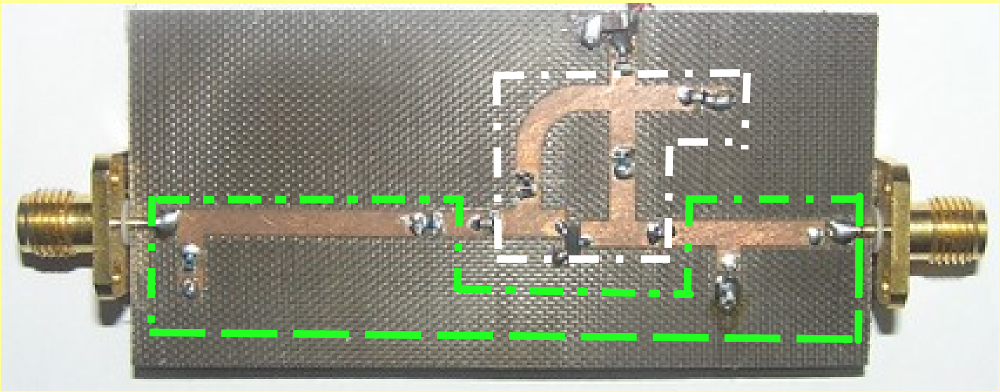

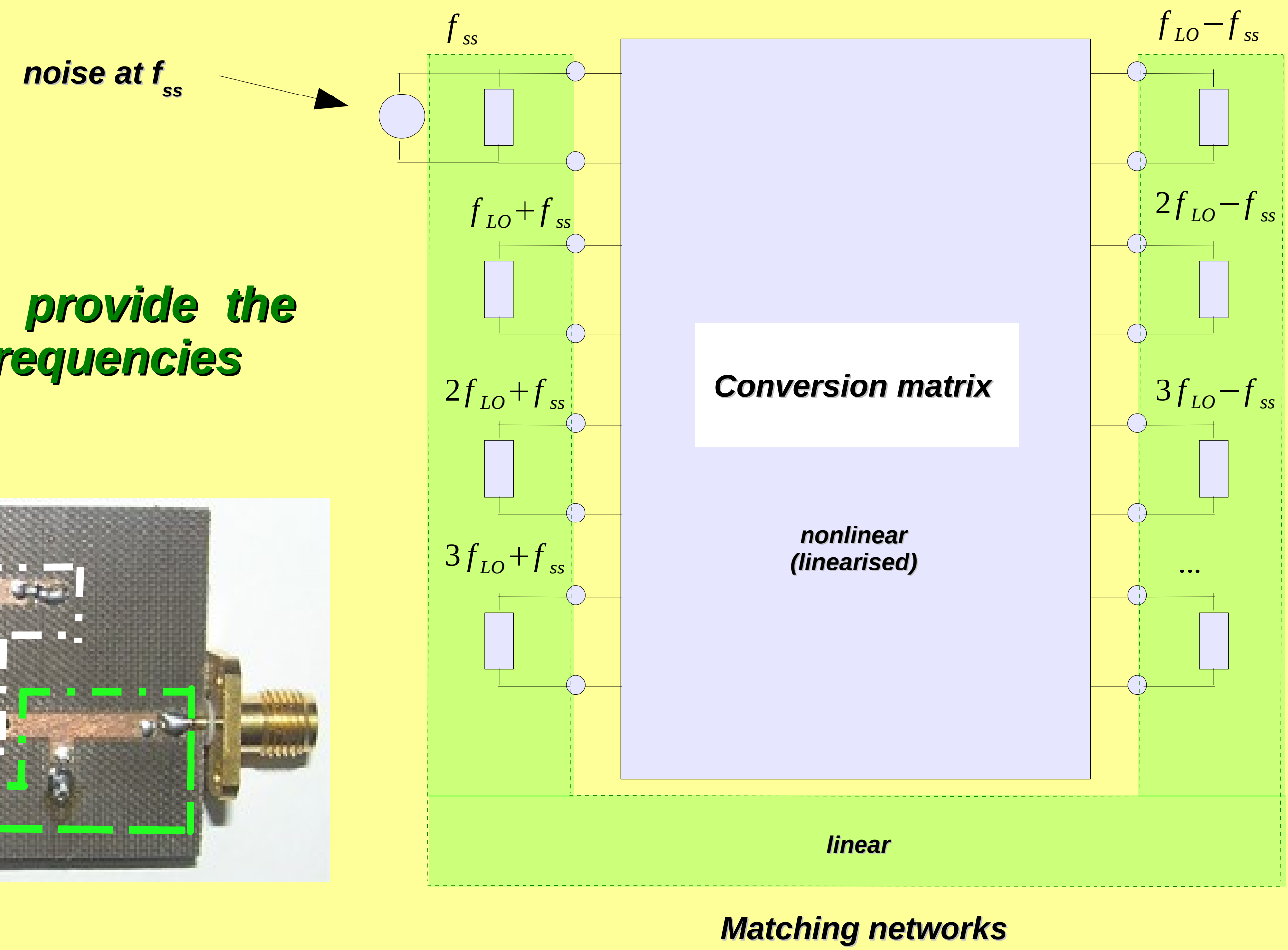

Stability (Rizzoli, 1985):

- Removal of the small-signal excitation

- Linear, homogeneous equations system

- Determinant of the system = 0 ?

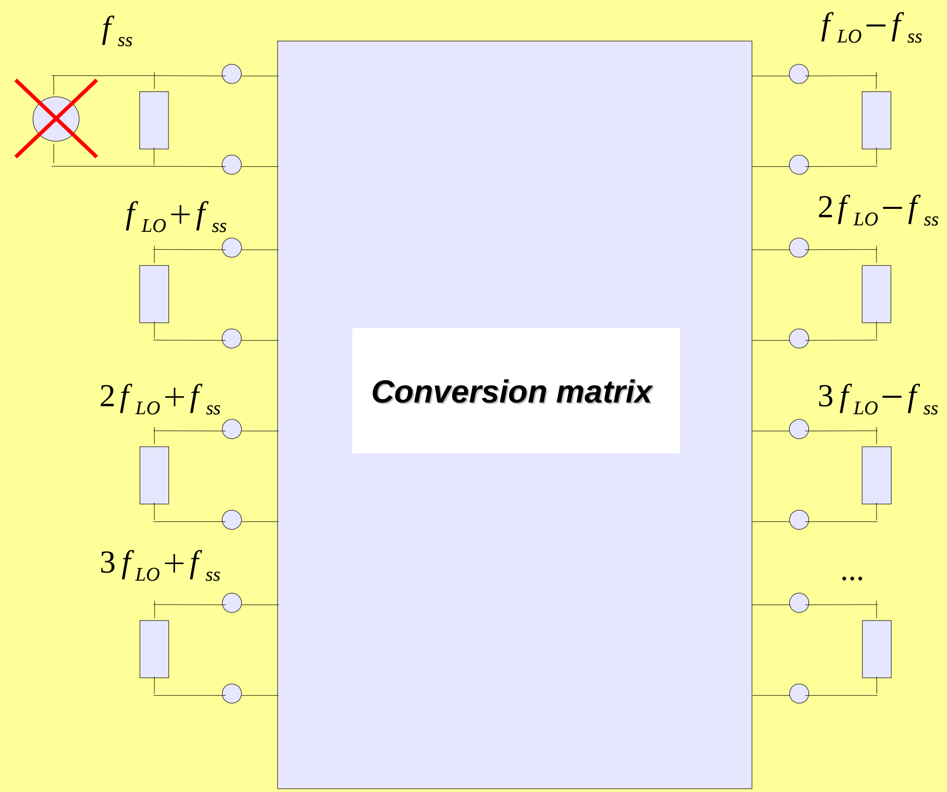

Non-trivial solution at small-signal frequency: oscillation -> instability

(provided that the Rollett proviso is fulfilled)

Stability (Rizzoli, 1985):

The determinant is a function of the small-signal frequency ω_{ss}

Onset of oscillation:

complex frequency $\sigma = \alpha_{ss} + j\,\omega_{ss}$

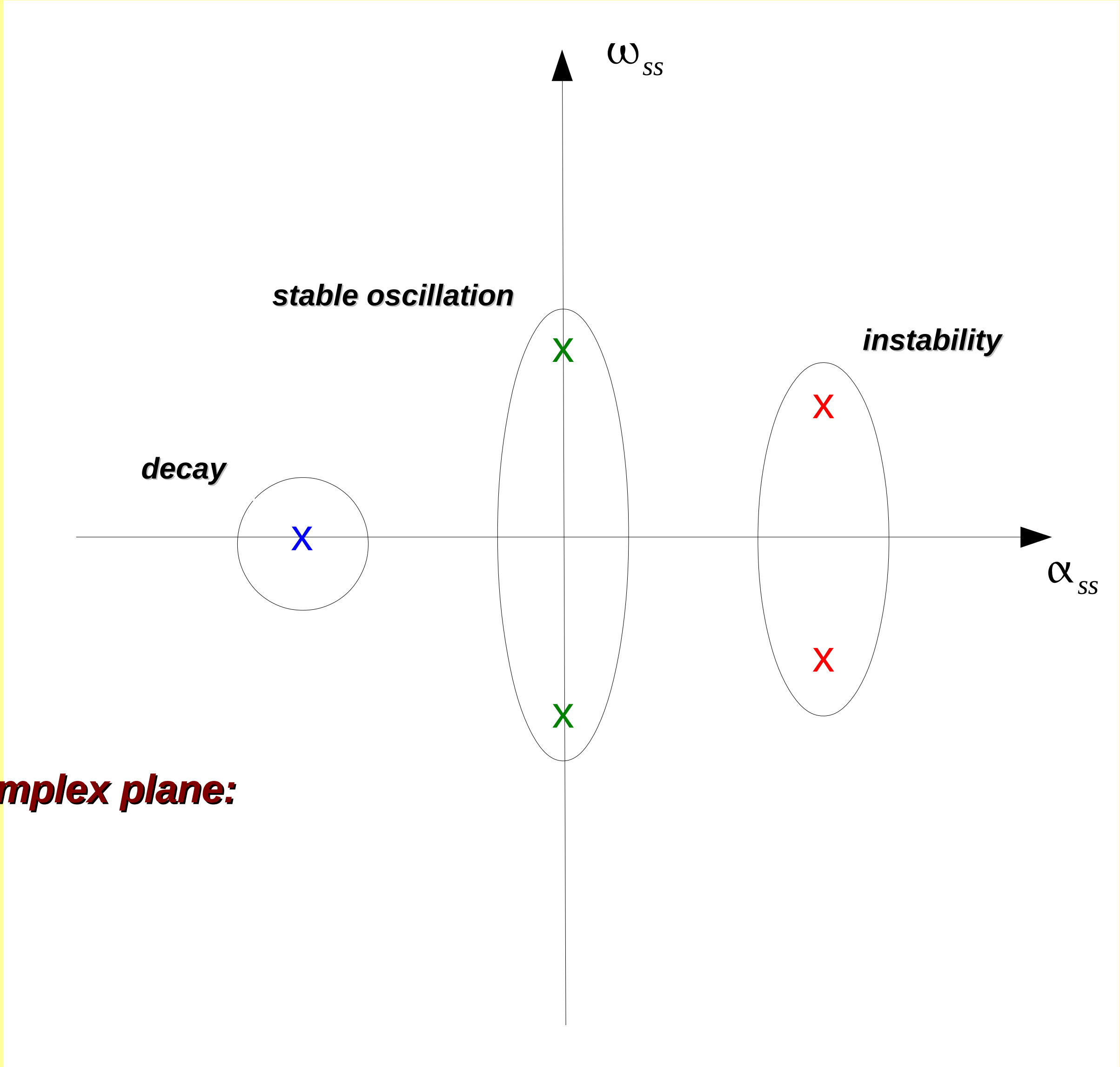

The zeros of the determinant in the complex plane:

Stability (Rizzoli, 1985):

Calculation of the determinant in theLaplace domain $\sigma = \alpha_{ss} + j\,\omega_{ss}$

Not possible with currently available CAD programs!

⇩

Calculation along the imaginary axis $\sigma = j\,\omega_{ss}$

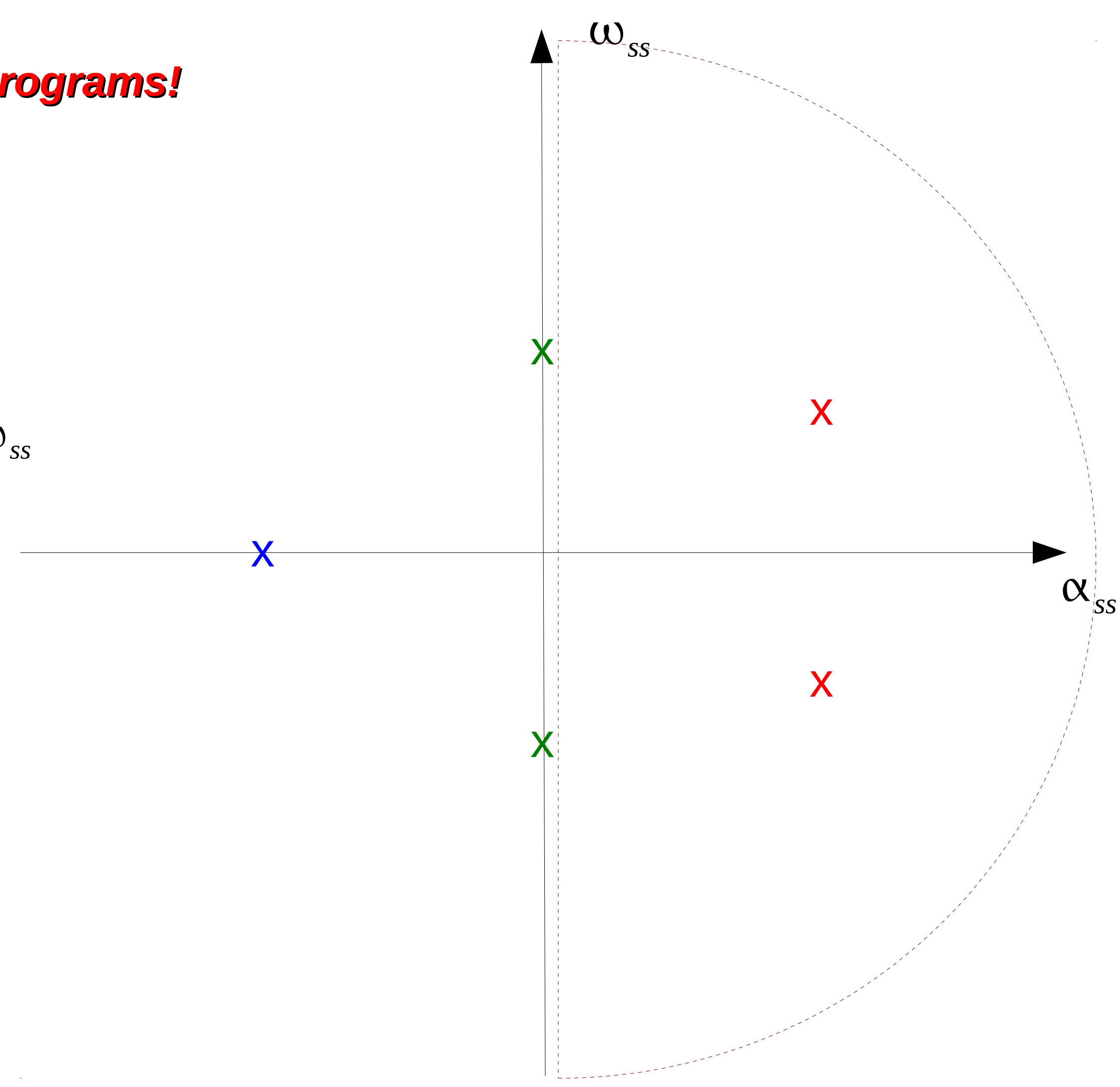

Encirclements of the origin
=
Zeros in the RHS half-plane

Stability (Rizzoli, 1985):

The conversion matrix is periodic as a function of frequency:

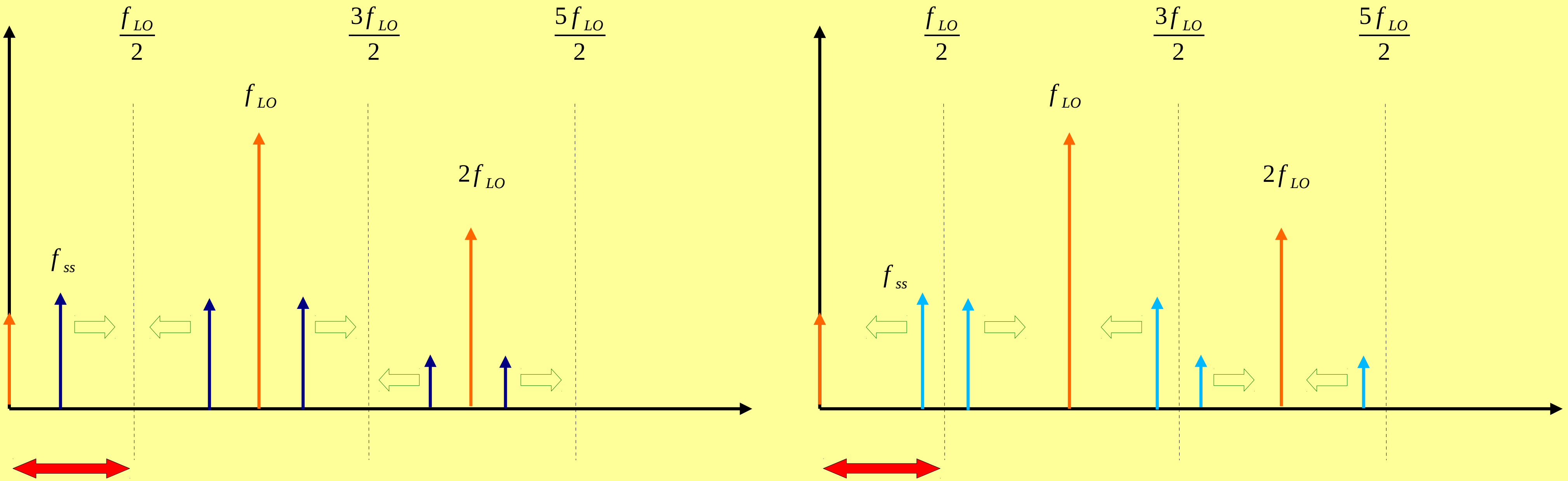

and symmetric with respect to $\frac{f_{LO}}{2}$ ⟹ **Calculation in the range:** $0 \div (\frac{f_{LO}}{2})$

Stability (Rizzoli, 1985):

Example – frequency divider (Rizzoli, 1985)

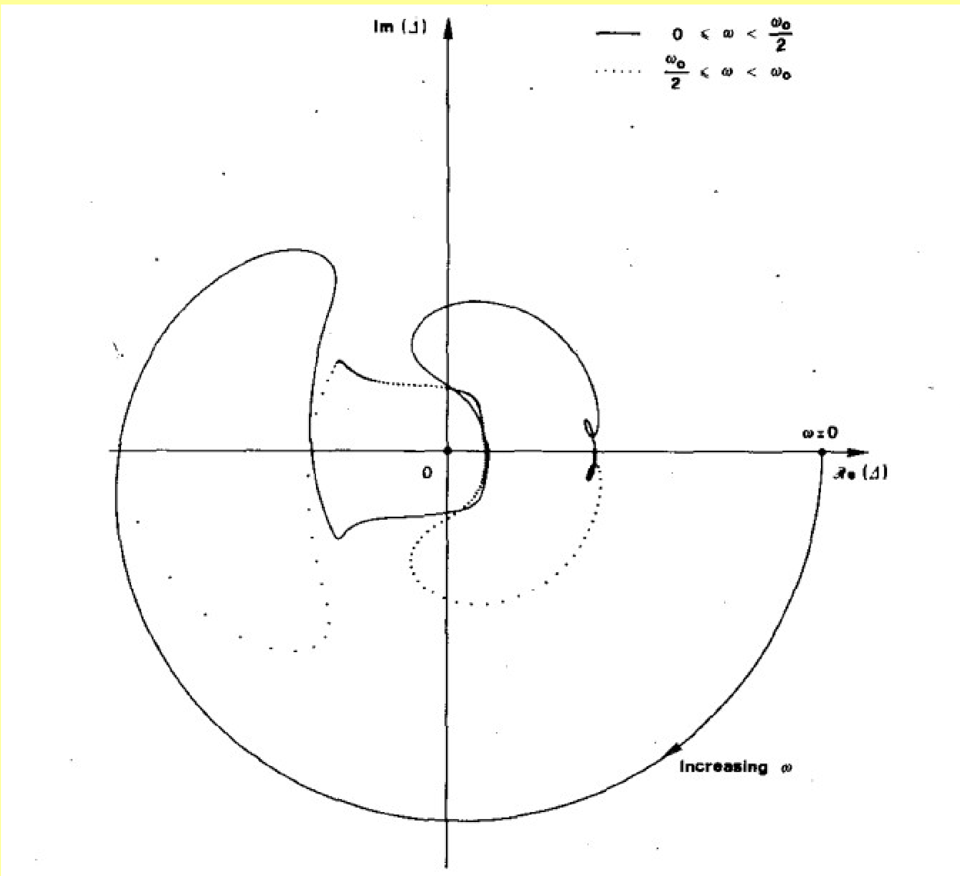

Fig. 5. Nyquist plot for a stable equilibrium condition of the frequency divider (nominal operating regime).

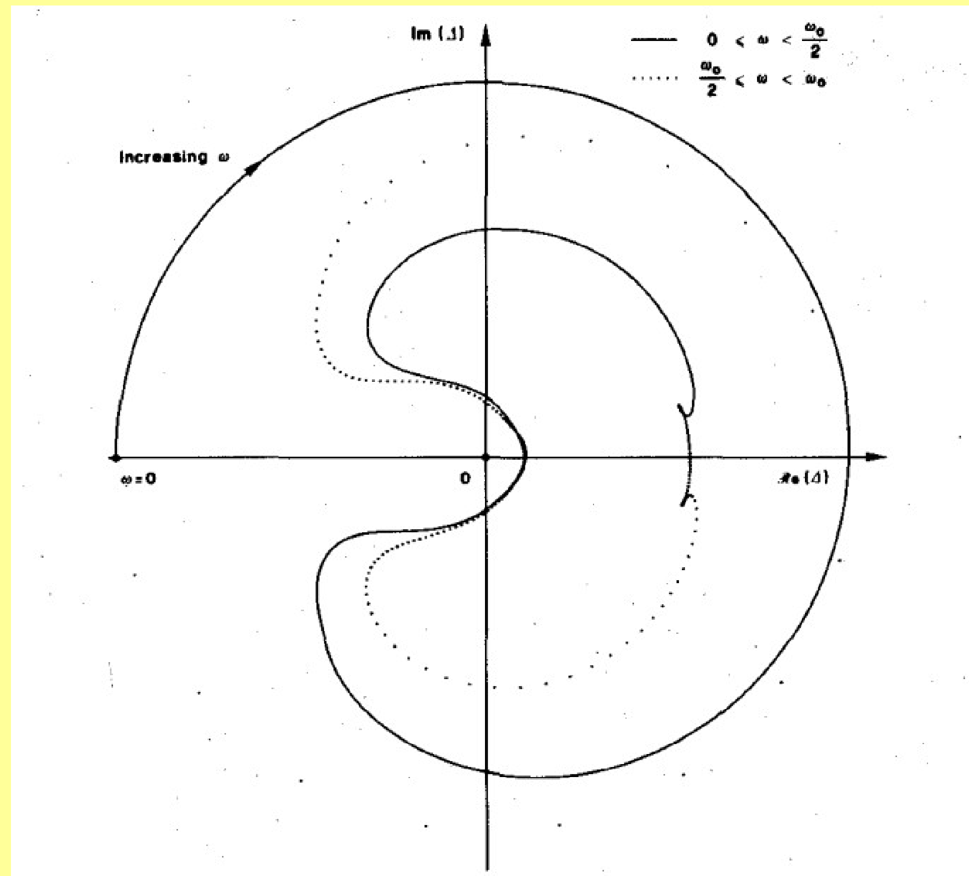

Fig. 6. Nyquist plot for an intrinsically unstable equilibrium condition of the frequency divider (hysteresis region).

Stability (Rizzoli, 1985):

Example – frequency divider (Leuzzi, Pantoli, 2009)

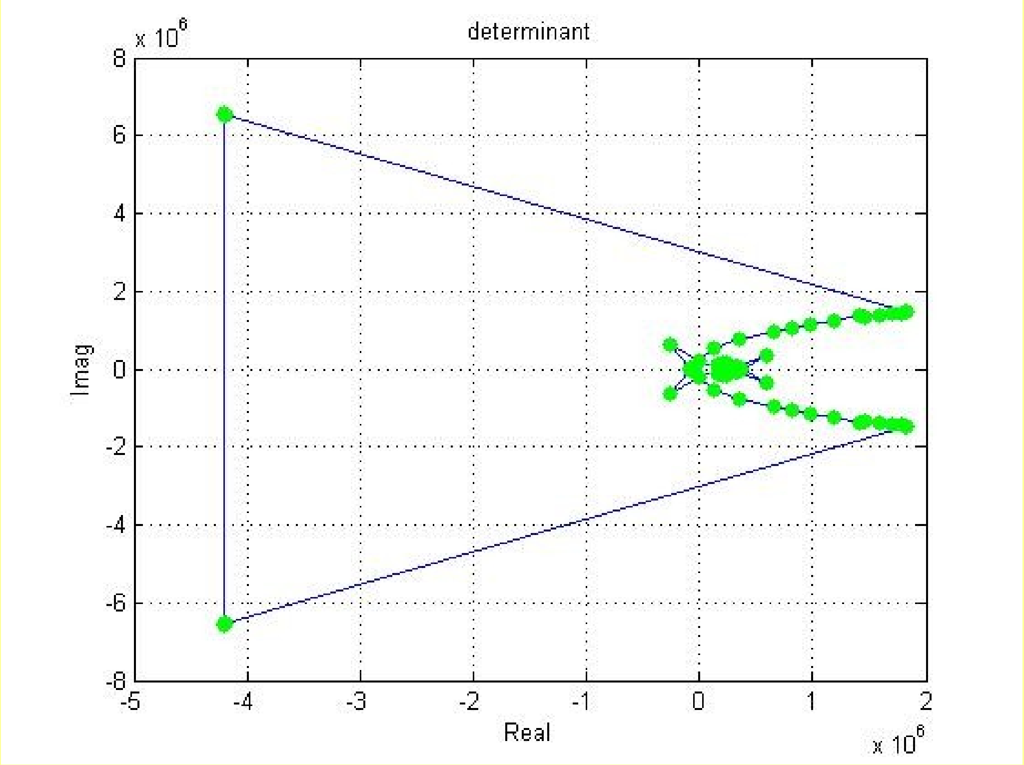

stable

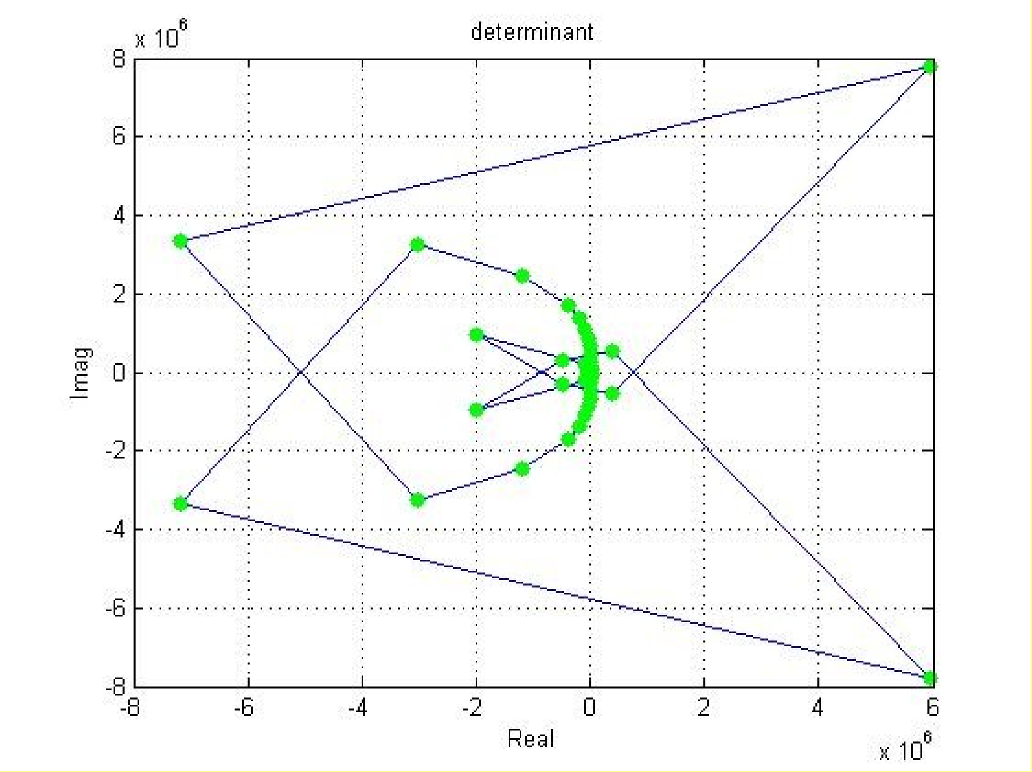

unstable

⇨ **Not practical: results are often confusing and unstable**

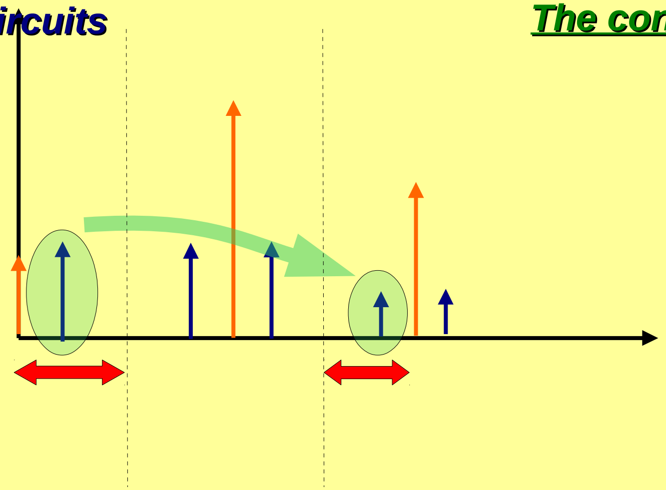

Stability (Collantes, 2001):

- Conversion gain between two ports
- Frequency sweep in the range $0 \div \left(\frac{f_{LO}}{2}\right)$
- Fit to a polynomial function of the frequency

$$CG(j\omega_{ss}) = \frac{k\cdot(\omega_{ss}-z_1)\cdot(\omega_{ss}-z_2)\cdot\ldots}{(\omega_{ss}-p_1)\cdot(\omega_{ss}-p_2)\cdot\ldots}$$

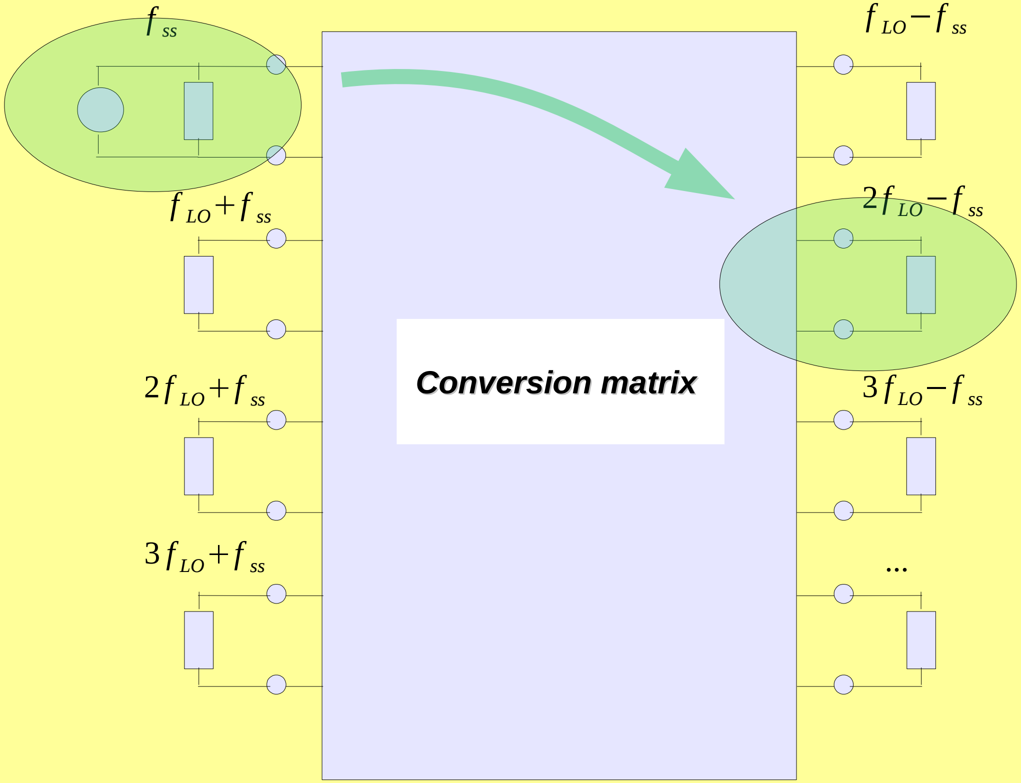

⇒ Identification of the (complex) poles of the conversion gain function

Stability (Collantes, 2001):

Poles position may change with input power

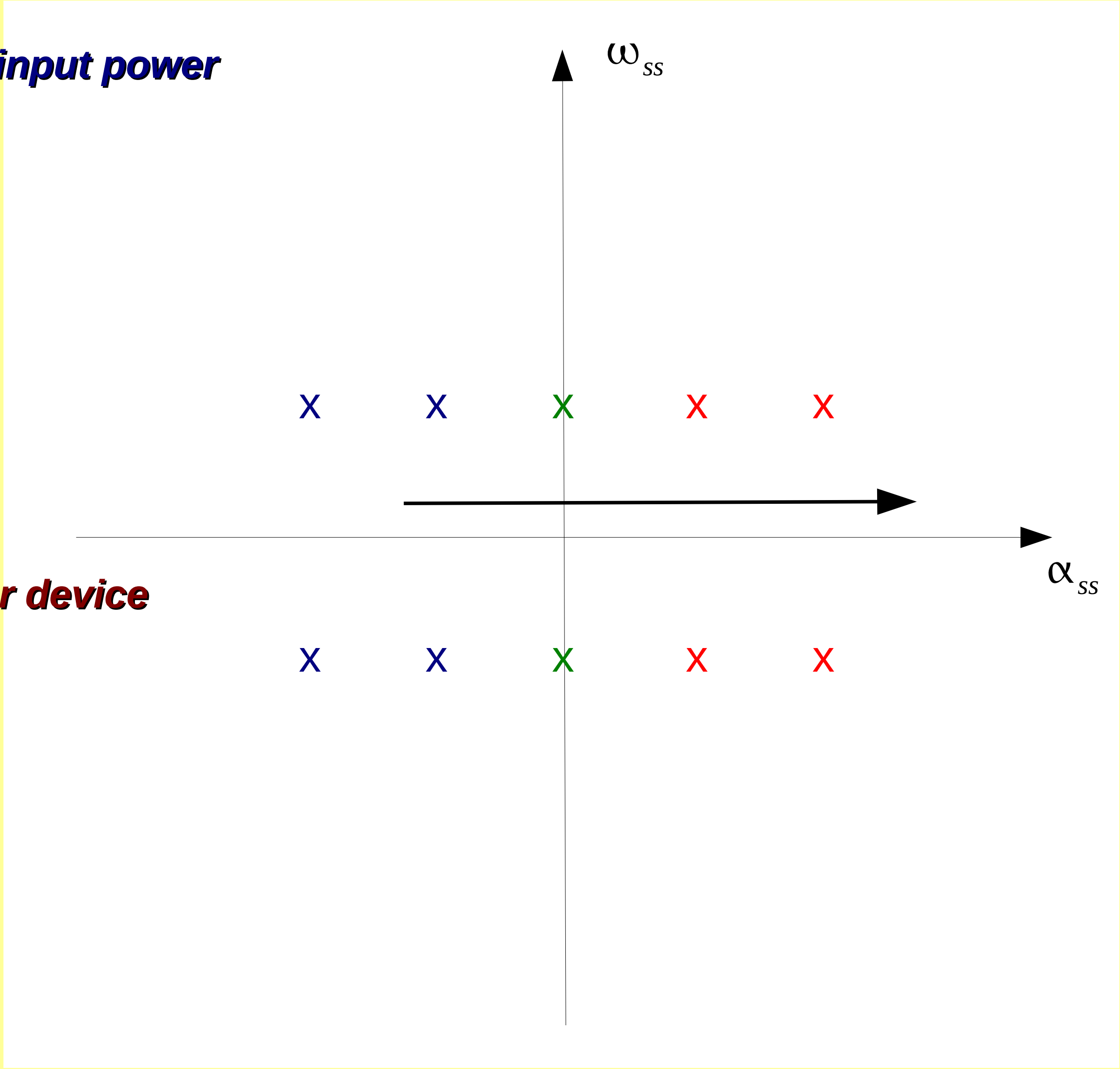

Increasing input power

⇩

Increasing conversion gain of the nonlinear device

⇩

Increasing potential instability

Stability (Collantes, 2001):

Poles position may be moved by redesign of the circuit:

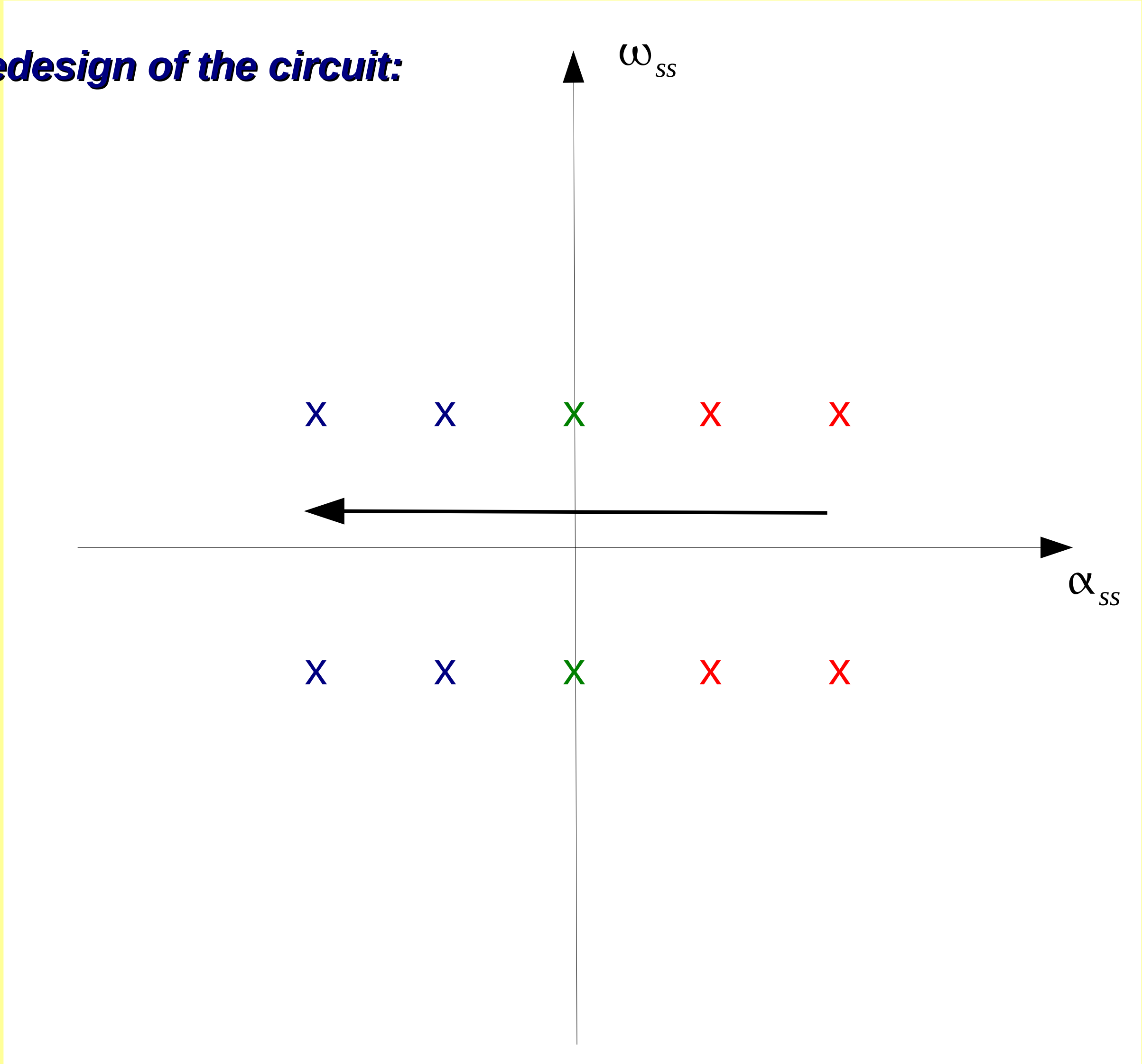

- Component values can be optimised

- No explicit design condition

Stability (Collantes, 2001):

Example – Pin-diode limiter (Gatard, 2006; Pantoli, 2009)

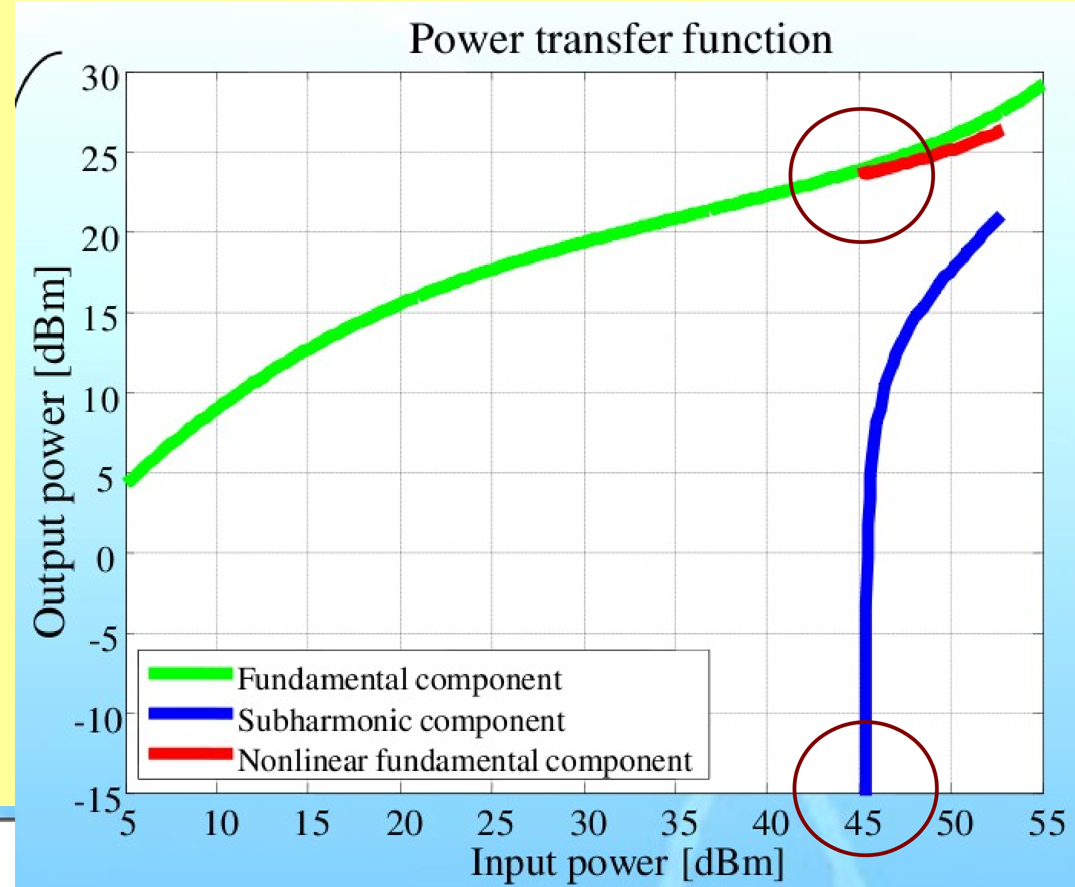

Poles cross the y-axis when a spurious subharmonic signal appears

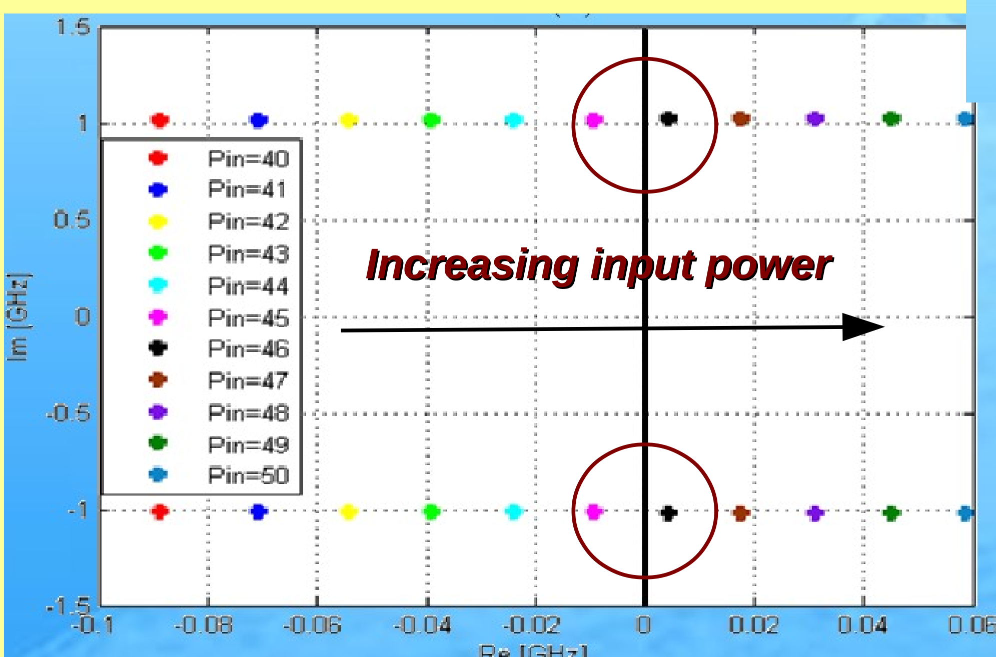

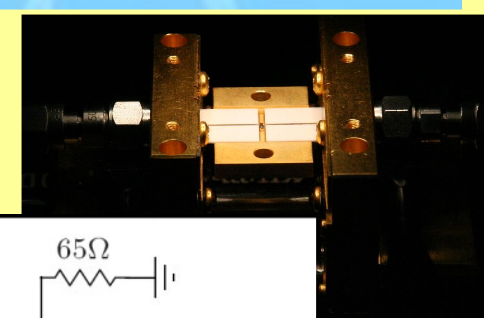

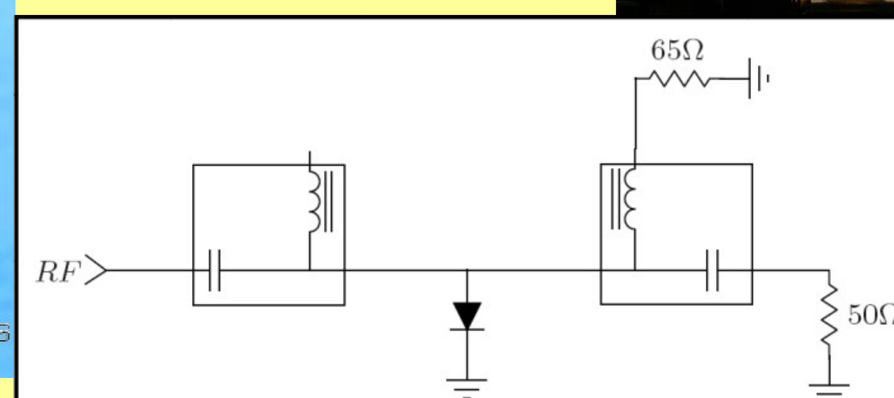

Stability (Collantes, 2001):

Example – Pin-diode limiter (Gatard, 2006; Pantoli, 2009)

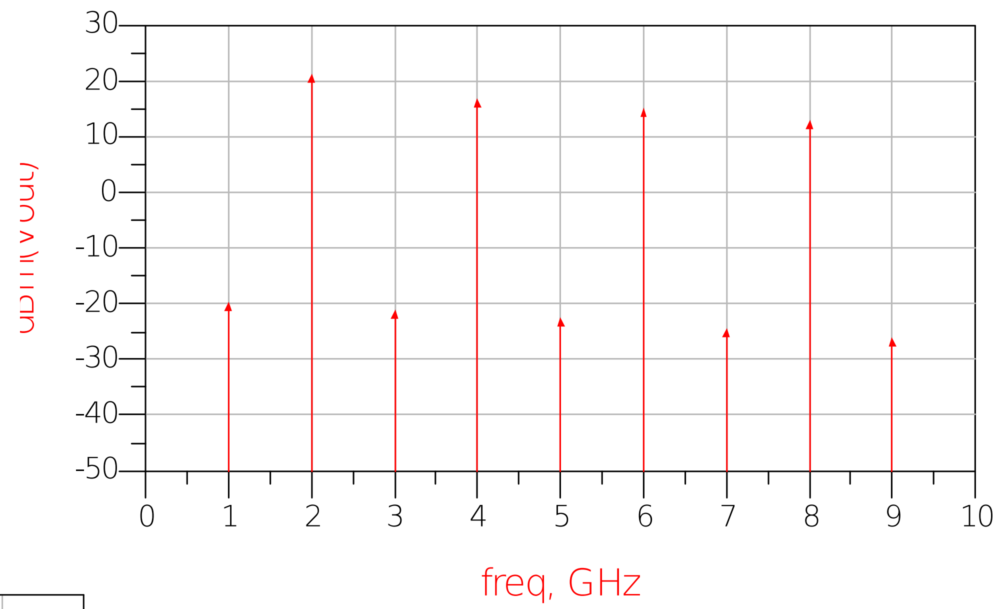

Harmonic balance with auxiliary generator

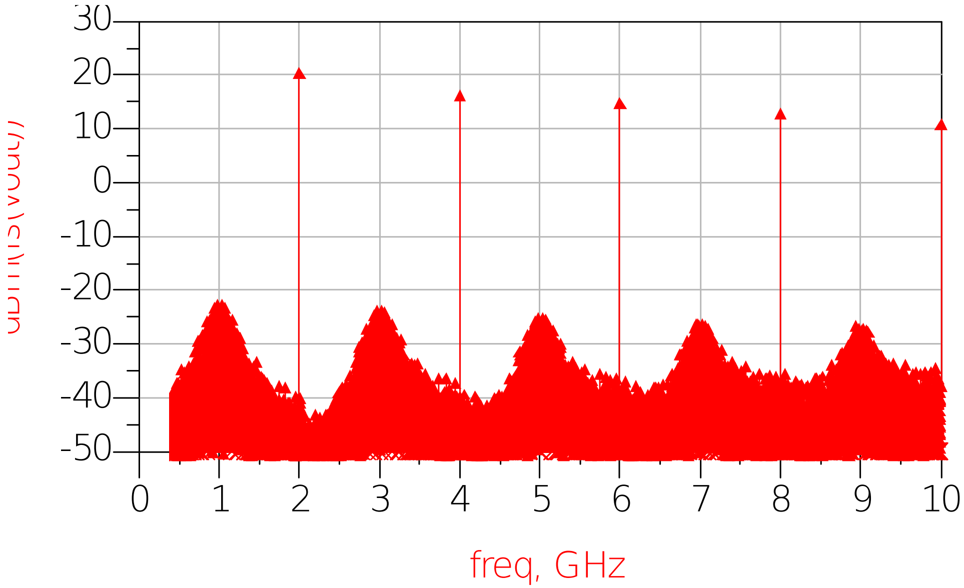

Time-domain analysis

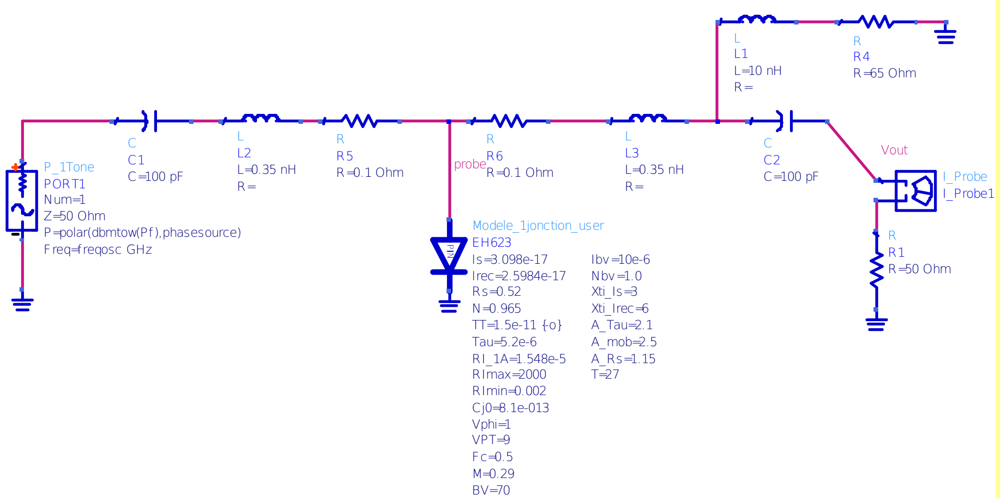

Stability (Di Paolo, 2002):

- Removal of the small-signal excitation

- Reduction to a one-port or two-port network

- Linear stability design

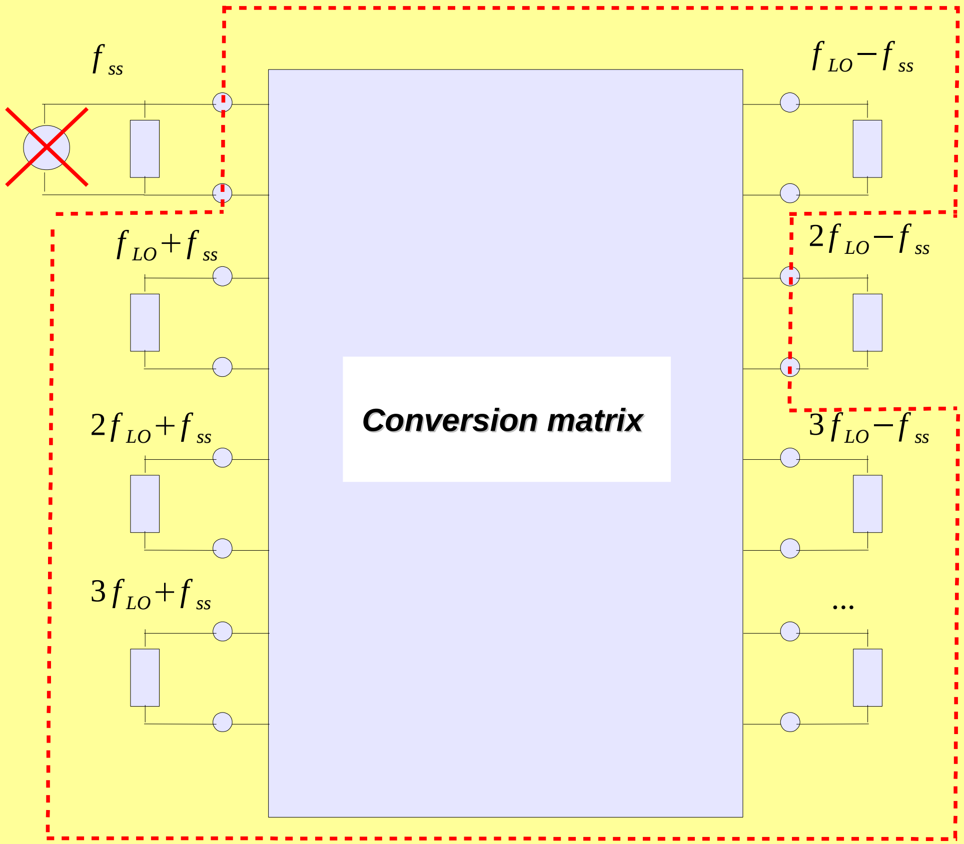

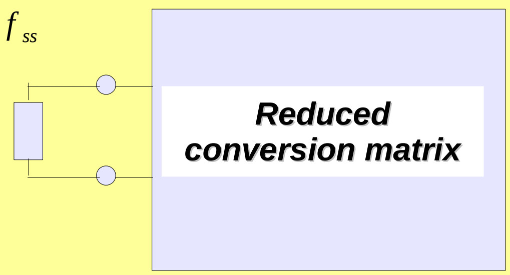

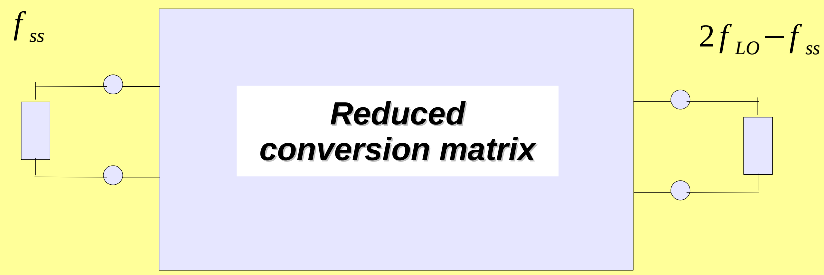

Stability (Di Paolo, 2002):

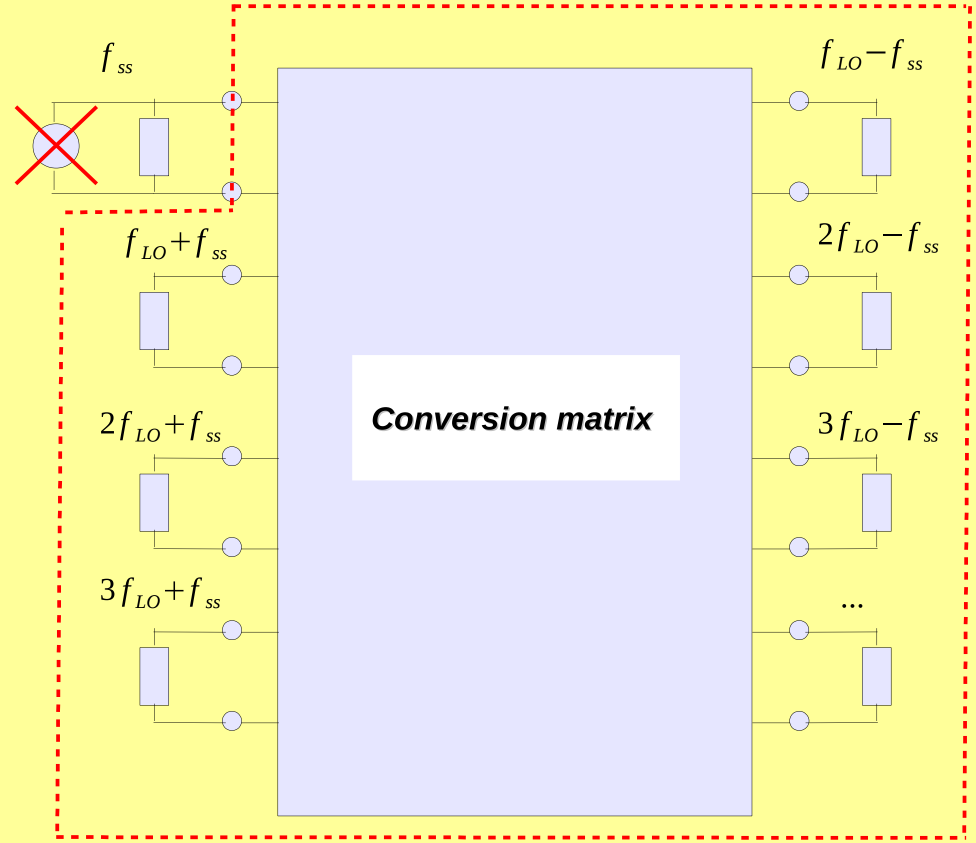

Linear stability design (one port):

Stability $|\Gamma_i(\omega_{ss})|<1$

Potential instability $|\Gamma_i(\omega_{ss})|>1$

Oscillation $\Gamma_L(\omega_{ss})\cdot\Gamma_i(\omega_{ss})=1$

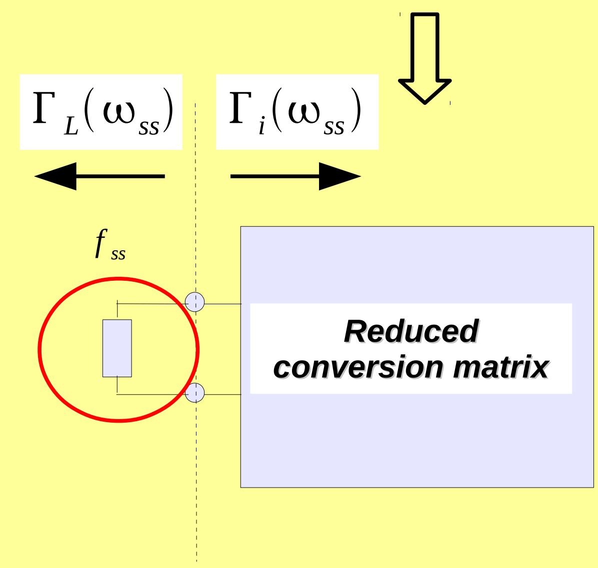

Redesign of $\Gamma_L(\omega_{ss})$ **for stability**

Stability (Di Paolo, 2002):

Redesign of the linear networks:

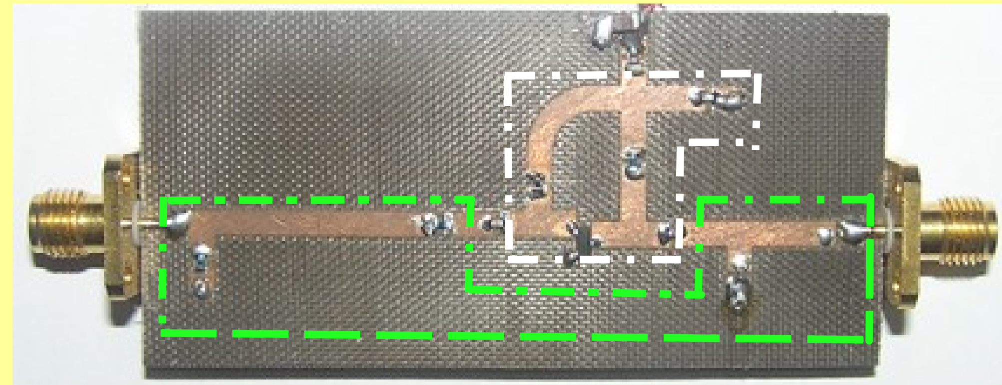

Impedance adjustment at converted frequencies

$Z_L(nf_{LO} \pm f_s)$

No impedance change at large-signal fundamental and harmonic frequencies

$Z_L(nf_{LO})$

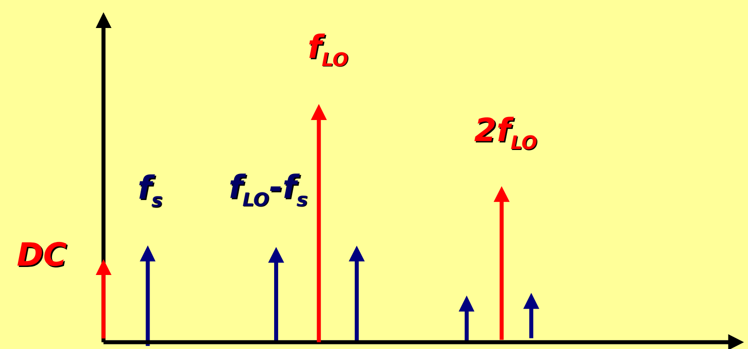

Otherwise the conversion matrix must be recomputed, and the large-signal performances change

Special case: $f_{ss} = \frac{f_0}{2}$

$a(\frac{\omega_O}{2})$

$b(\frac{\omega_O}{2})$

$\Gamma_i(\frac{\omega_O}{2})$

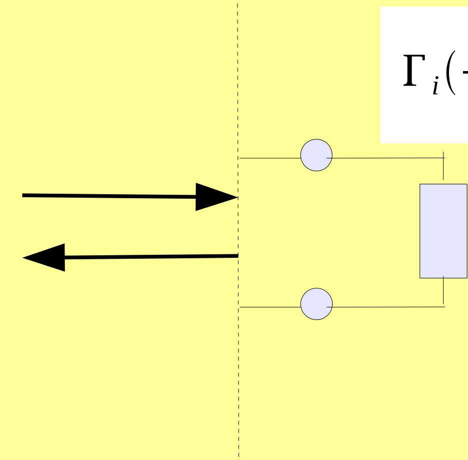

The conversion matrix assumes a different formalism

$$\begin{bmatrix} b_r \\ b_i \end{bmatrix} = \begin{bmatrix} \Gamma_{11} & \Gamma_{12} \\ \Gamma_{21} & \Gamma_{22} \end{bmatrix} \cdot \begin{bmatrix} a_r \\ a_i \end{bmatrix}$$

$$a = a_r + j a_i$$

$$b = b_r + j b_i$$

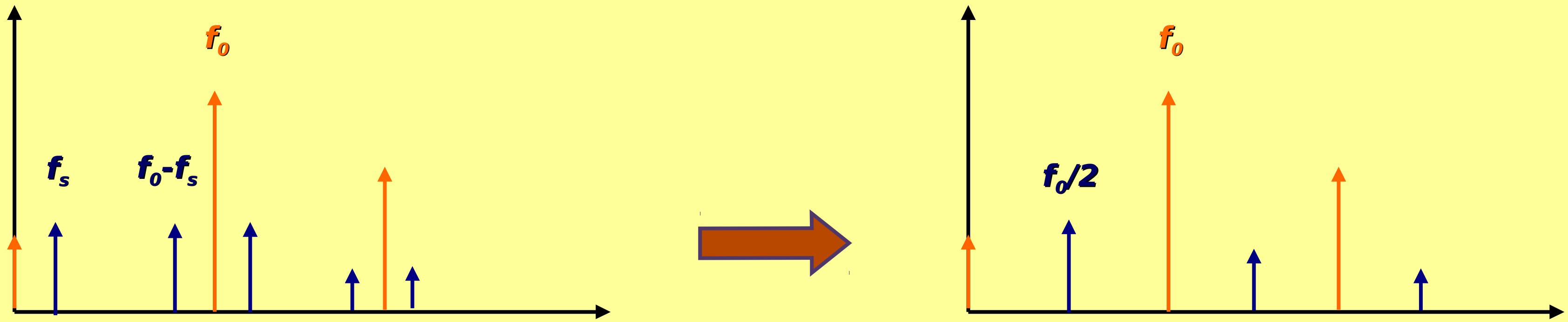

Special case:

$$f_{ss} = \frac{f_0}{2}$$

The reflection coefficient depends on the phase of the incident wave

$$\Gamma_i\left(\frac{\omega_O}{2}\right)$$

$$a\left(\frac{\omega_O}{2}\right)$$

$$b\left(\frac{\omega_O}{2}\right)$$

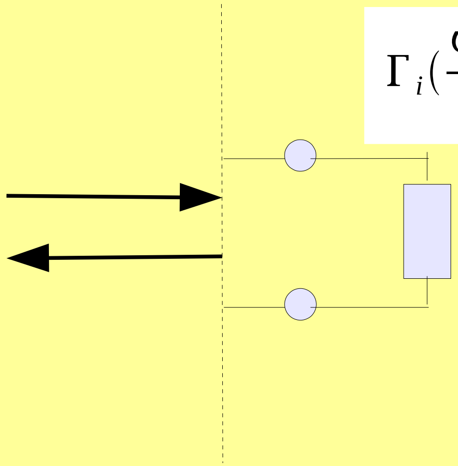

$$\begin{bmatrix} b_r \\ b_i \end{bmatrix} = \begin{bmatrix} \Gamma_{11} & \Gamma_{12} \\ \Gamma_{21} & \Gamma_{22} \end{bmatrix} \cdot \begin{bmatrix} a_r \\ a_i \end{bmatrix}$$

$$a = a_r + j\,a_i$$

$$b = b_r + j\,b_i$$

|b| < |a|

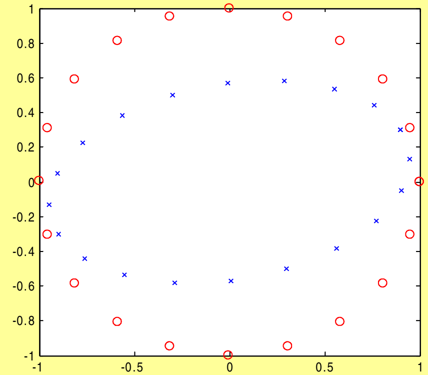

|b| > |a|

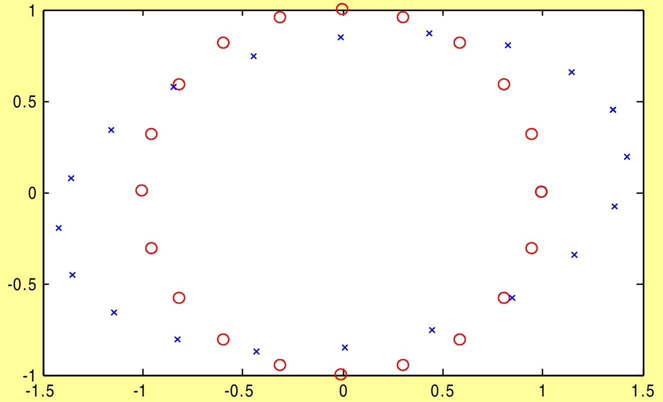

The phase reference is the phase of the large signal at f_0

(Measurements by D.Schreurs)

Special case: $f_{ss} = \frac{f_0}{2}$

The oscillation condition becomes:

$$\Gamma_S = \frac{1}{\Gamma_i}$$

$$det\left(\begin{bmatrix} \Gamma_{S,r} & -\Gamma_{S,i} \\ \Gamma_{S,i} & \Gamma_{S,r} \end{bmatrix} + \begin{bmatrix} \Gamma_{in11} & \Gamma_{in12} \\ \Gamma_{in21} & \Gamma_{in22} \end{bmatrix}\right) = 0$$

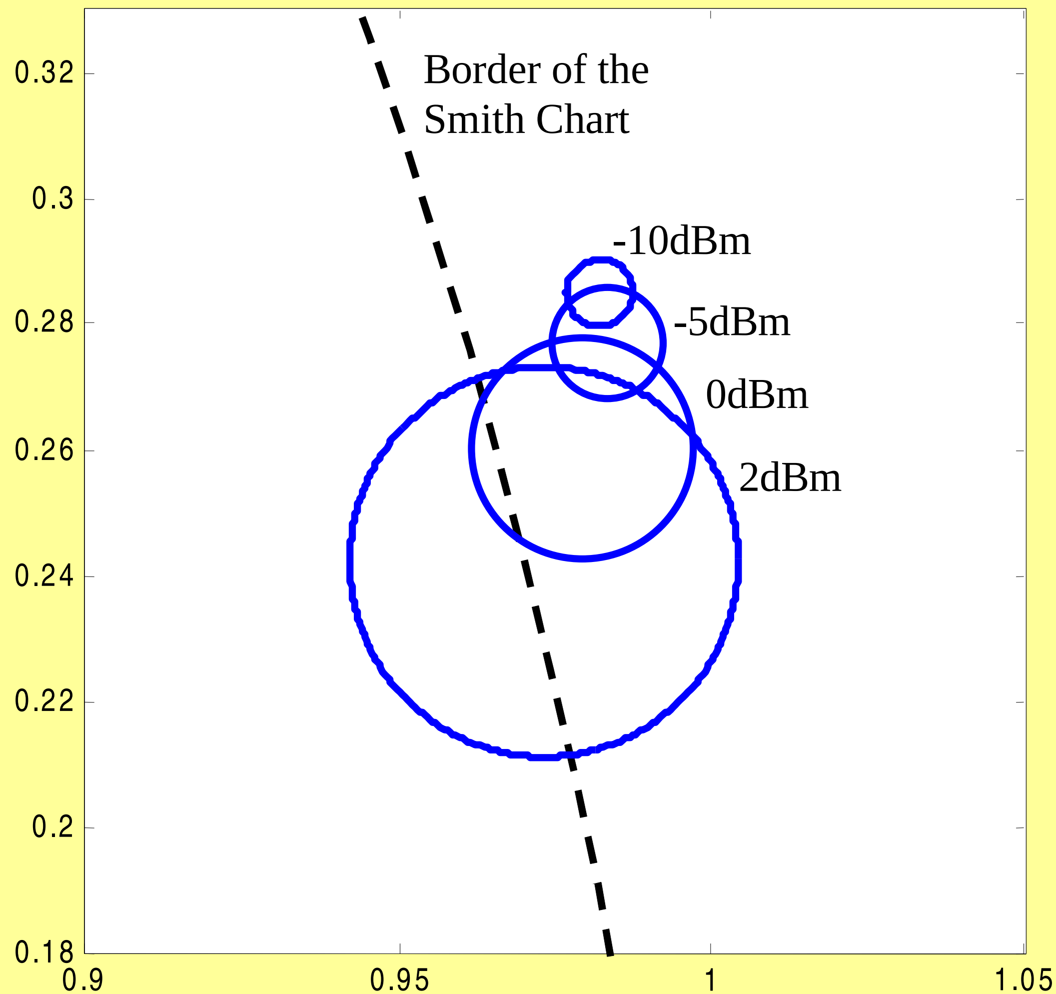

The loads giving oscillation form a circle

Applications: medium-power amplifier

First design: stable amplifier

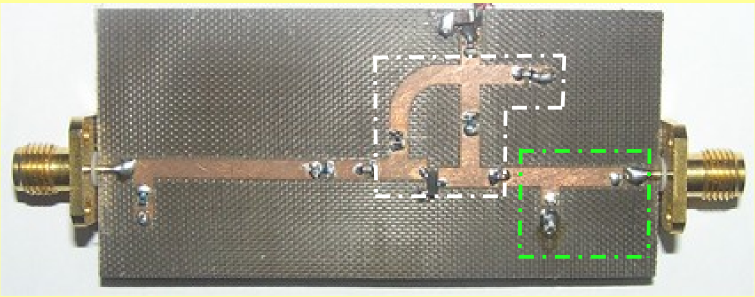

Second design: modified, unstable amplifier

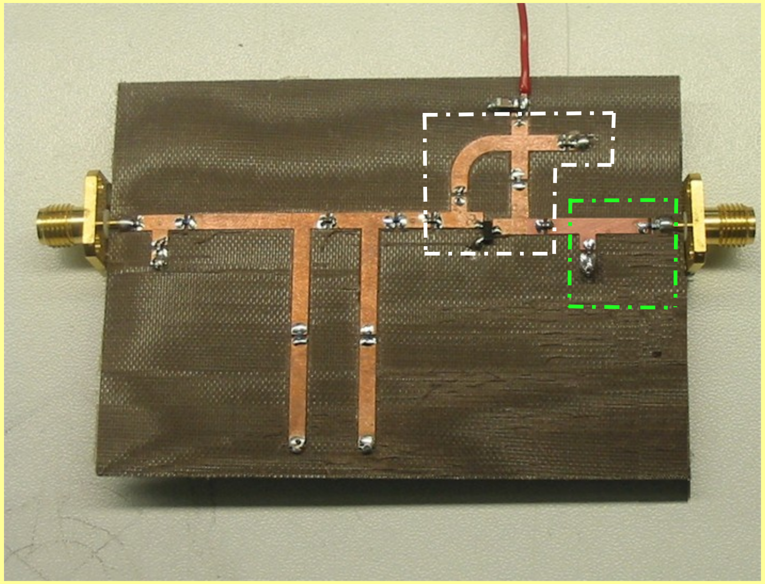

- Same biased transistor
- Same output matching network
- Modified input matching network

Applications: medium-power amplifier

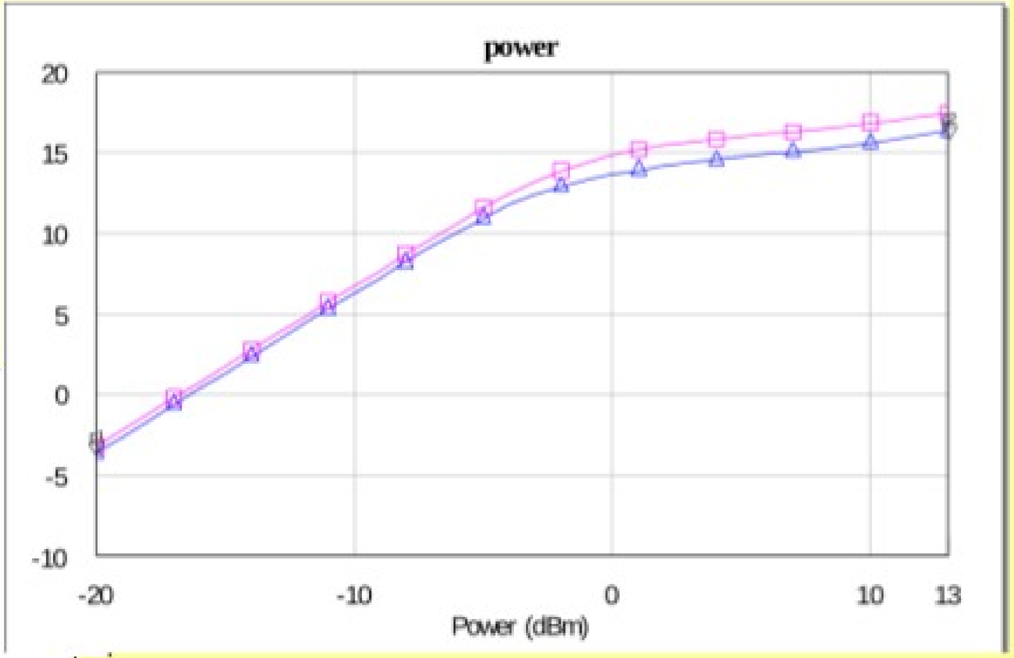

Harmonic balance simulations

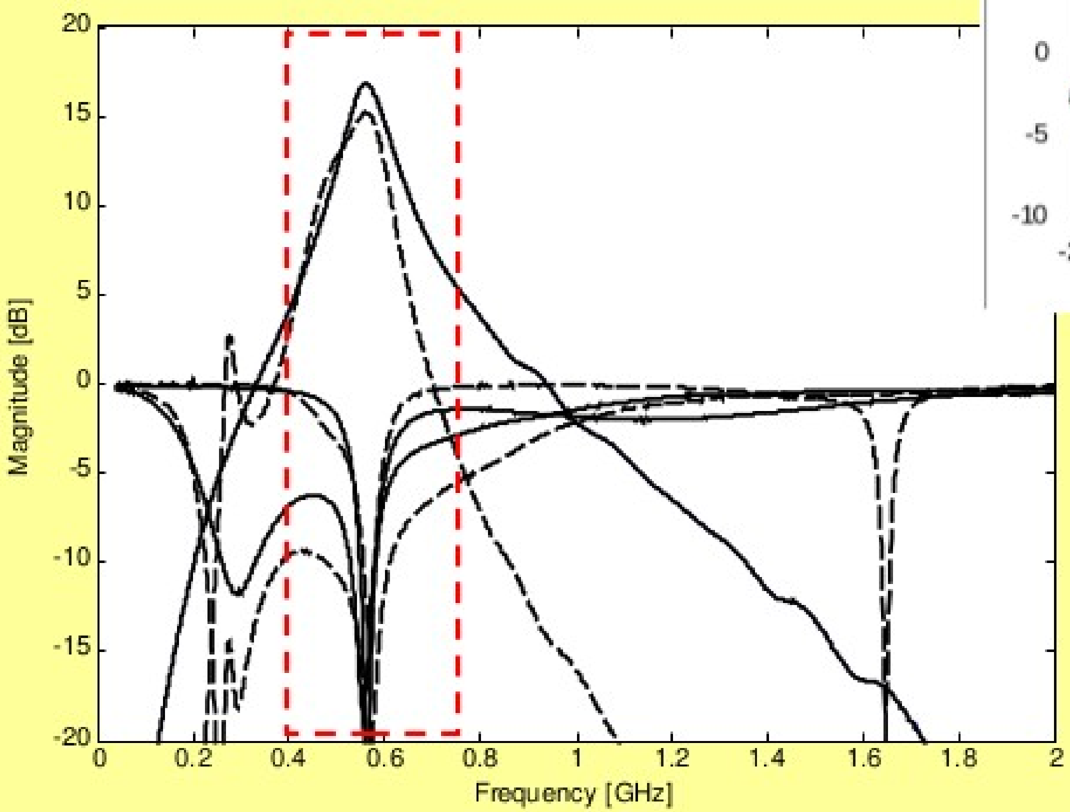

Measured S-parameters

The stable amplifier

Output power

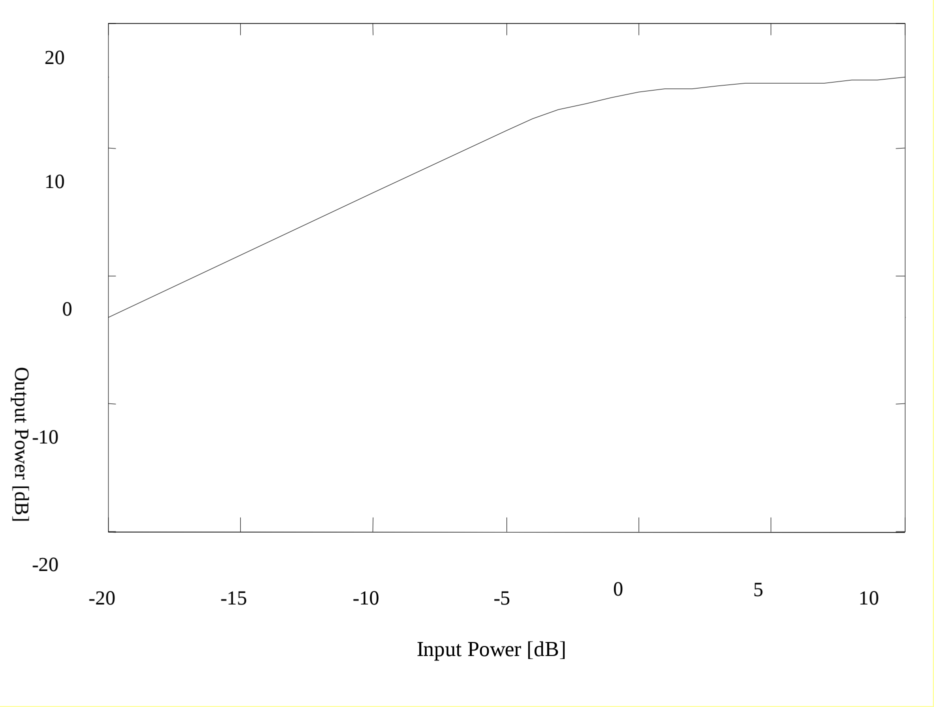

Output power spectrum

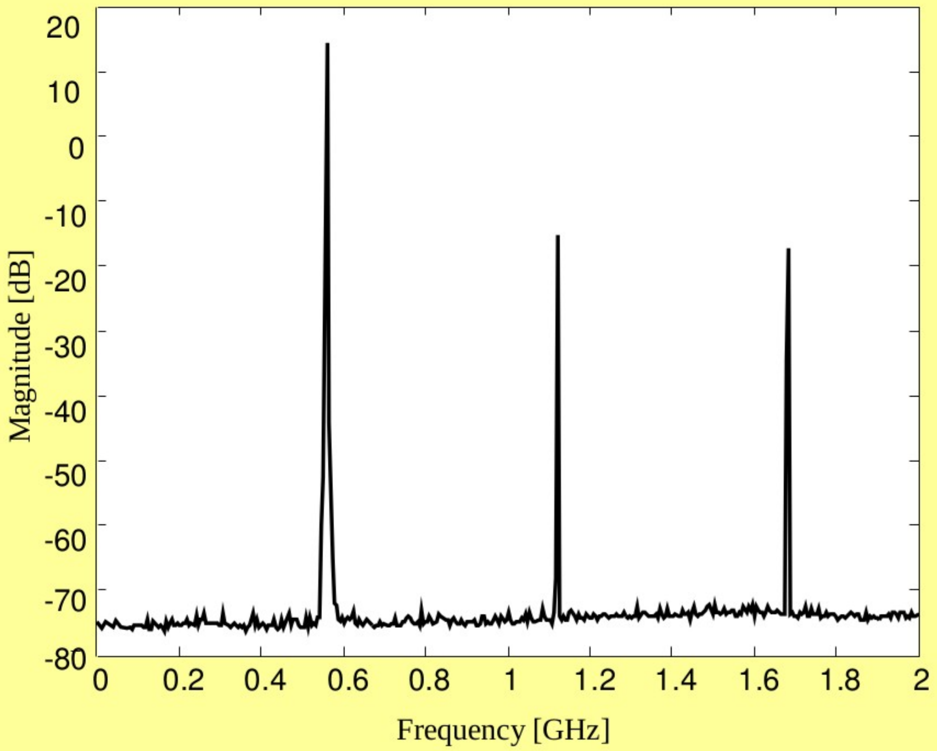

Stability check of the amplifier

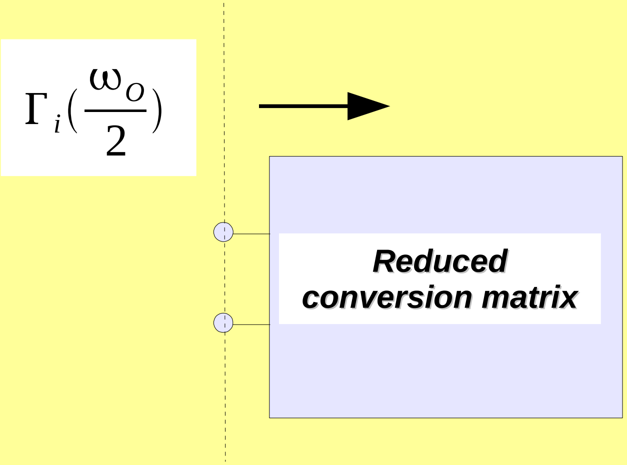

Conversion matrix

↓

Reflection coefficient at $f_0/2$

↓

Potential instability

Stable amplifier

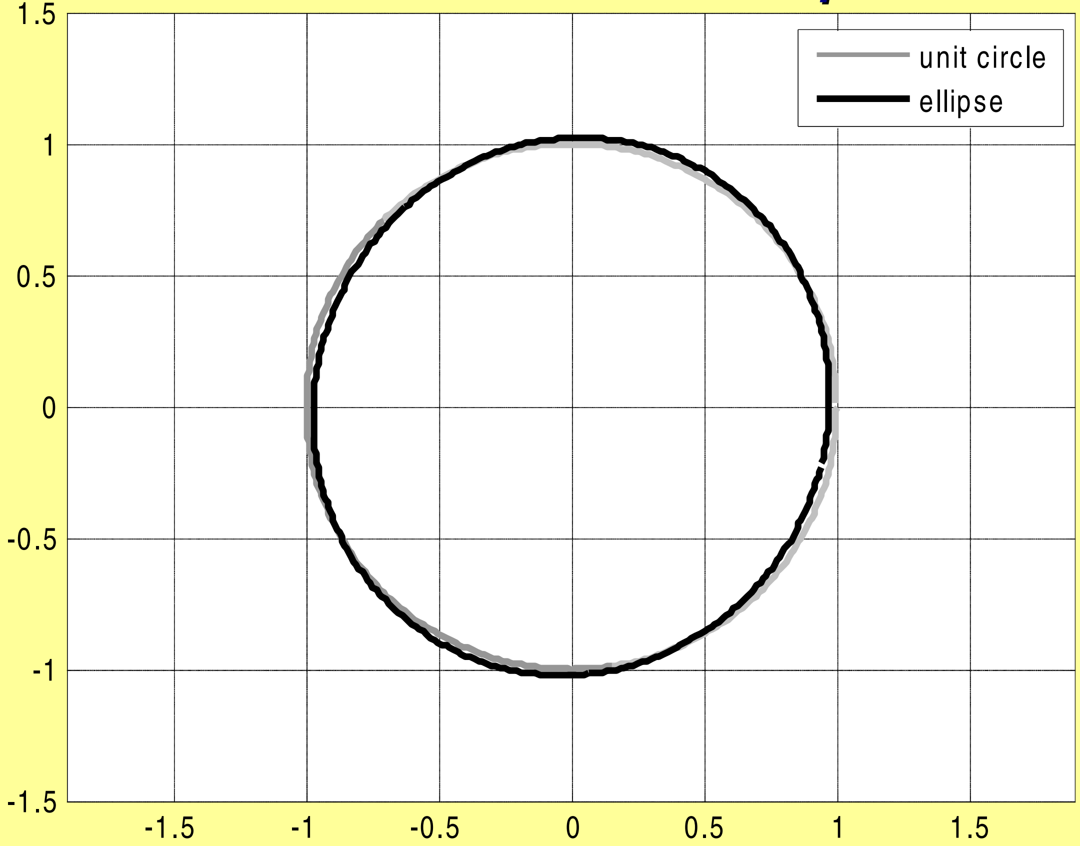

Redesign of the amplifier for instability at $f_{ss} = \frac{f_0}{2}$

Unstable region at $f_0/2$ at input

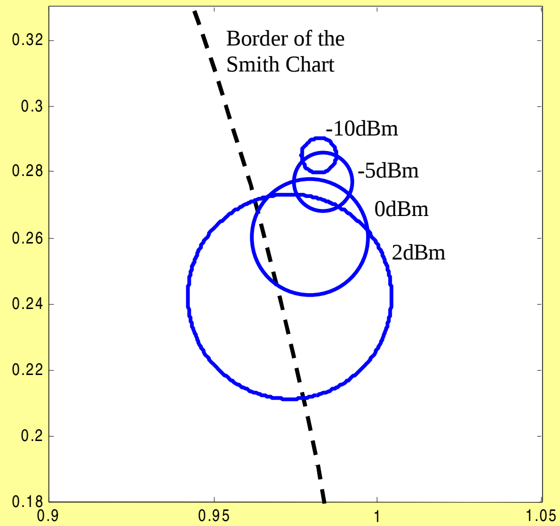

Modified loads at fractional frequencies

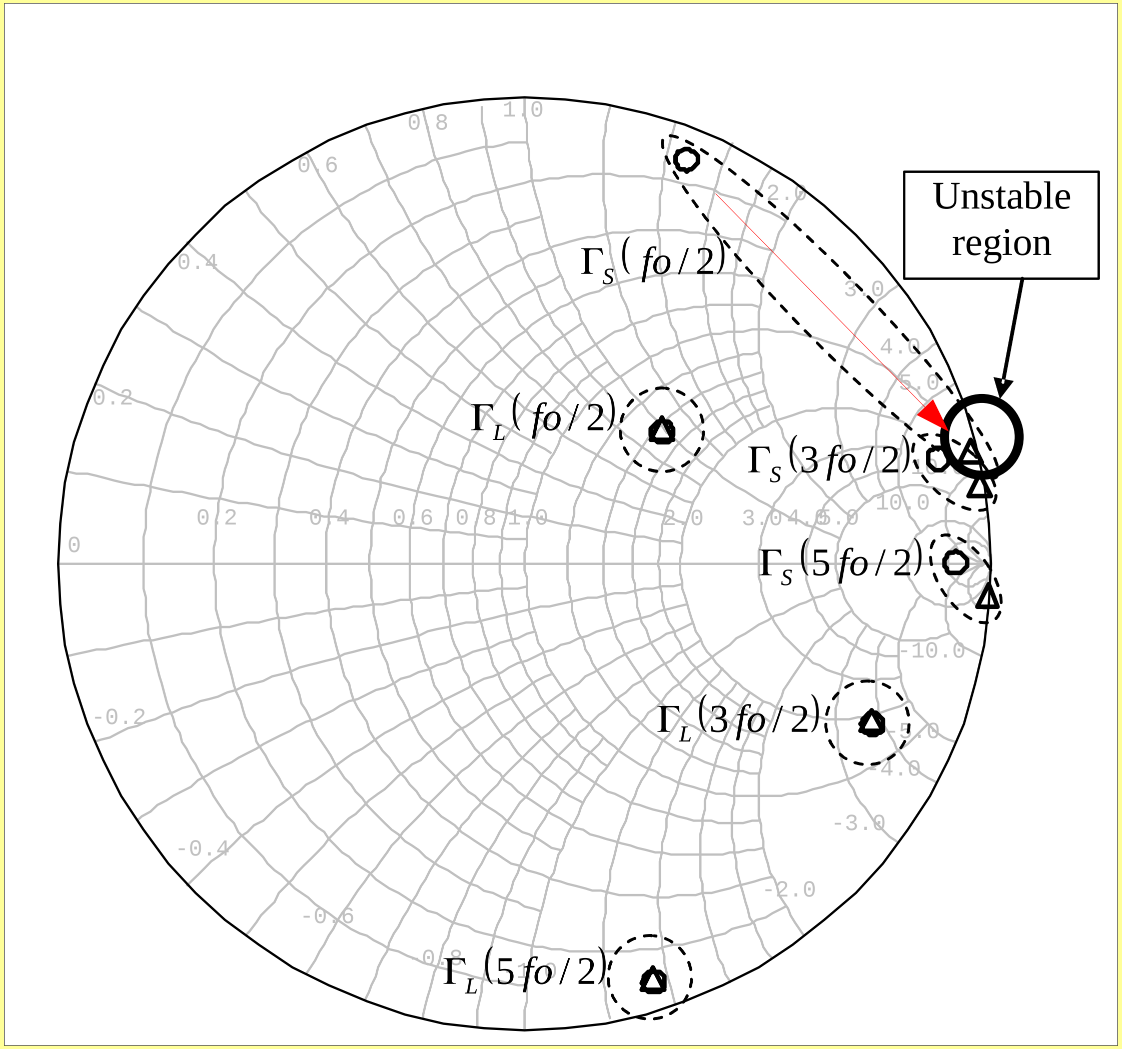

Only one load at input has been changed

The output matching network is unchanged

Redesign of the amplifier for instability at $f_{ss} = \frac{f_0}{2}$

Loads at fundamental frequency and harmonics are unchanged

The conversion matrix remains the same

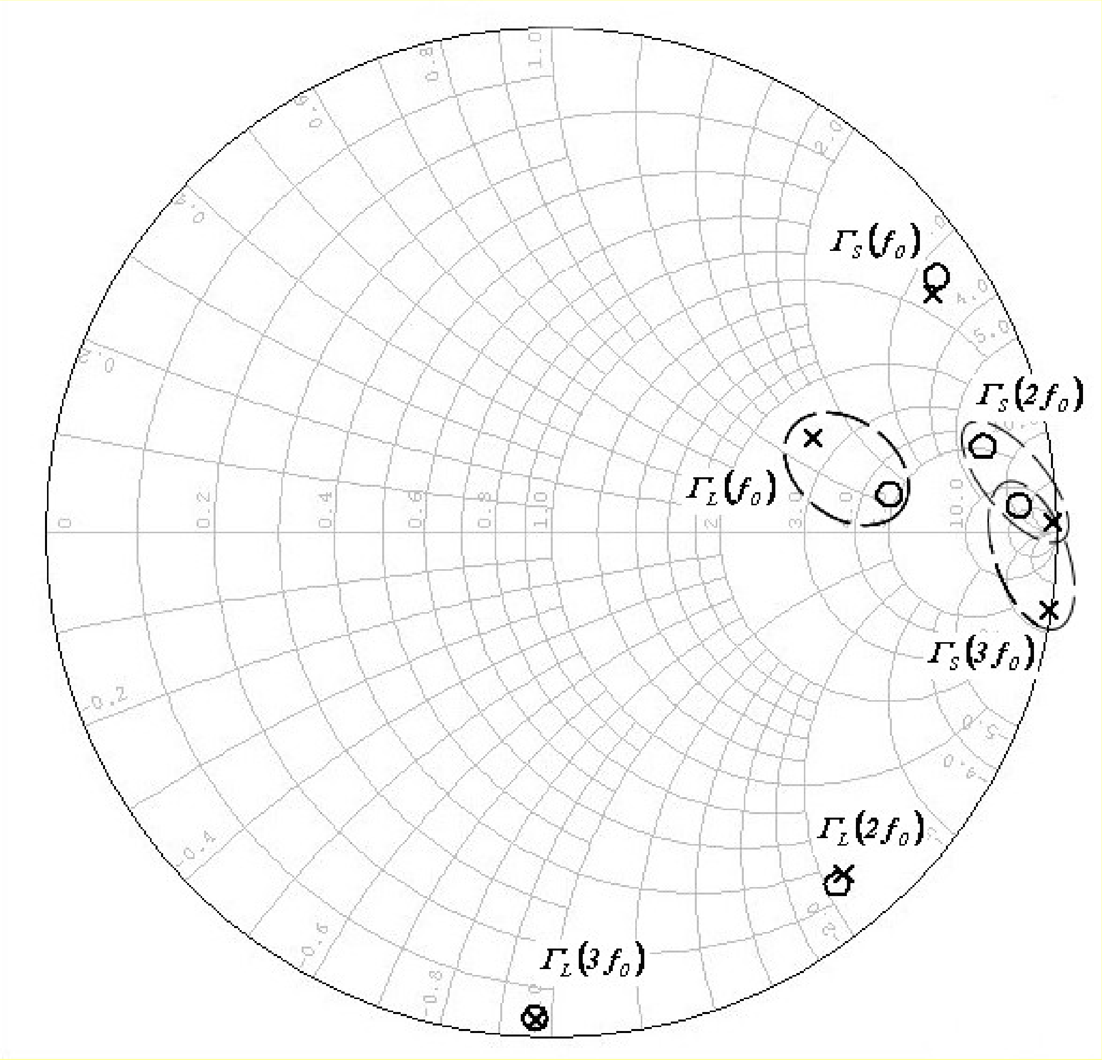

Redesigned amplifier - unstable

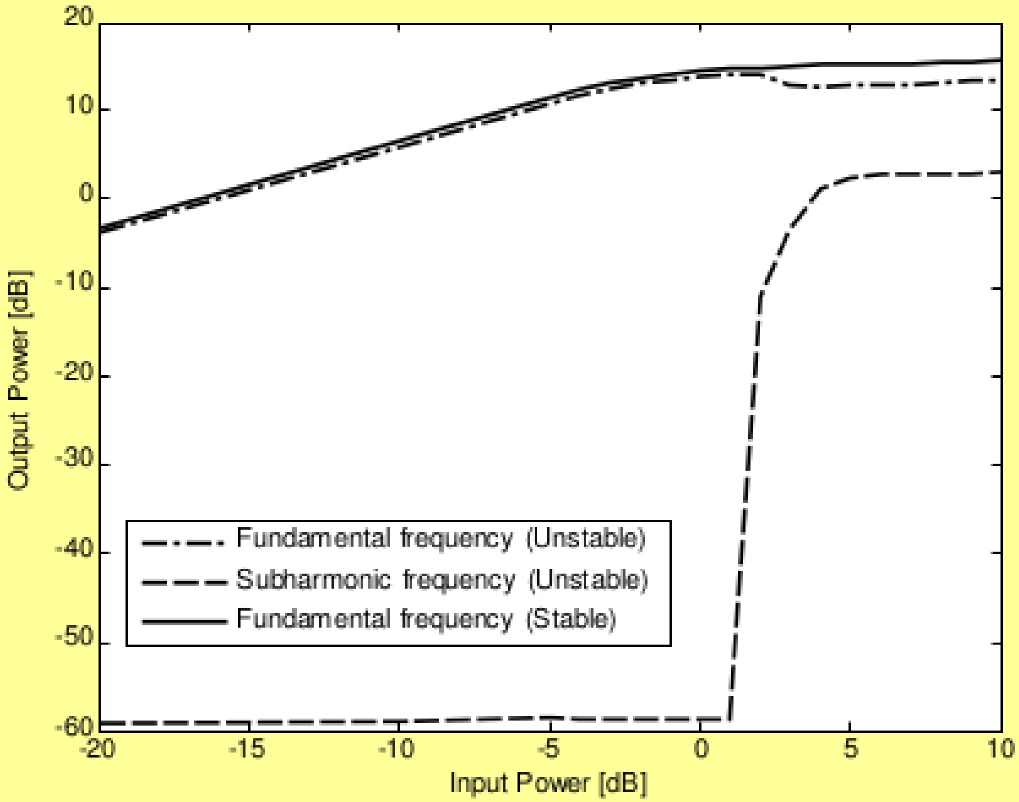

Output power spectrum

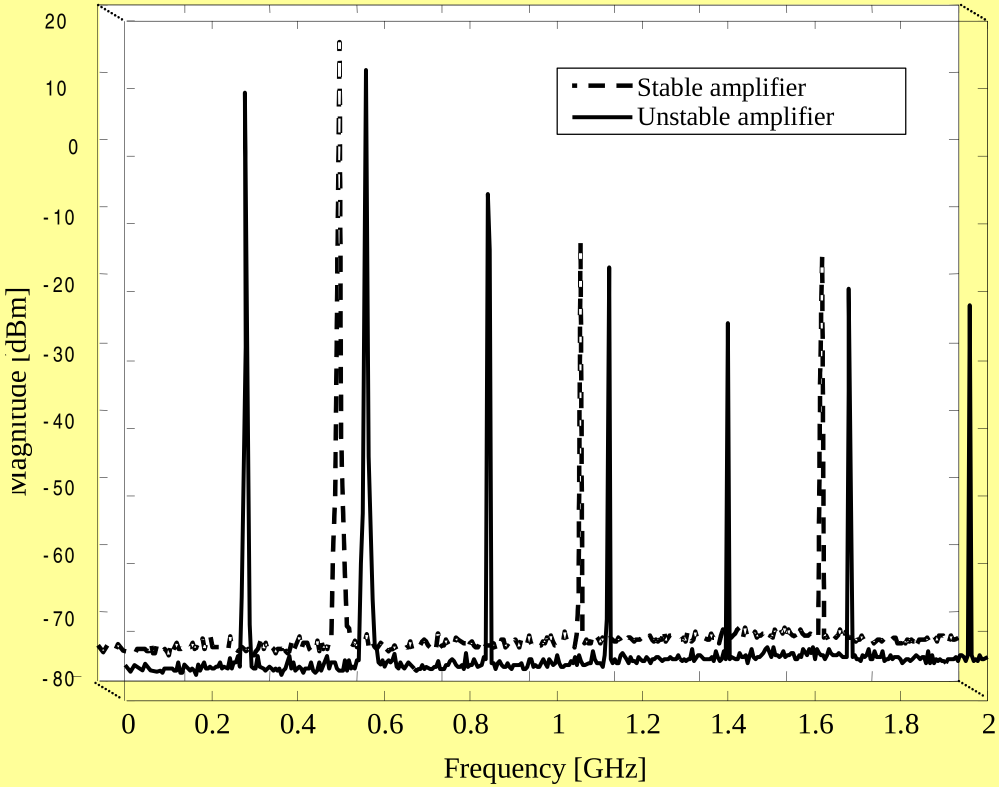

Special case: parallel power amplifier

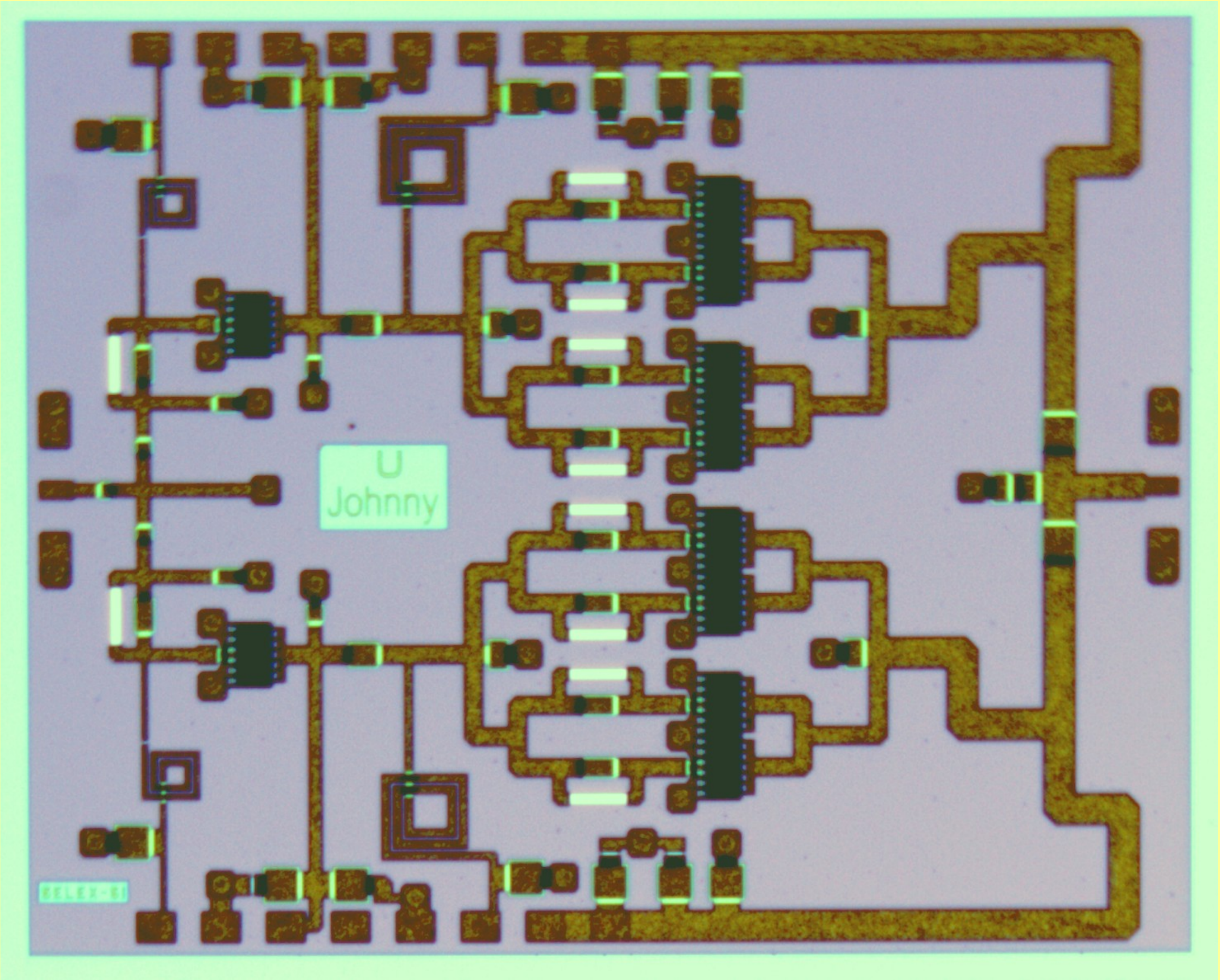

Single-transistor approach:

The symmetry of the amplifier is exploited

The amplifier must be symmetric wrt a longitudinal axis

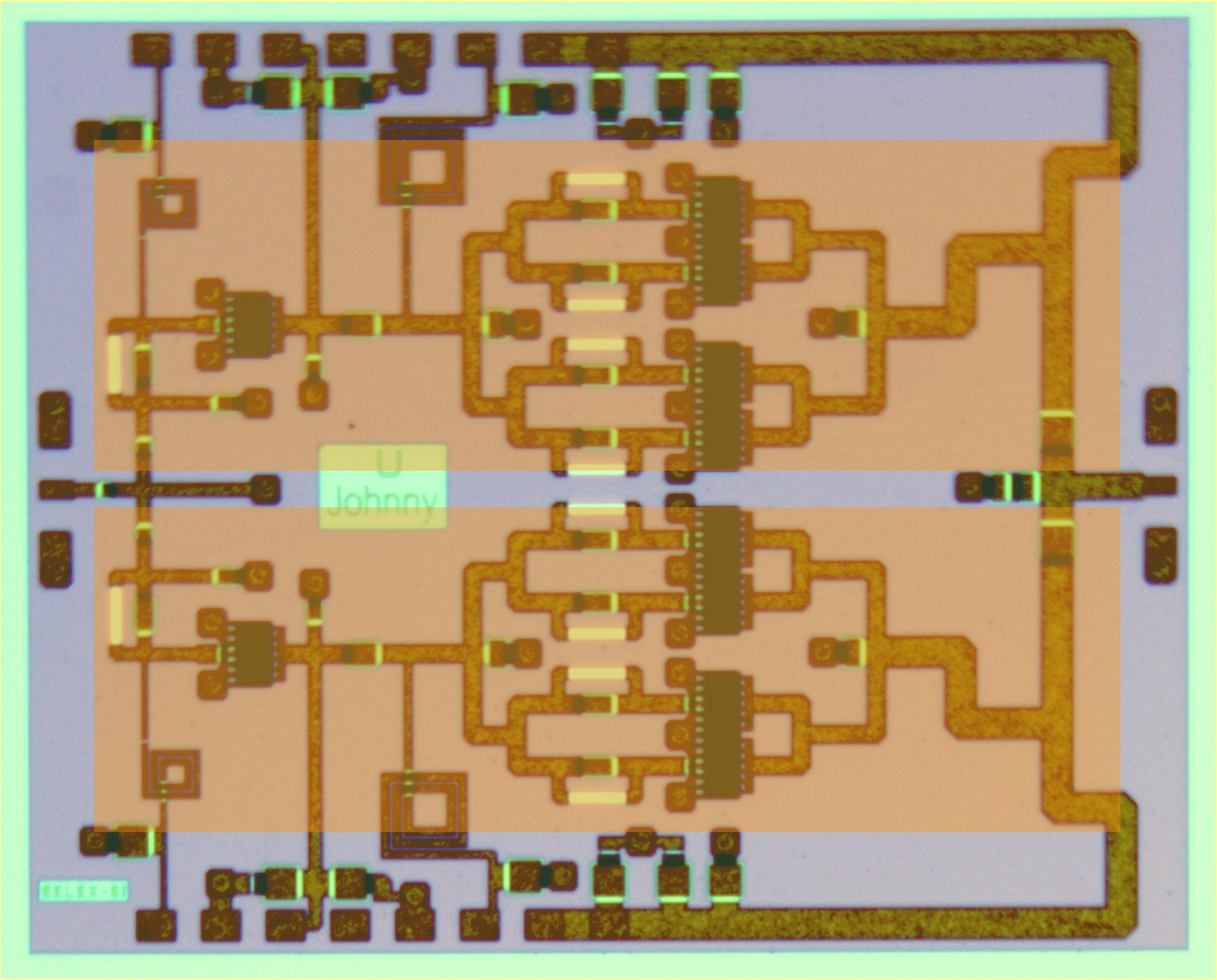

Single-transistor approach:

The symmetry of the amplifier is exploited

The amplifier must be symmetric wrt a longitudinal axis

Each half must in turn be symmetric wrt its longitudinal axis

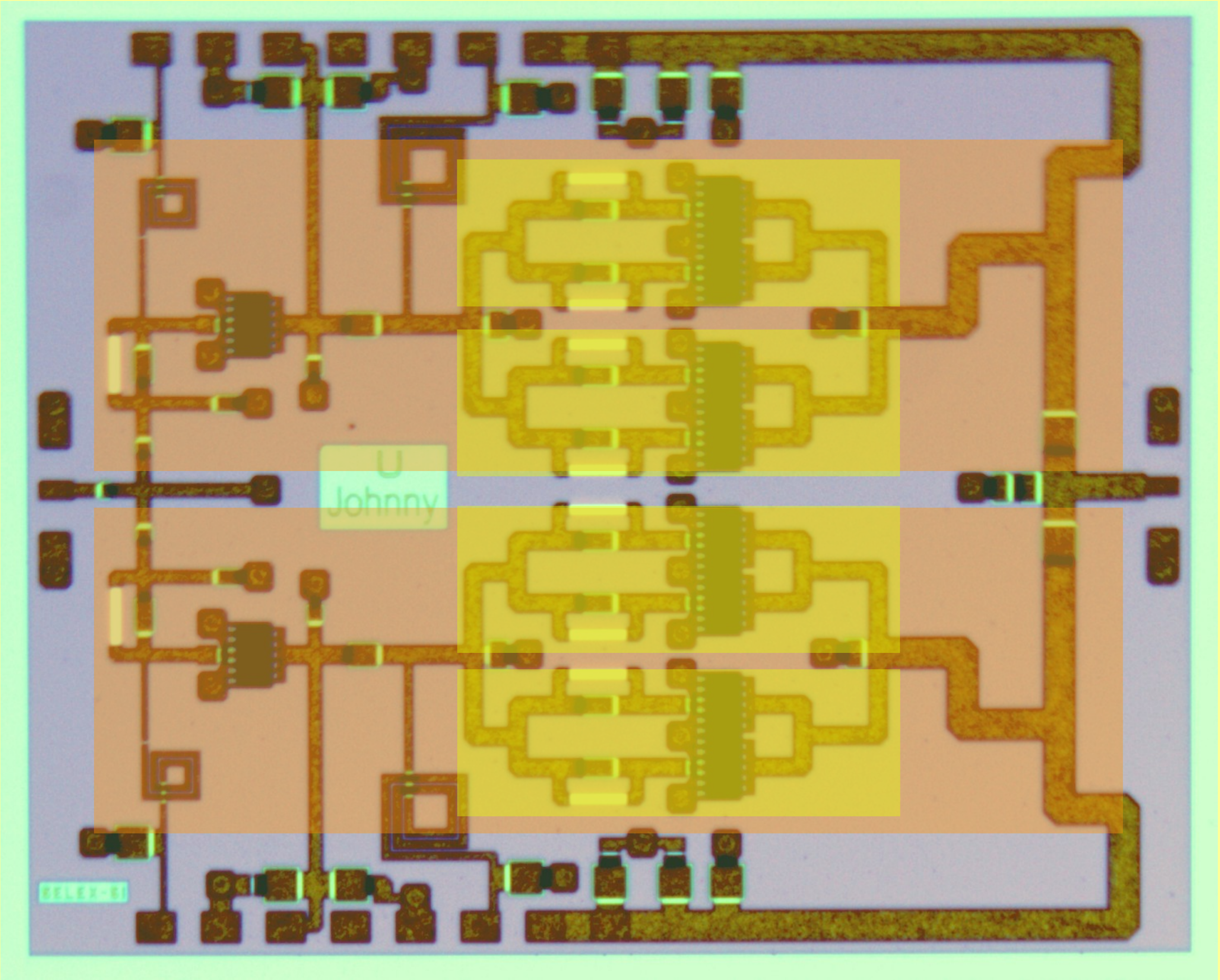

Single-transistor approach:

The symmetry of the amplifier is exploited

The amplifier must be symmetric wrt a longitudinal axis

Each half must in turn be symmetric wrt its longitudinal axis

...and so on.

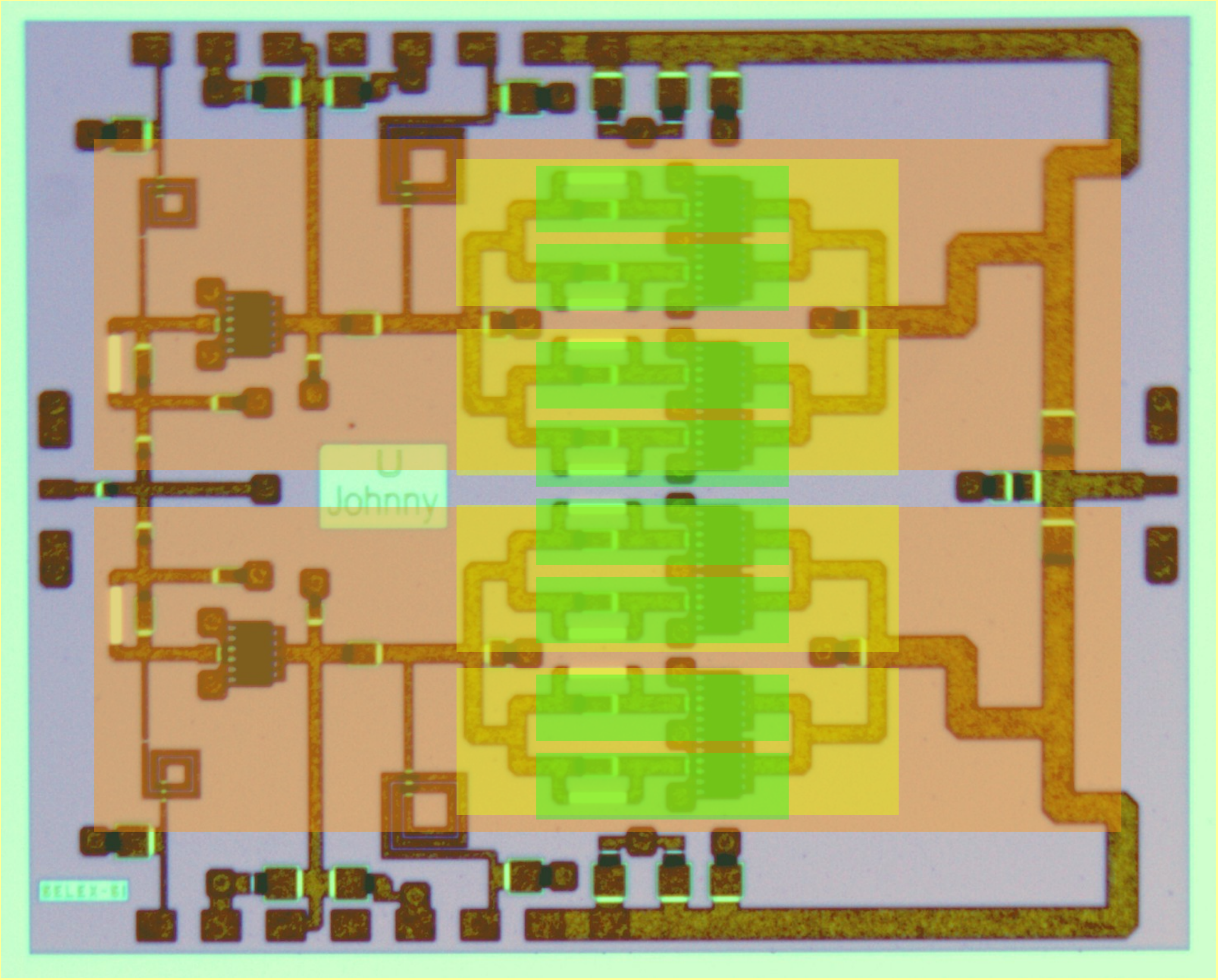

Single-transistor approach:

Identification of the symmetry modes

Example: a 4-transistor amplifier

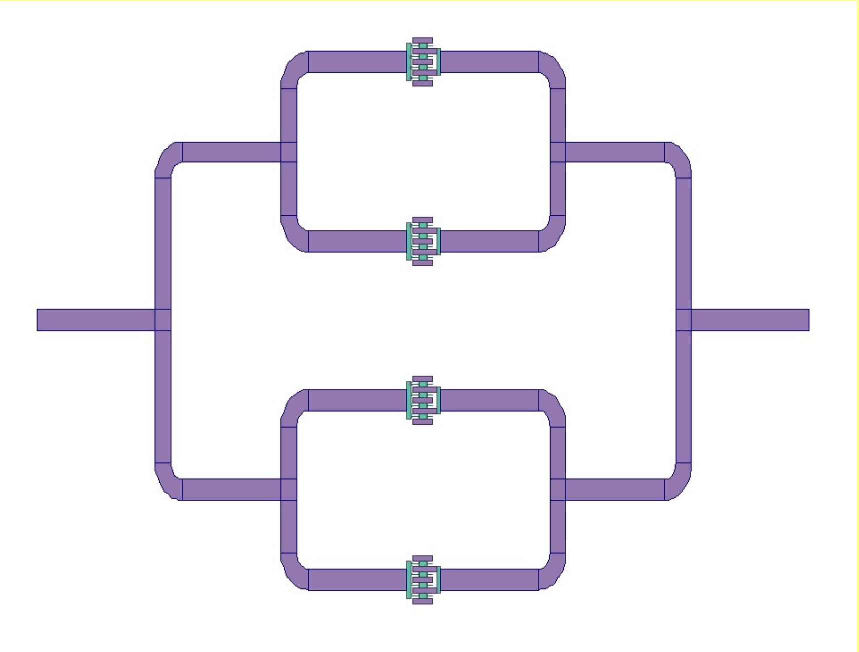

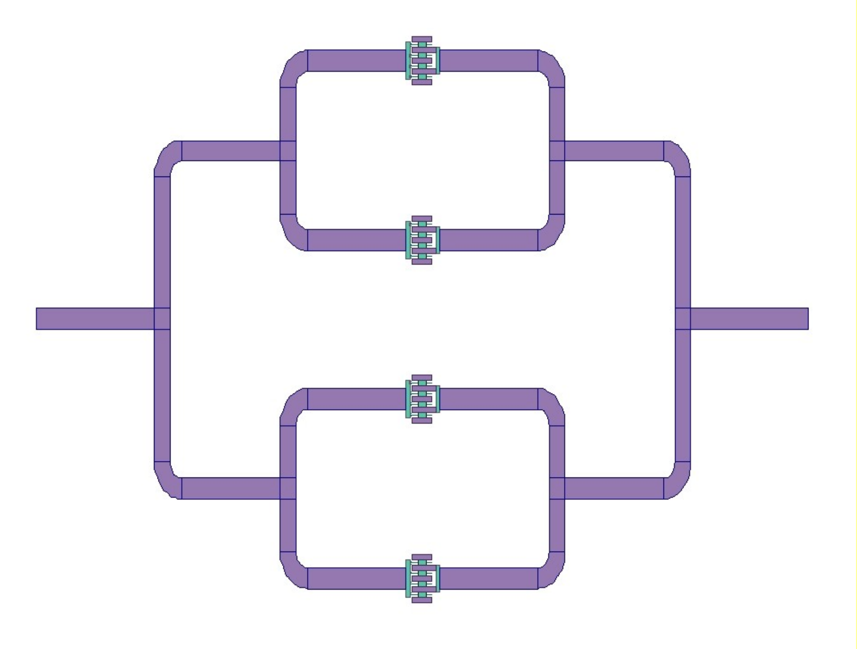

Single-transistor approach:

Identification of the symmetry modes

Example: a 4-transistor amplifier

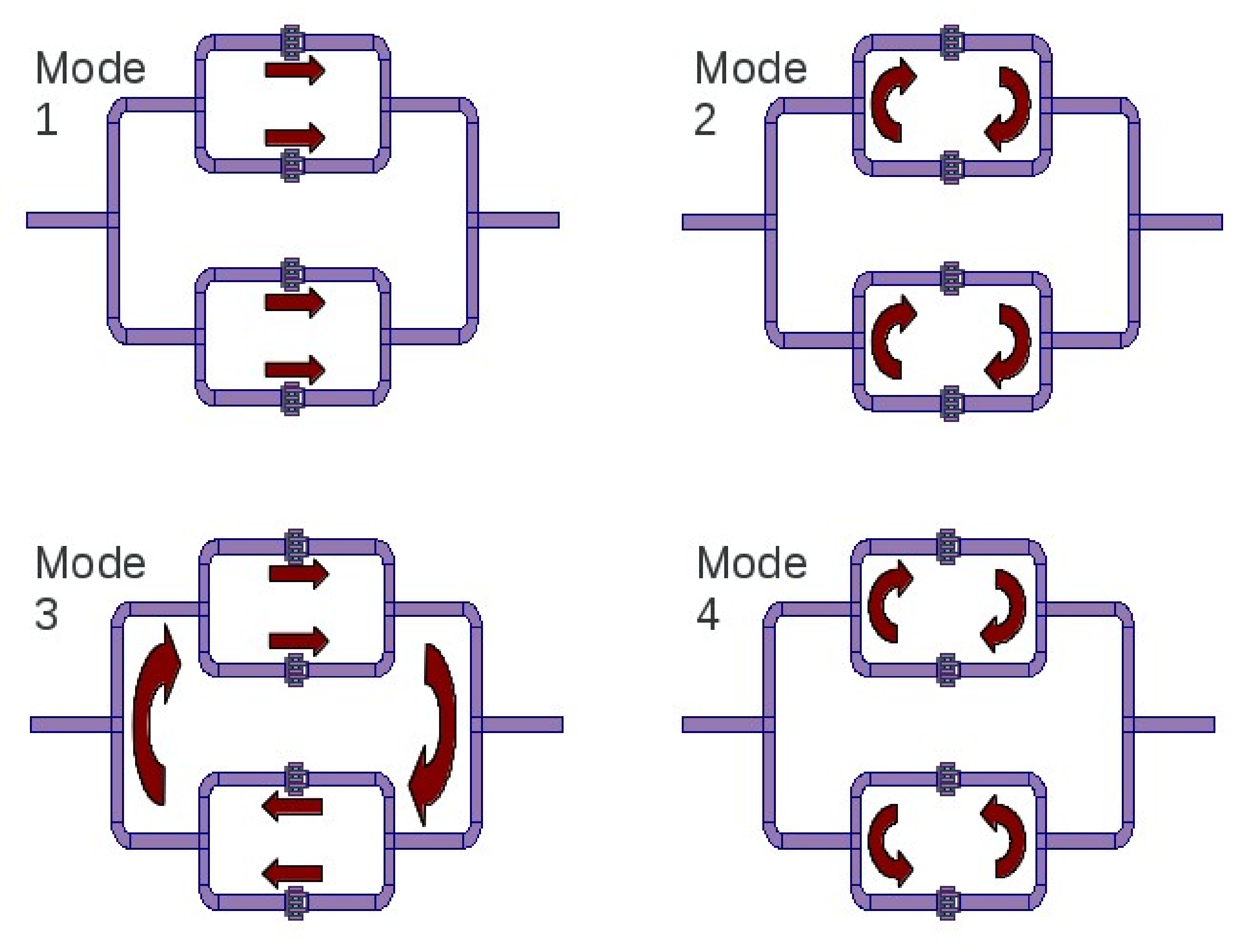

Four modes are found

Single-transistor approach:

Identification of the symmetry modes

Example: a 4-transistor amplifier

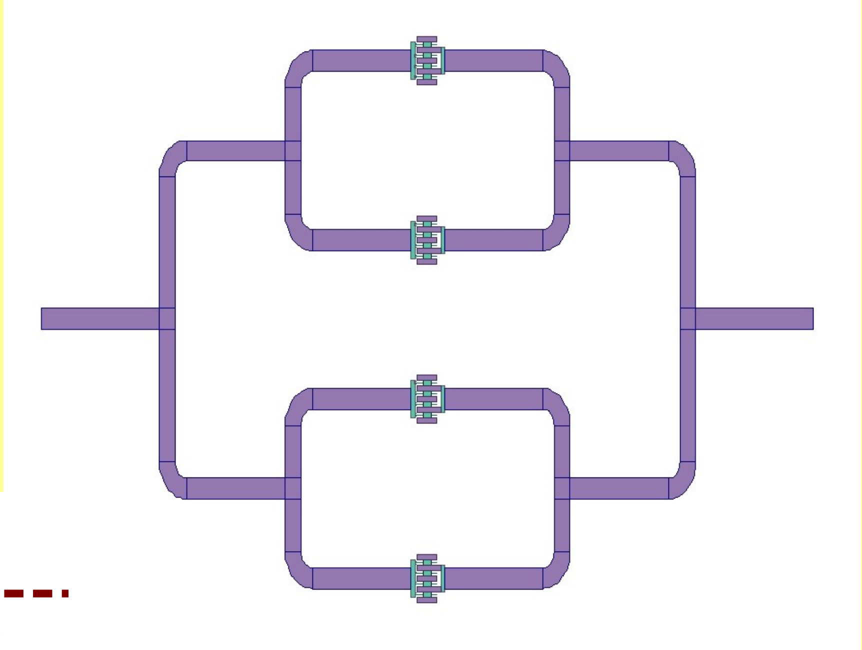

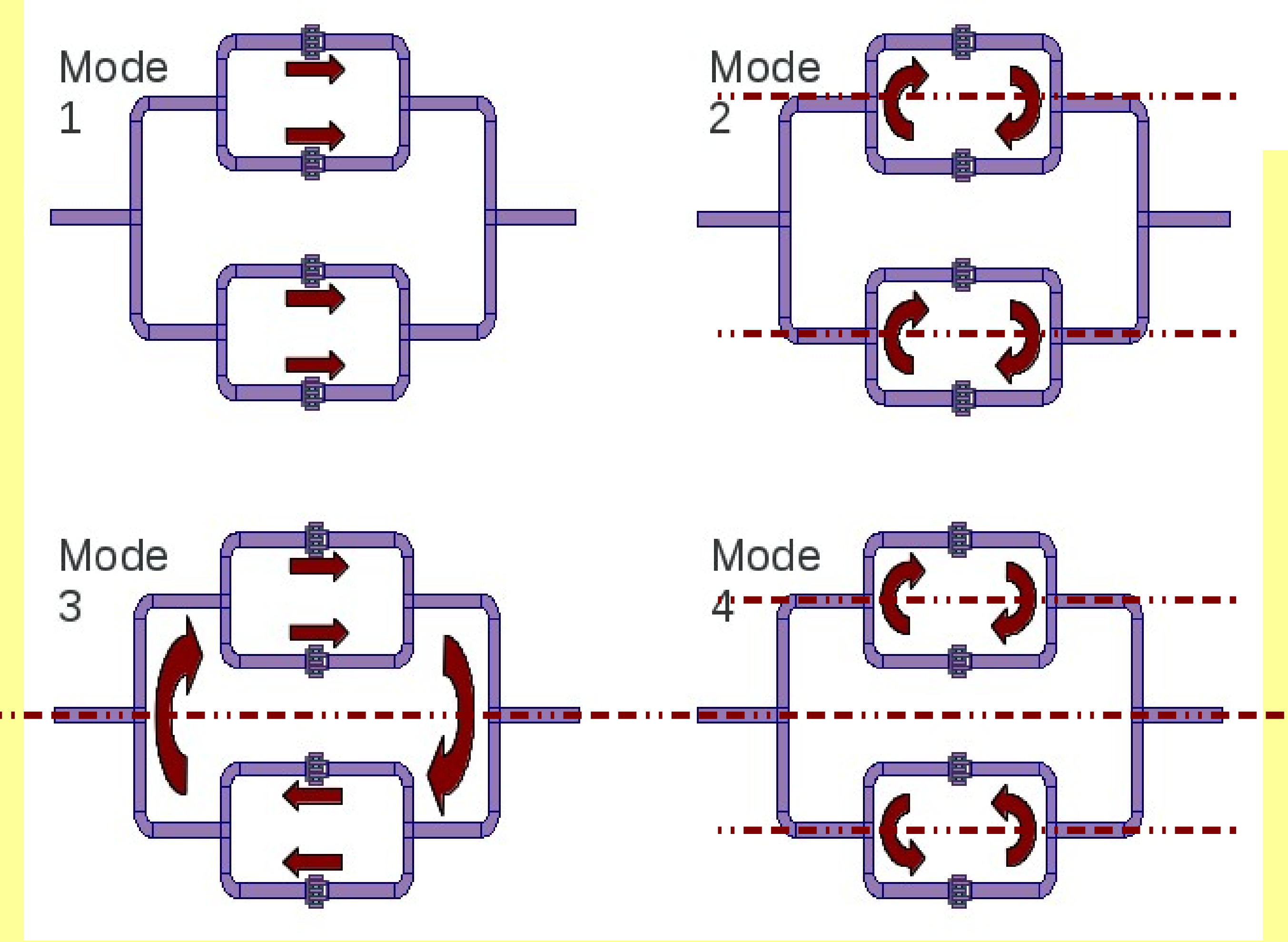

Four modes are found

Symmetry axes for each mode

Single-transistor approach: S-parameters of the matching networks

The input and output ports are loaded with Z_0

The symmetry of the networks is exploited

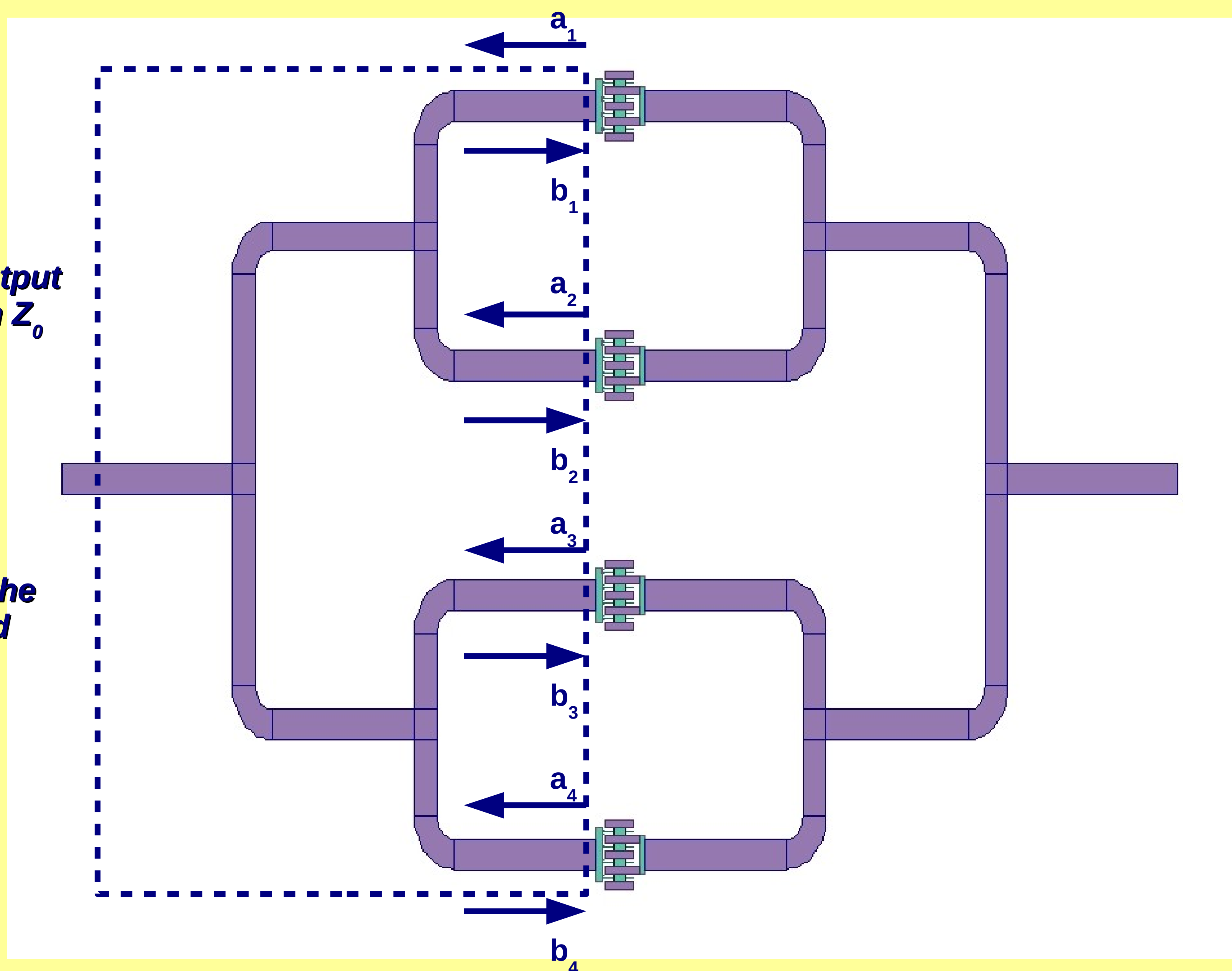

Single-transistor approach:

Modes identified from S-parameters

$$S_{11}=S_{22}=S_{33}=S_{44}=S_R$$
$$S_{12}=S_{21}=S_{34}=S_{43}=S_{MN}$$
$$S_{13}=S_{14}=S_{23}=S_{24}=S_{31}=S_{32}=S_{41}=S_{42}=S_{MF}$$

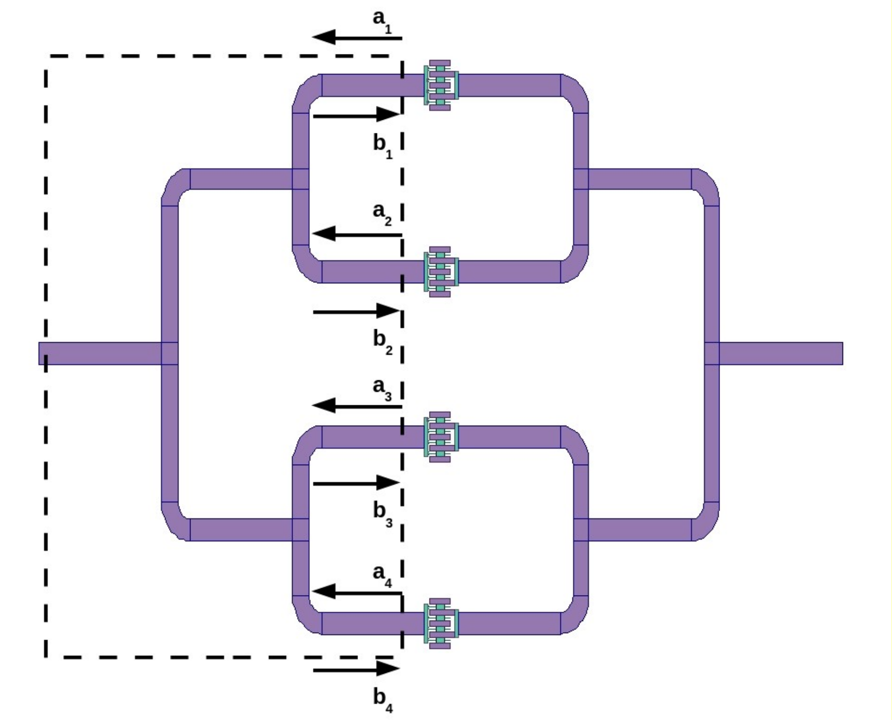

$$b_1=S_R\cdot a_1+S_{MN}\cdot a_2+S_{MF}\cdot a_3+S_{MF}\cdot a_4$$
$$b_2=S_{MN}\cdot a_1+S_R\cdot a_2+S_{MF}\cdot a_3+S_{MF}\cdot a_4$$
$$b_3=S_{MF}\cdot a_1+S_{MF}\cdot a_2+S_R\cdot a_3+S_{MN}\cdot a_4$$
$$b_4=S_{MF}\cdot a_1+S_{MF}\cdot a_2+S_{MN}\cdot a_3+S_R\cdot a_4$$

Four modes:

$$m_1=[1,1,1,1]$$
$$m_2=[1,-1,1,-1]$$
$$m_3=[1,1,-1,-1]$$
$$m_4=[1,-1,-1,1]$$

E.g. - mode 3 :

$$b_1=b_2=-b_3=-b_4=b$$
$$a_1=a_2=-a_3=-a_4=a$$

$$b=(S_R+S_{MN}-2S_{MF})\cdot a=\Gamma_3\cdot a$$

The stabilisation approach: Rizzoli's (Nyquist) method

Example – GaN power amplifier (Selex S.I.)

A high numer of harmonics and frequency points are required

Results are sometimes confusing and unstable

Example: 10 harmonics of the large signal

22-port conversion matrix

47 frequency points

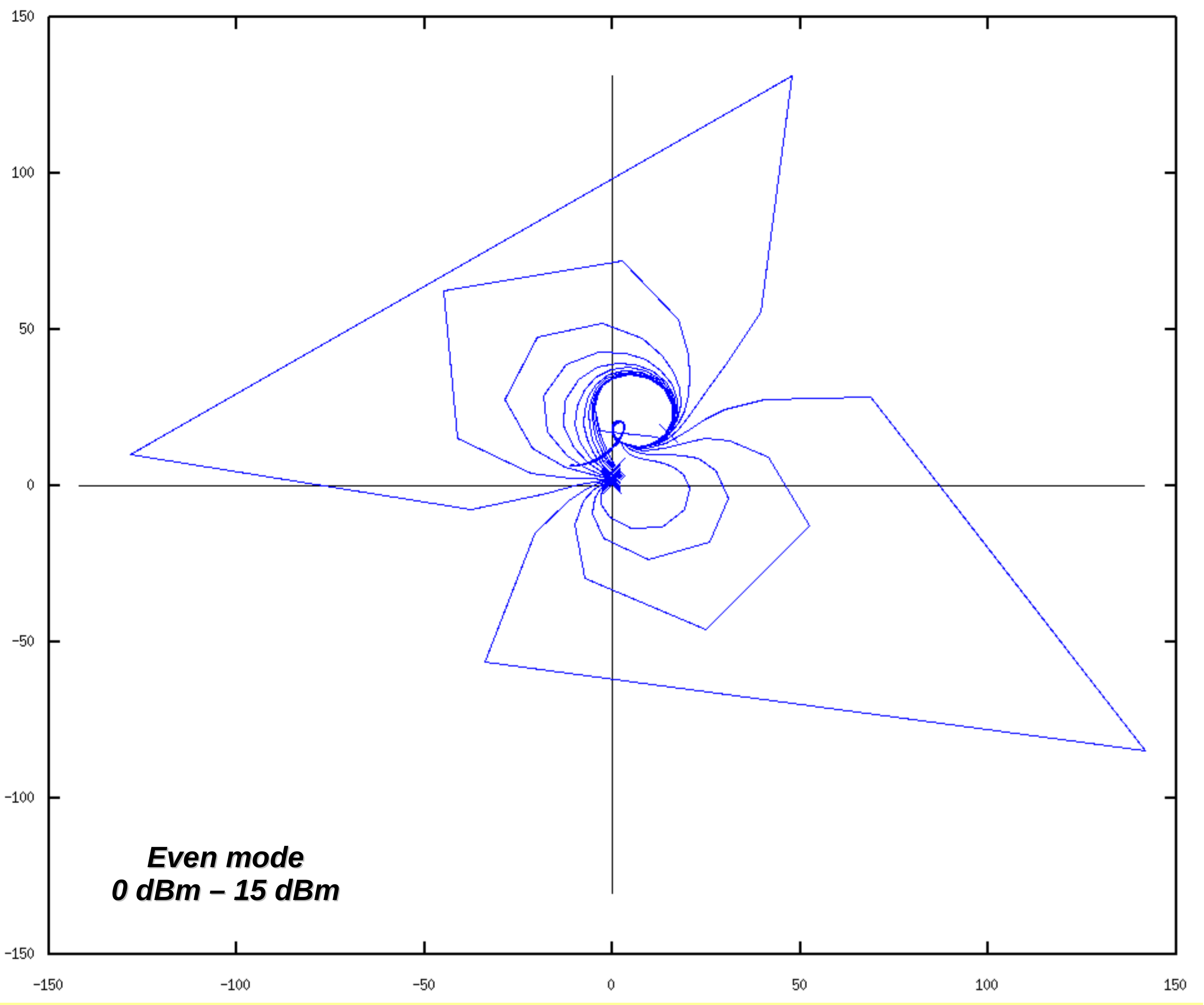

The stabilisation approach: Rizzoli's (Nyquist) method

Example – GaN power amplifier (Selex S.I.)

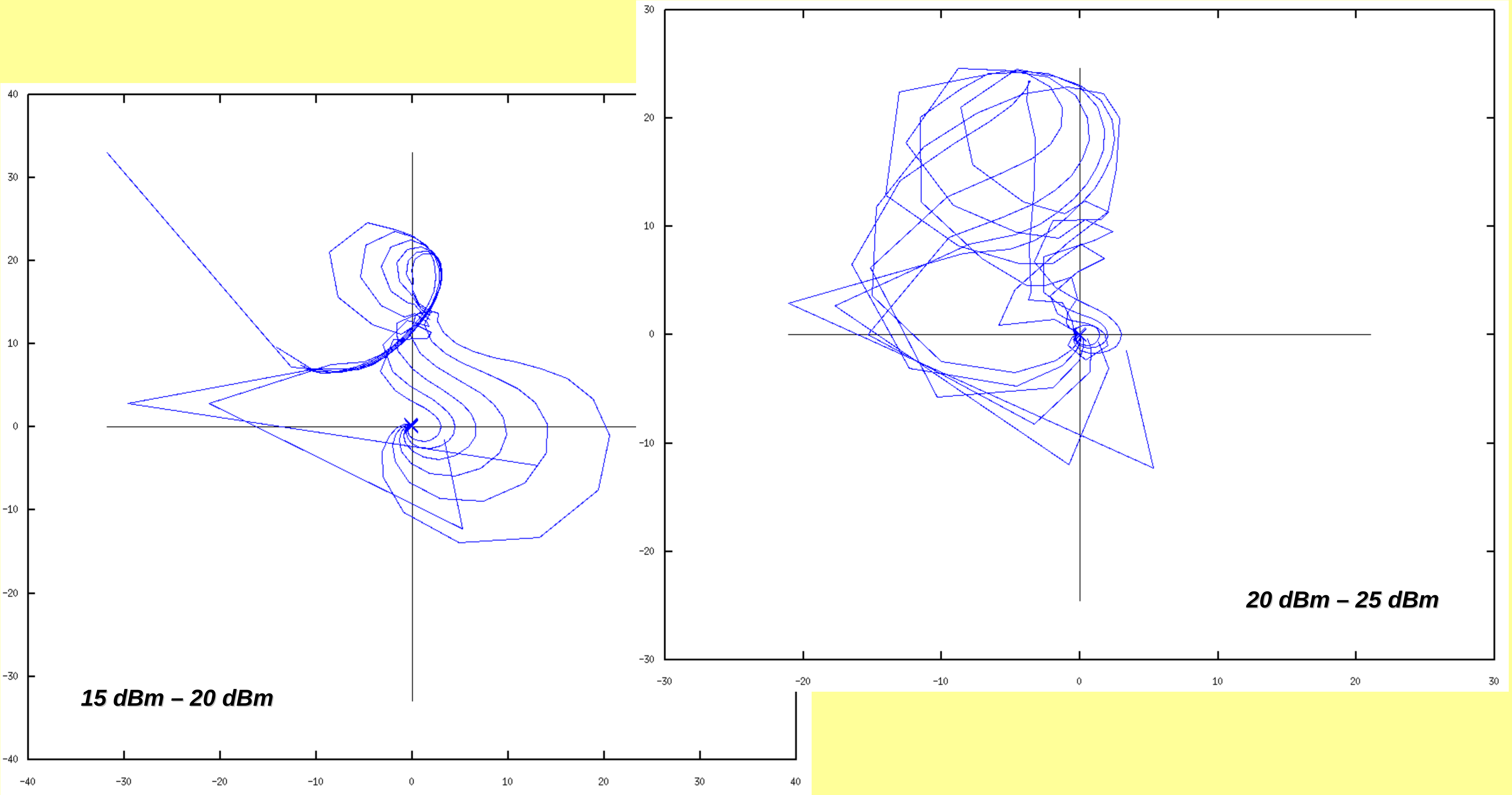

The stabilisation approach: Collantes' (pole-zero identification) method

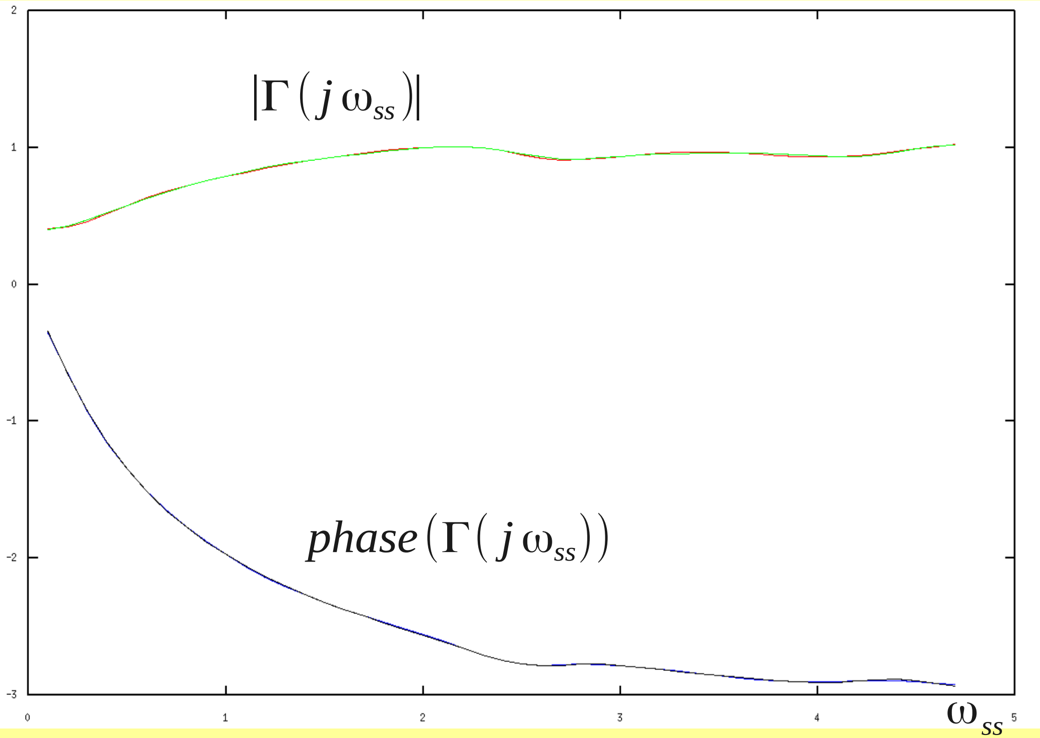

10th-order

Rational-function identification not unique

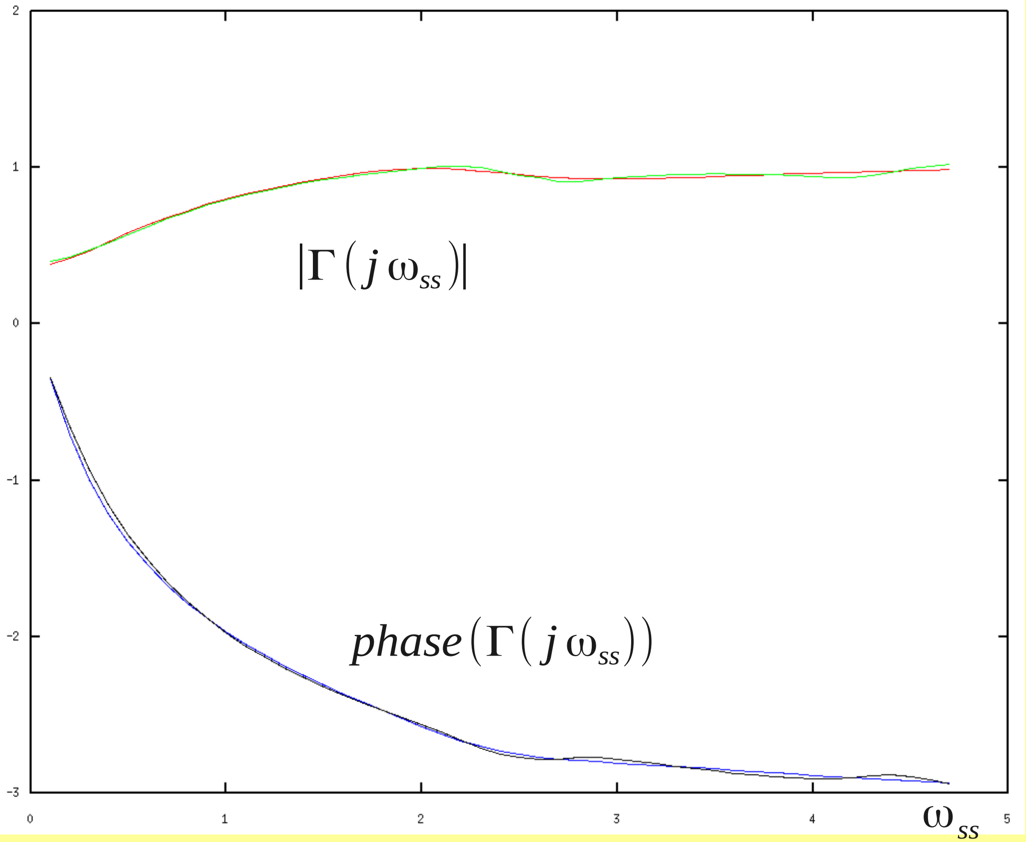

3rd-order

The stabilisation approach: Collantes' (pole-zero identification) method

Pole-zero cancellation

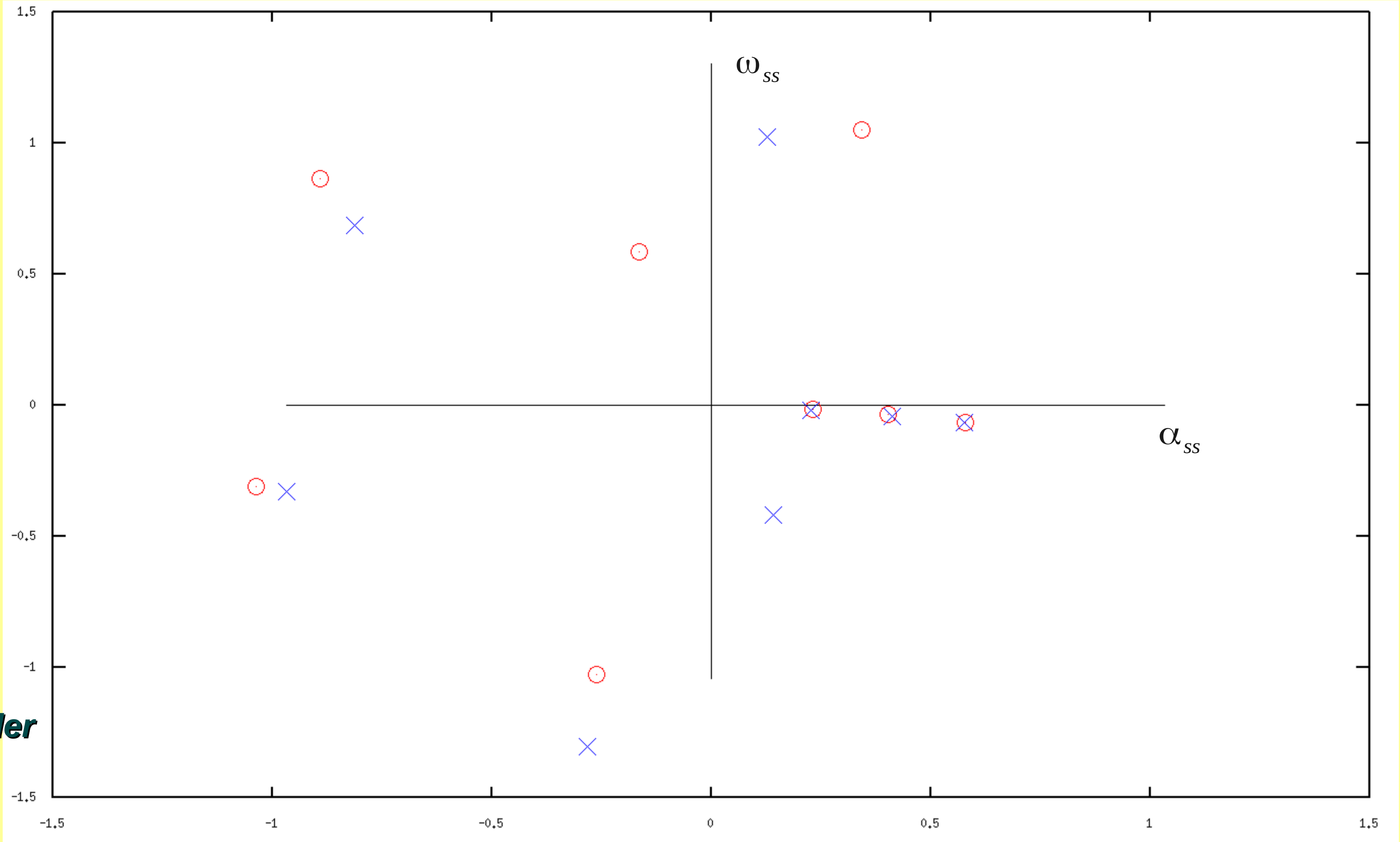

8th-order

Examples:

8-FET monolithic power amplifier

Two-stage, 9-GHz power amplifier from Selex S.I.

12 mm total periphery
0.4-µm GaAs HEMT

34 dBm output power at 1dB gain compression
16 dB linear gain

Divider-by-two
2-FET driver
Two dividers-by-four
8-FET power stage
Combiner-by-eight

Driver stage linear

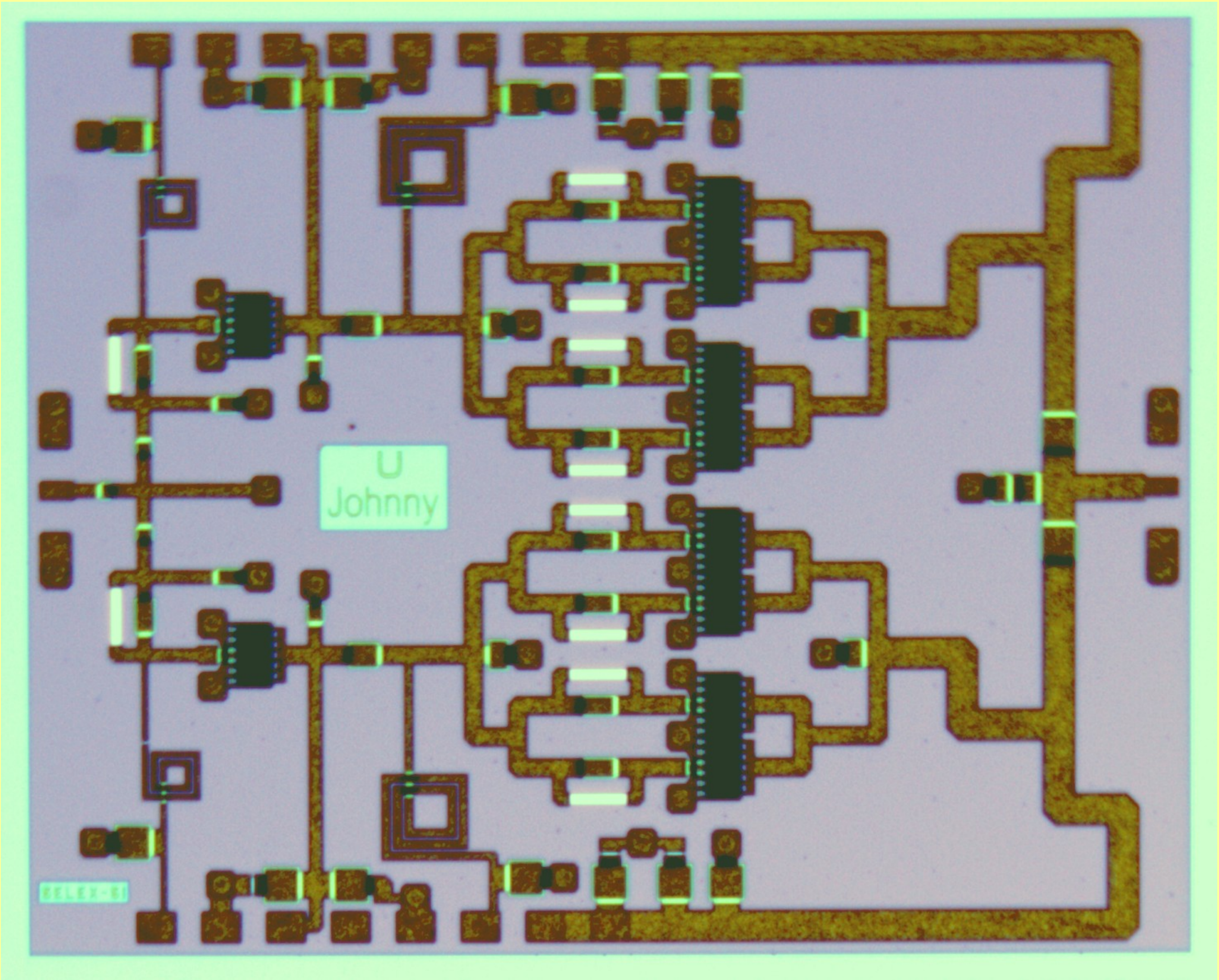

Examples:

8-FET monolithic power amplifier

The amplifier is linear under small-signal conditions

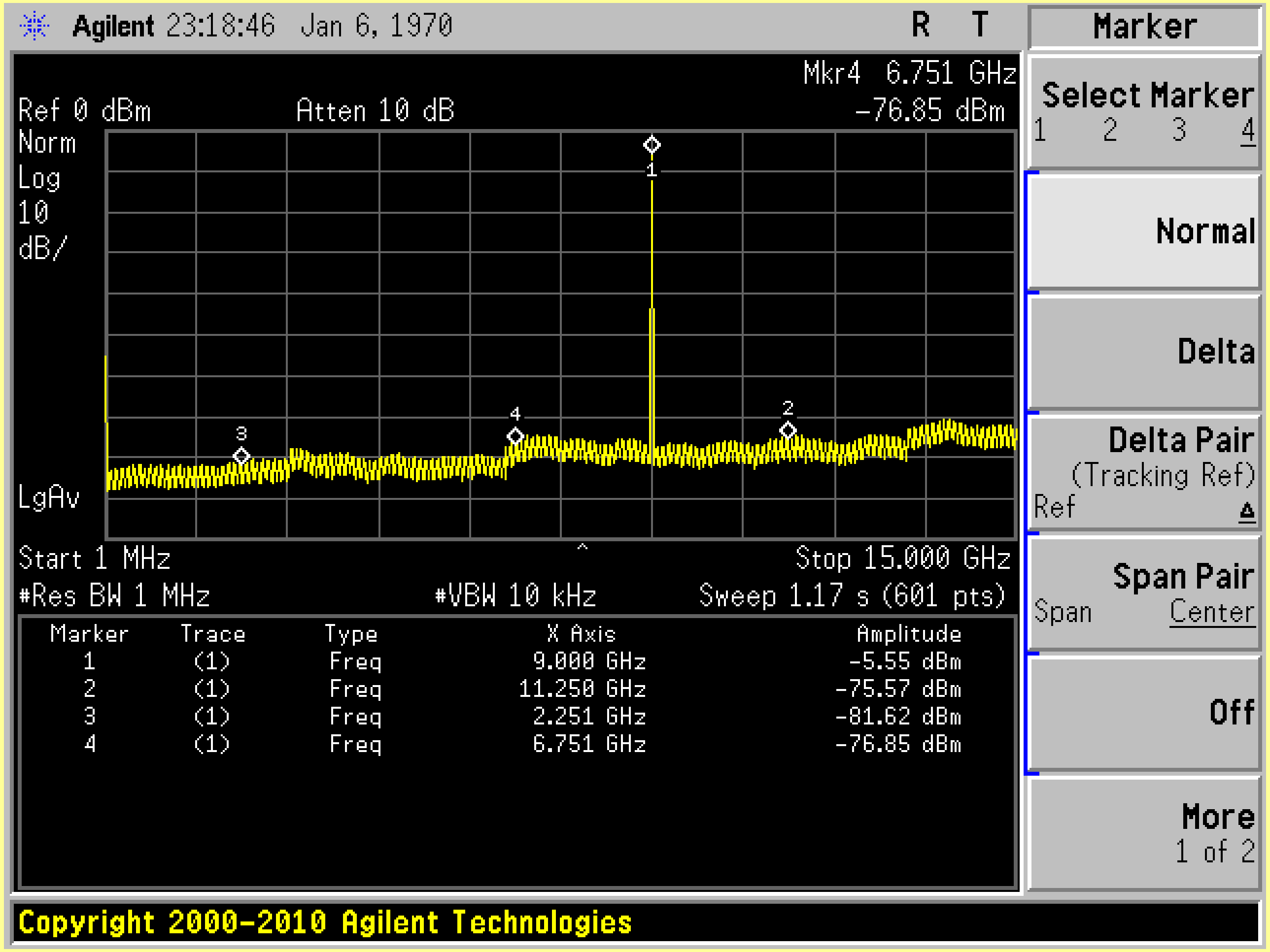

Examples:

8-FET monolithic power amplifier

A spurious signal appears under large-signal drive (Pin = 15 dBm)

The spurious frequencies are correlated

f_s

$f_0 - f_s$

$f_0 + f_s$

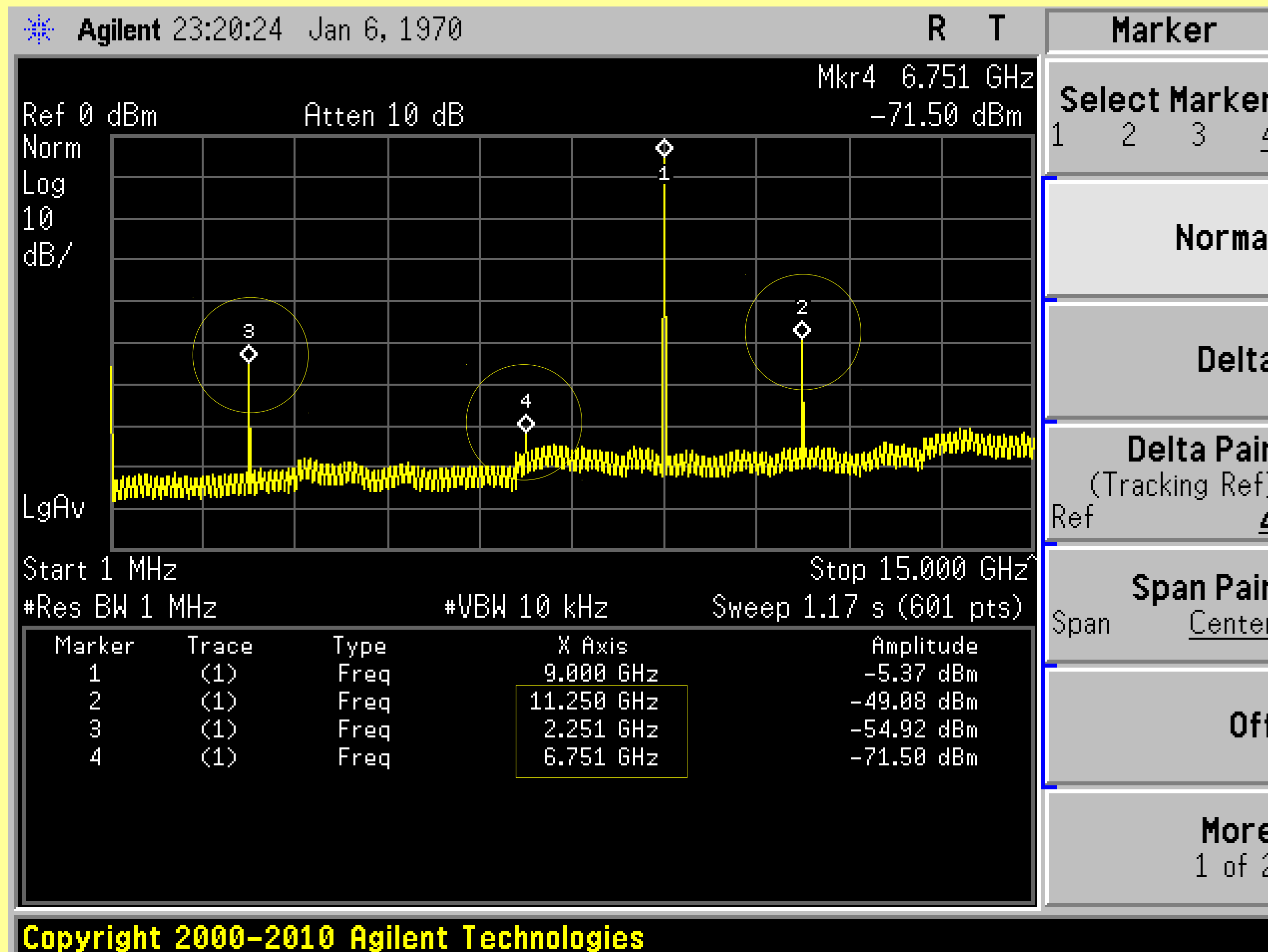

Examples:

8-FET monolithic power amplifier

The load falls into the unstable area

The one-port stability criterion (Lee) shows instability

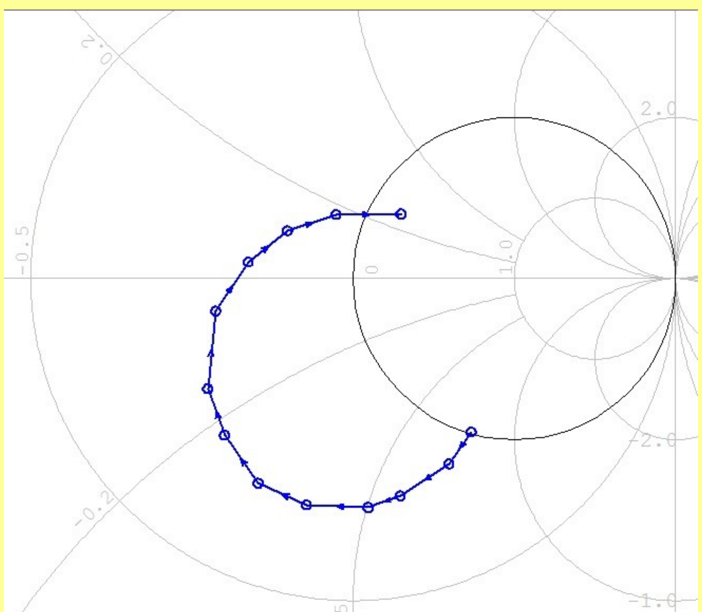

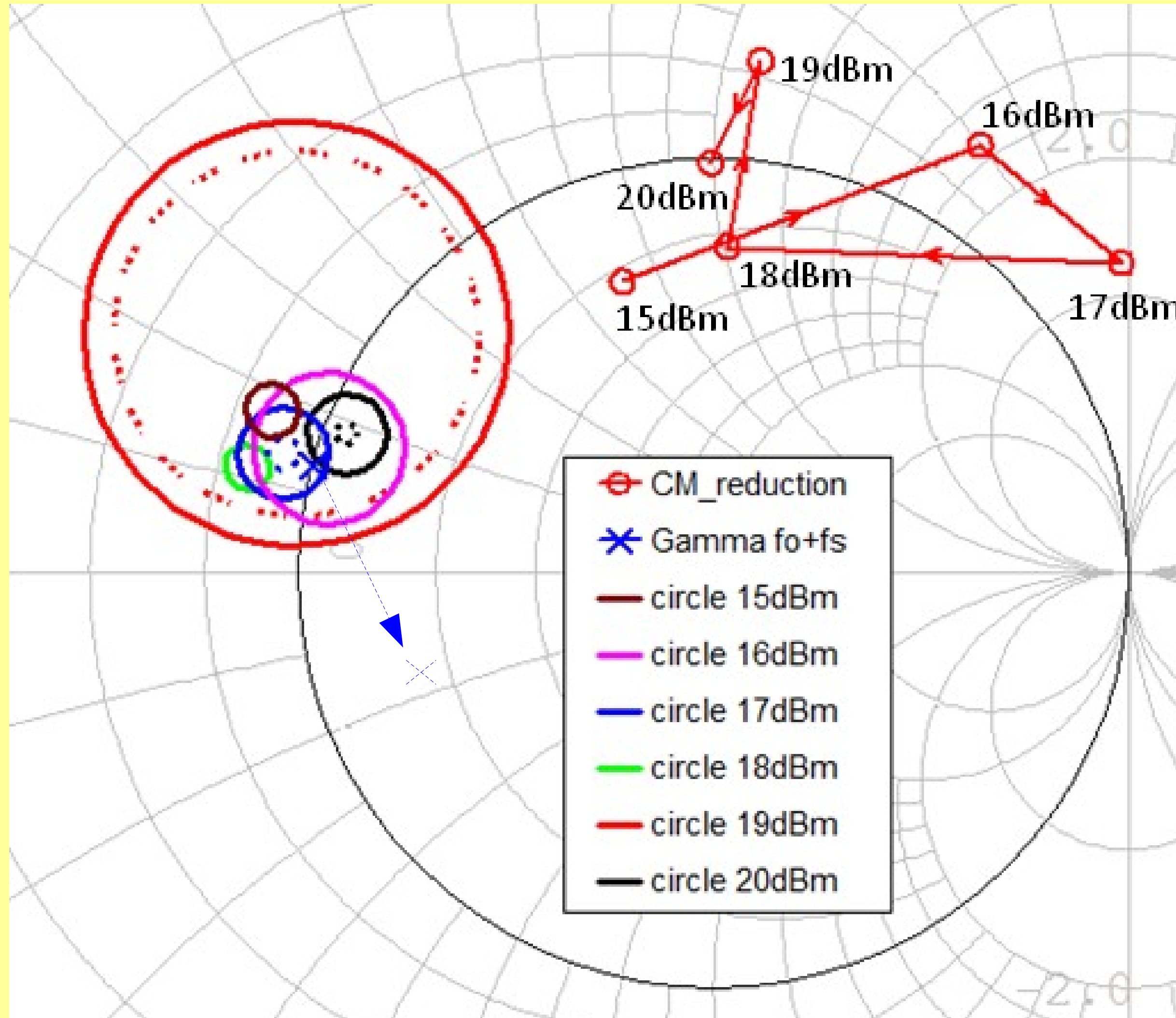

Solution: move the load outside of the unstable area

Examples:

2-device hybrid balanced power amplifier

Two versions (600 MHz):

First amplifier stable under small- and large-signal drive

Second amplifier redesigned for large-signal instability

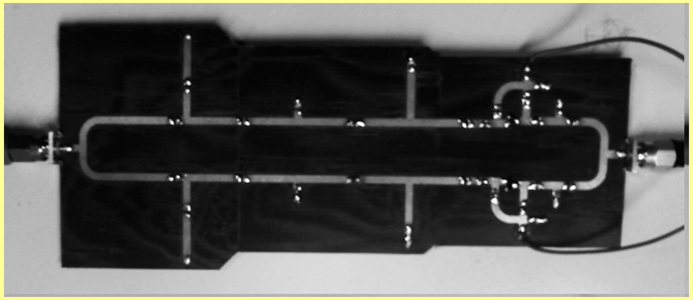

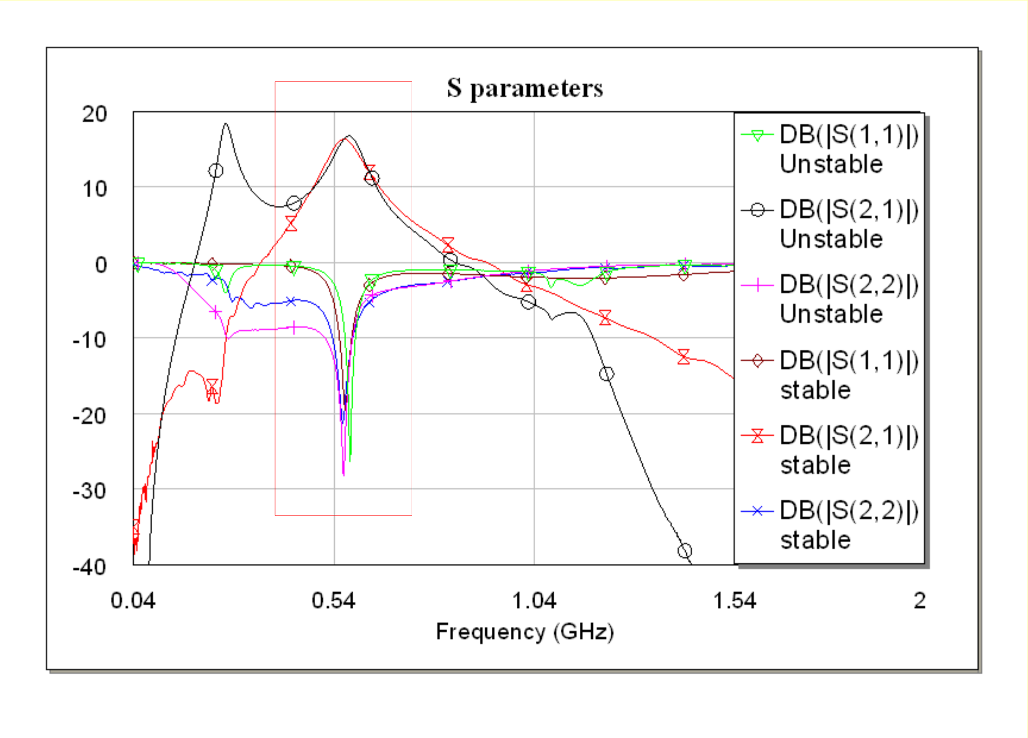

Linear performances very close at large-signal frequency

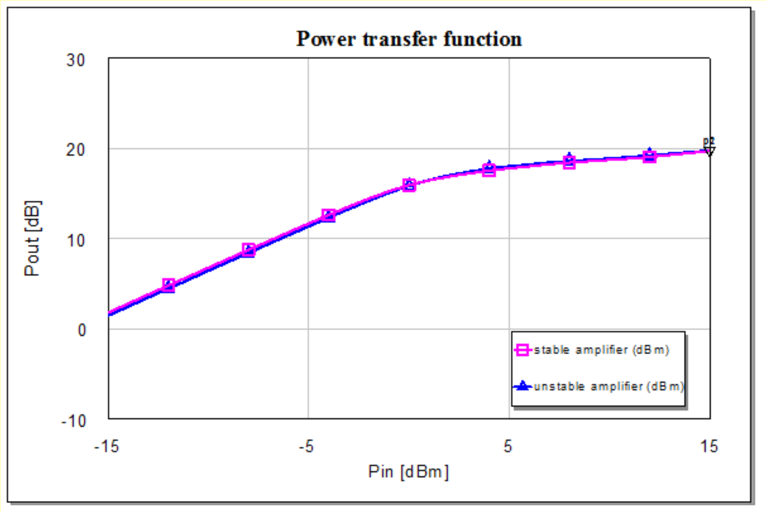

Simulated output power are very close

Examples:

2-FET hybrid balanced power amplifier

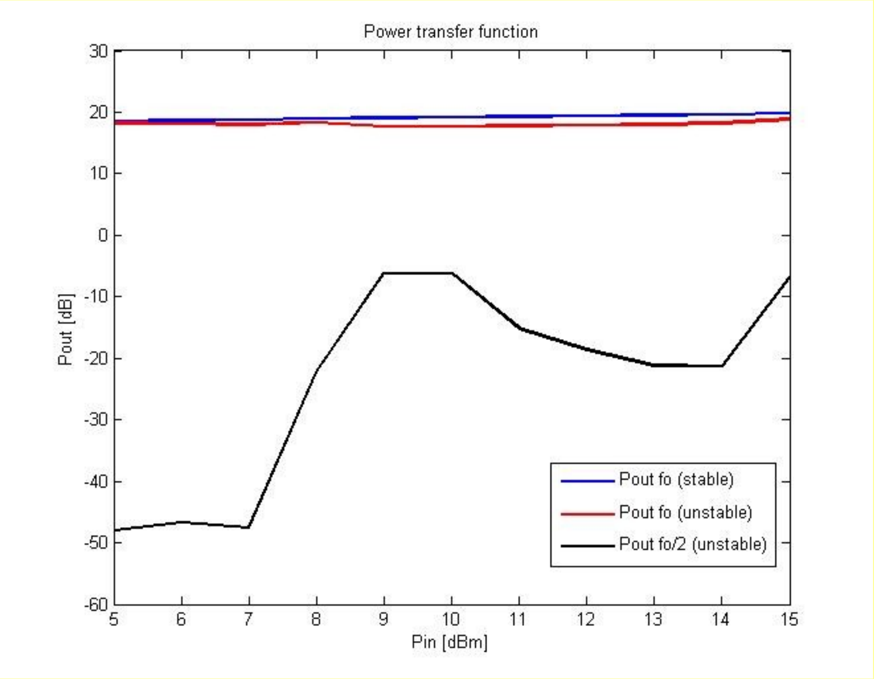

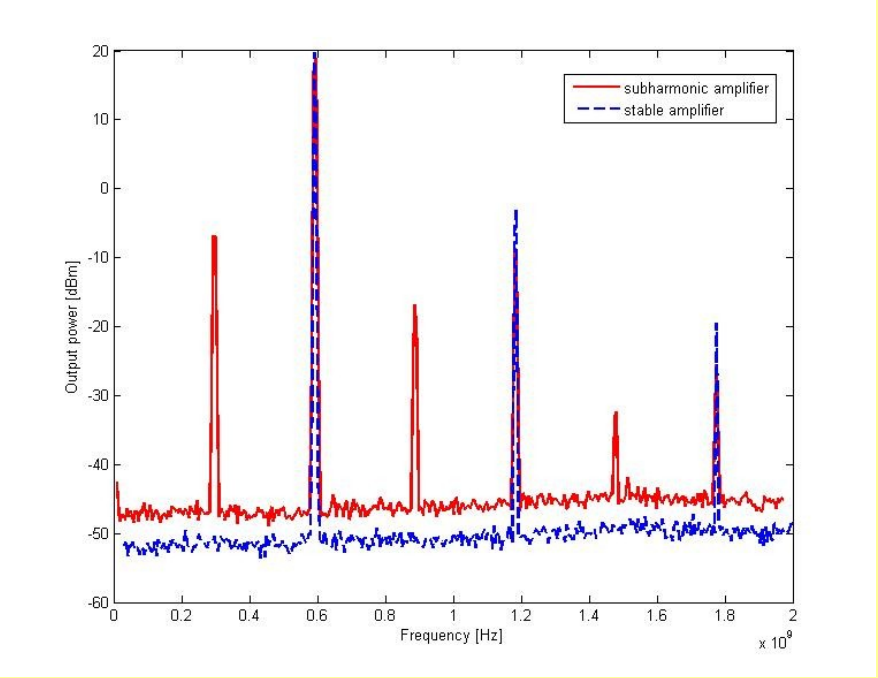

Measured output power very different

Spectra show a spurious signal at f_0 / 2

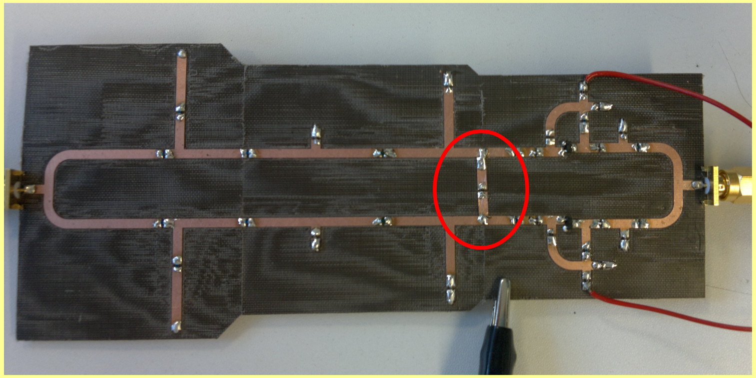

Instability suppressed with a shunt resistance

Conclusions:

* Stability under large-signal conditions can be addressed via the conversion matrix

* Poles of a conversion function can be located and moved by optimisation

* Stability can be enforced by direct design of loads in stable / unstable regions of the Smith Chart